Development and Application of an Inverse Spatially Offset Raman Spectroscopic Method for the Detection of Concealed Substances

By Thomas Bedward

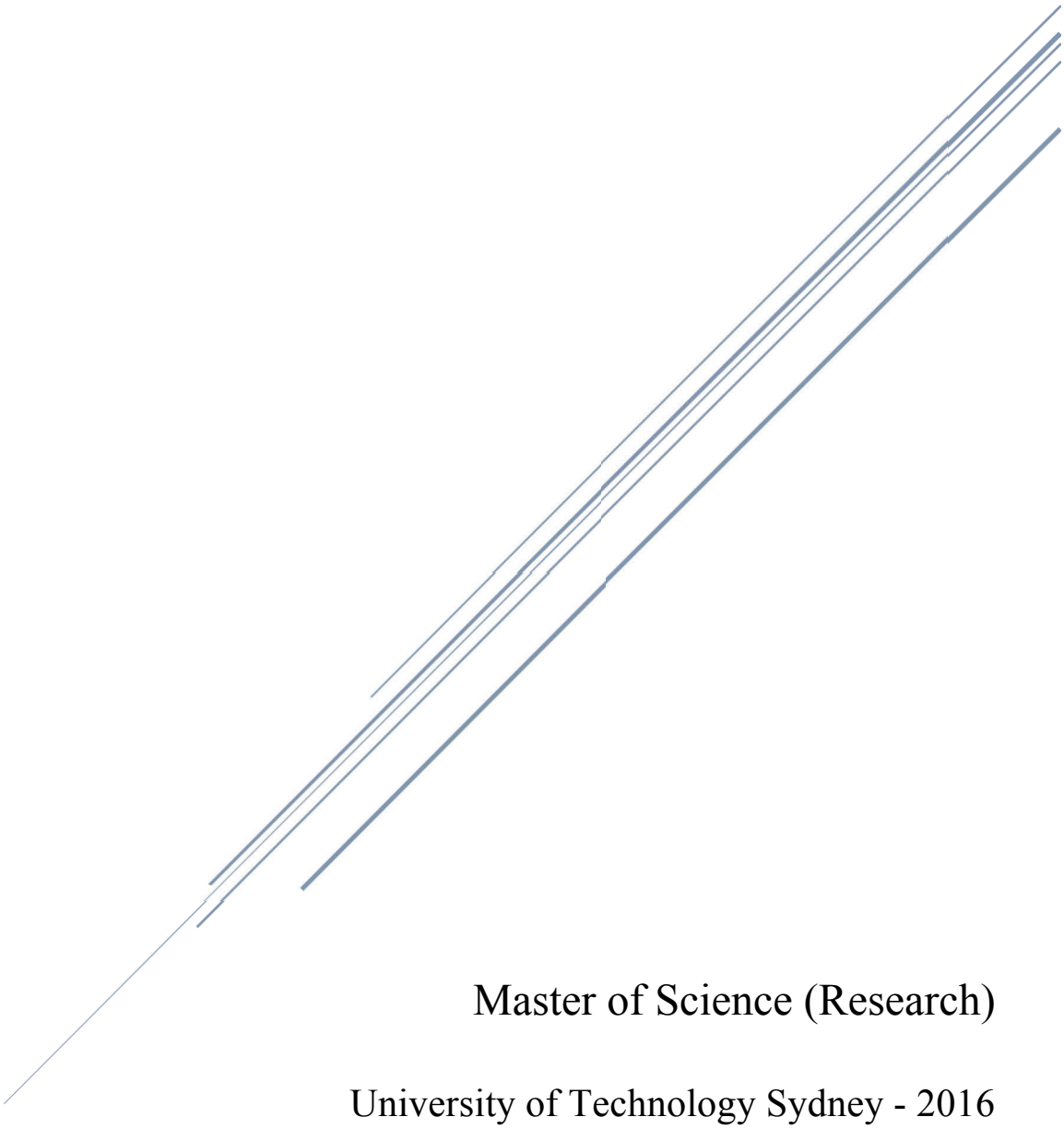

Master of Science (Research)

University of Technology Sydney - 2016

A Thesis submitted for the Master of Science (Research)

Faculty of Science

University of Technology Sydney

2016

Certificate of Authenticity & Originality

I certify that the work in this thesis has not previously been submitted for a degree, nor has it been submitted as part of the requirements for a degree except as fully acknowledged within the text.

I also certify that the thesis has been written by me. Any help that I have received in my research work and the preparation of the thesis itself has been acknowledged. In addition, I certify that all the information sources and literature used are indicated in the thesis.

Thomas Bedward

3rd of August, 2017

Table of Contents

List of Figures

List of Tables

Abbreviations

AFP	Australian Federal Police
ALS	Alternating Least Squares
API	Active Pharmaceutical Ingredient
BTEM	Band-Target Entropy Minimisation
CCD	Charge Couple Device
DEA	Drug Enforcement Administration
FBI	Federal Bureau of Investigation
HCl	Hydrochloride
HDPE	High Density Polyethylene
GSM	Grams per Square Metre
LDPE	Low Density Polyethylene
LOD	Limit of Detection
LOQ	Limit of Quantification
MCR	Multivariate Curve Resolution
MDMA	3,4-Methylenedioxymethamphetamine (Ecstasy)
NA	Numerical Aperture
NIR	Near Infrared
NIPALS	Non-linear Iterative Partial Least Squares
PARAFAC	Parallel Factor Analysis
PCA	Principal Component Analysis
PED	Performance Enhancing Drug
PLS	Partial Least Squares

PLS-R	Partial Least Squares Regression
PVC	Polyvinyl Chloride
PMMA	Poly(methyl methacrylate)
RMSE	Root Mean Square Error
RMSEP	Root Mean Square Error of Prediction
S	Slope
SD	Standard Deviation
SESORS	Surface Enhanced Spatially Offset Raman Spectroscopy
SNR	Signal to Noise Ratio
SNV	Standard Normal Variate
SORS	Spatially Offset Raman Spectroscopy
UNODC	United Nations Office on Drugs & Crime
WCO	World Customs Organisation
WHO	World Health Organisation

Abstract

Since the creation of the 'Dark Net' in mid-1990's, the way in which drugs are bought, sold, and transported has changed dramatically (Bartlett 2014). A digital age of drug trade has begun, and it has only been growing, with tens of thousands of websites now available on the Darknet, many of which are dedicated to the sale and trade of illicit substances (Anderson 2015). While techniques utilised by Customs and Border Security offices, both domestically and internationally, have evolved to stem this growing problem, the methodologies used by drug transporters and vendors have advanced even more rapidly, causing there to be a growing need for new detection techniques.

In 2016, the postal system has become one of the largest channels through which illicit substances are trafficked, with suppliers simply mailing their products to customers, greatly reducing and even removing the risk of ever being caught. Furthermore, suppliers have adopted a new, 'scatter-gun' approach, in which large shipments are broken down and sent in smaller, less obvious quantities. This approach has two main benefits, firstly, shipments are easier and cheaper to transport, and secondly, if one or two smaller parcels are intercepted, the bulk of the shipment is still far more likely to slip by Customs and Border Security offices. It is the combination of these practises, as well as the inability to examine every piece of mail that is sent and received that has helped to create a growing problem and a damaging trend.

In this paper, a Spatially Offset Raman Spectroscopy (SORS) method was developed and implemented specifically to detect, identify, and quantify samples of illicit substances concealed within twenty-five common packaging types. Utilising an axicon, conventional Raman

spectrometer and chemometric software, it was shown that a rapid and non-destructive SORS method could be easily and successfully implemented for the bulk of packaging materials commonly encountered within Australia and at Australian borders, as well as potentially aiding in the detection and identification of many concealed drug samples.

Ultimately, it was found that nineteen of the twenty-five packaging types could be successfully interrogated using the developed method, with strong signals and accurate detections made through envelopes, padded bags, and a variety of tapes, plastics, and papers. Furthermore, it was found that the method could detect and identify complex, powdered samples involving up to four components, as well as detecting target substances through more complex multi-layered parcels with a relatively high degree of accuracy and certainty.

Chapter One: Introduction

The war on drugs has been an internationally fought campaign, with victories found on both sides of the battlements. A constant battle, smugglers and customs agencies are both constantly involving their methods of detection and concealment, constantly developing new and more advanced ways in which they can apply their respective trades.

Currently, the drug smugglers appear to be winning, with an estimated total of 246 million drug users (1 out of every 20 people) between the ages of 15 and 64 in 2013, and an increase of 3 million users from the year before (UNODC 2015). The magnitude of the world drug problem becomes more apparent when considering that more than 1 out of 10 drug users is a problem drug user, suffering from drug use disorders or drug dependence. In other words, some 27 million people, or almost the entire population of a country the size of Malaysia, are problem drug users (UNODC 2015).

While new and more intricate smuggling methods are being applied, the majority of recreationally used illicit substances are known to arrive through parcels and in simple packaging delivered by mail, and it is therefore this prolific method of smuggling that requires the most immediate focus.

One of the most discussed and researched techniques for such methods of identification and quantification in current years, is that of Raman spectroscopy. The prominence of Raman spectroscopy in the field of drug detection and quantification is largely attributed to the technique's ability to provide rapid, sensitive, non-destructive, and in-situ analysis of a variety of

drug samples (West and Went 2011). A large number of recorded developments into the technique, including the use of multivariate analysis techniques, improved and specialised enhancement techniques, and the improvements in instrumentation such as a wider variety of laser wavelengths and the implementation of Kerr gated fluorescence rejection (Littleford, Matousek et al. 2004) has served to make the technique more reliable and suitable for the identification of a variety of drug types, ultimately leading it to become the technique of choice for most narcotic related applications (West and Went 2011).

While relevant literature regarding contemporary spectroscopic methods indicate that the use of Raman spectroscopy as a quantitative method is limited, continuing advances in the instrumentation and methodologies applied have proved that suitable methods can be successfully developed and implemented. Unfortunately, while the use of chemometric processes such as Partial Least Squares Regression has dramatically improved the accuracy and rapidity of quantitative analysis, there are still concerns regarding the correct ethical procedures applied when analysing potential illicit substances, such as ensuring the proper handling and processing of samples, and removing possible allegations of evidence tampering in forensic case work

In an effort to subvert this issue, as well as to further simplify and improve the basic method of Raman spectroscopy, the new technique of Spatially Offset Raman Spectroscopy (SORS) has been created. This technique has been ideally reported to be able to produce accurate identification of both solids and liquids within containers in a number of previous trials (Bloomfield, Loeffen et al. 2010). Importantly, this technique is able to analyse substances without the need for any sample pre-treatment, meaning that a suspected illicit substance can be identified and potentially quantified without disturbing or opening its packaging. While literature

regarding this technique is still limited, there is sufficient evidence to prove that SORS is a prominent and highly important modern spectroscopic technique.

In this paper, a SORS method that is amenable to conventional Raman spectrometers will be presented. The method developed will serve to detect, identify, and quantify various mixed samples involving atropine and a number of adulterants through twenty-five common and frequently used packaging types, as well as testing of more complex mixed powders and multi-layer parcels.

Chapter Two – Raman Spectroscopy

2.1 Background

The Raman Effect was first predicted in 1923 by Austrian theoretical physicist Adolf Smekal in his paper 'Zur Quantentheorie der Dispersion' ('The Quantum Theory of Dispersion') however it wasn't until five years later that the effect was first experimentally observed (Smekal 1923). Sir Chandrasekhar Raman and K. S. Krishnan were the first to experimentally observe the Raman Effect in liquids, publishing their observations in a paper entitled 'A New Radiation' in 1928 (Raman 1928), with the effect later being observed in solid forms by Russian physicists Grigory Landsberg and Leonid Mandelstam in the same year (Landsberg and Mandelstam 1928, Raman 1928).

Initially, great favour was placed upon the newly discovered Raman Effect, which was largely accredited to the relative ease and accuracy of being able to photographically record the wavenumber shift of the Raman Effect, instead of the more complex and tiresome point-by-point plotting of moving coil galvanometer signals that were being used in infrared spectroscopy. This early favour, though short lived, allowed Raman spectroscopy to be named as one of the most prominent contemporary methods for identifying molecular structures, and was initially prompted to surpass infrared spectroscopy as the most prolifically used methodology.

Despite the initial fervour of interest, the use of Raman spectroscopy in chemical investigations declined rapidly due to the onset of a number of prominent issues. The incipience of strong fluorescence emissions that would often eclipse the weaker Raman signals and often saturated

the photographic emulsions used in spectrographic recording was a dire disadvantage that severely limited the application and use of the method (Chalmers, Edwards et al. 2012). It was the growing modernisation of materials and technology that allowed for the prevalent disadvantages of Raman spectroscopy to be overcome, and in doing so brought favour back to the long maligned technique. The invention of tuneable laser excitation, improvements in method of detections, and the ability to computerise data acquisition and analysis meant that the functionality of Raman spectroscopy could be improved tenfold. The need for this more modern technology to fully realise Raman spectroscopy's potential meant that its widespread acceptance in forensic analysis was initially slow. As a result, it wasn't until the 1990's that Raman spectroscopy was truly accepted and applied to forensic casework, while the more widely accepted mid-infrared spectroscopy techniques had been in operation in forensic analyses since the early 1950's (Chalmers, Edwards et al. 2012).

Destruction of the sample, either by chemical or mechanical means, is an incredibly prominent disadvantage for spectroscopic techniques, particularly when considering forensic applications. The loss or destruction of important evidence, and possible restrictions on the quantity or size of available specimens were extreme issues for techniques of that age, and it was the need to overcome these obstacles, along with a realisation of new technology that lead to an important revelation in the mid-twentieth century. For the first time, modern advancements in spectroscopic instrumentation allowed for modern methods of truly non-destructive testing, allowing for the rapid acquisition of chemical molecular data that could be achieved from very small quantities of valuable samples (Edwards and Chalmers 2005) (Caliberto and Spoto 2000) (Vandenabeele, Edwards et al. 2007).

The advancement of technology and expanses in research meant that increased sensitivity and further utilisation of spectroscopic methods in forensic analysis was now a practical possibility. The later coupling of Raman and infrared spectroscopic methods with a microscope enabled smaller, finer samples to be tested non-destructively, an advancement that allowed for greater strides in providing chemical identification data to be achieved. The first successful coupling of the two technologies was achieved by Michel Delhaye and Paul Dhamelincourt in the University of Lille, France, in 1976 (Chalmers, Edwards et al. 2012), and their achievement was found to be an almost instant triumph. The newly coined Raman microspectrometer was soon quickly and effectively put to work investigating fragments from oil paintings, and analysing mediaeval manuscripts in museum collections under the direction of Bernard Guineau (Guineau, Lorblanchet et al. 2001), and ushered in a new age of practical Raman spectroscopy.

The next great advancement in the field of Raman spectroscopy came in the form of portable and handheld spectrometers that were capable of performing in-situ testing and analysis of samples. A series of studies from Michael D. Hargreaves et al (Hargreaves, Page et al. 2008) focused upon the effectiveness of these new portable Raman spectrometers, and helped pioneer an increased focus and innovation in this field. Since then, the latest advancements in Raman spectroscopy have been centred predominantly around the invention of new methodologies for sampling and testing specimens, aiming to better the accuracy and rapidity of detecting and quantifying molecular compounds.

The development and implementation of several advanced spectroscopic techniques such as Surface Enhanced Raman spectroscopy, Resonance Raman spectroscopy, and Spatially Offset Raman spectroscopy, along with the use of computerised, chemometric software, and a continual focus on reducing and removing fluorescence effects in samples and increasing sensitivity, reproducibility, and accuracy have also been prominent modern advancements (Das and Agrawal 2011).

2.2 Theory

Raman spectra arise from the graphical plotting of the inelastic scattering of monochromatic radiation generated as a consequence of interactions with molecular vibrations. The principles behind Raman spectroscopy have been well studied and documented since Smekal first theorised it, and a number of renowned scholars have since been focused upon understanding and improving the known principles (Chalmers and Griffiths 2001) (Schrader 1995) (Long 2002) (Eliasson and Matousek 2007).

The decades of study and intense focus revealed the prominent requisite for Raman spectroscopy, that is for a molecular vibration to be Raman active there must be a change in polarisability present during the normal mode of vibration. Furthermore, it is understood that the irradiation of a molecule with a laser or other monochromatic light source will always result in two types of light scattering, namely, elastic Rayleigh scattering and inelastic Raman scattering. The difference between these two forms of scattering, is that in the elastic scattering, there will be no apparent change in photo frequency and no appreciable change in the wavelength or energy or the light. The opposite is found in inelastic scattering, where there will be a measurable

shift in the photo frequency due to excitation or deactivation of particular molecular vibrations, where a photon may lose or gain energy (Kaur 2006).

When monochromatic light of a particular wavelength (λ) strikes a sample, the light is scattered both elastically and inelastically in all directions. While the majority of this scattered light will be elastic, a small percentage (approximately 1 part in 10^6) will be inelastic. This elastic light will have its wavelength changed by a measureable amount, either increased ($\lambda + \lambda_v$) or decreased ($\lambda - \lambda_v$) by an amount that corresponds to the sample's Raman active vibrational mode wavelength (λ_v). It is this change that is measured and commonly referred to as the Raman Shift (Edwards and Chalmers 2005).

The Raman shift generated may be either positive or negative relative to the unchanged, elastic wavelength; known as Stokes or Anti-Stokes respectively. In conventional Raman spectroscopy it is the positive Stokes-shifted Raman bands that are measured, predominantly as they are known to have a higher intensity and to be involved in transitions from an upper excited vibrational energy level undergoing vibrational transition to a lower vibrational energy level (Schrader 1995). A simple Raman scattering spectrum, such as that of Cocaine HCl shown below in Figure 1, will then be produced by measuring the light shifted to lower frequencies (longer wavelengths) and to higher frequencies (shorter wavelengths) corresponding to each of the unique vibrational modes present in the molecule (LaPlant 2010).

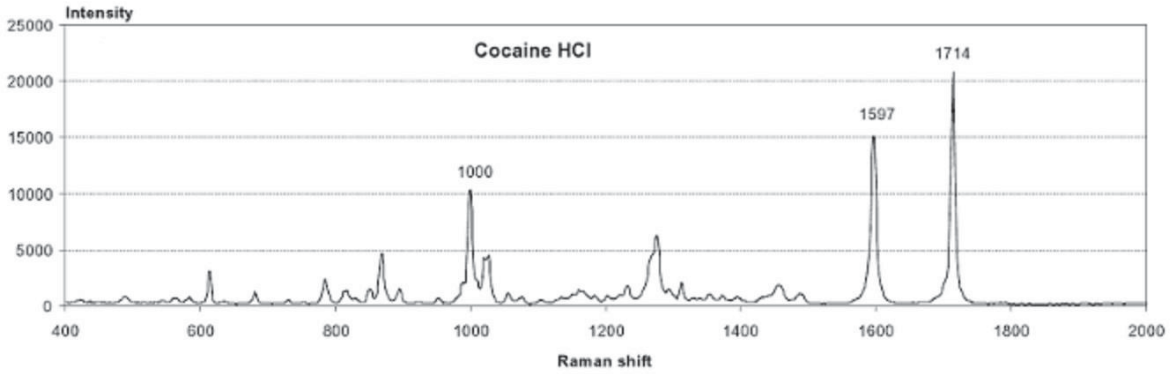

Figure 1 - Reference Raman spectrum of Cocaine HCl (Smith 2004).

In Figure 2 below, a simplified schematic of a conventional Raman spectrometer is shown. The sample being analysed is found at Point F, where the monochromatic light from the laser interacts with the vibrational modes and initiates the Rayleigh and Raman scattering of light. A filter then reduces the amount of light being transmitted to ensure that only the positively shifted inelastic scattering is allowed to reach the detector, producing an optimised Raman spectrum as a result.

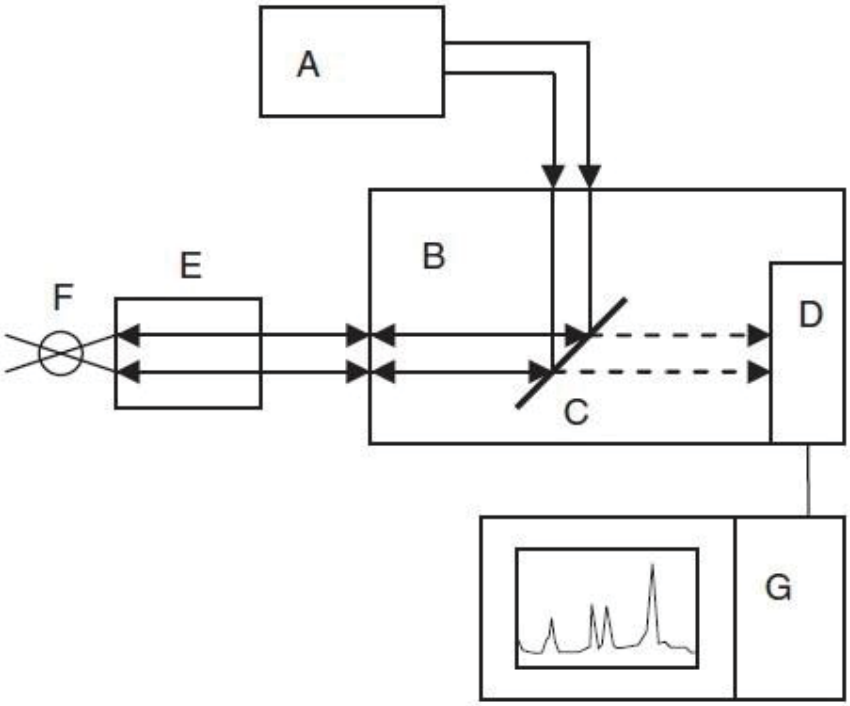

Figure 2 - Schematic of a Raman scattering setup consisting of a laser (A), Raman system (B), filter for Raman scattered light (C), charge-coupled device detector (D), microscope (E), sample (F), and computer monitor (G). Solid arrows indicate the direction of backscattered laser light, while dotted arrows indicate the direction of Raman scattered light (Elshout, Erckens et al. 2011).

Since the amount of inelastic Raman scattering that arises from irradiation is so small when compared to the elastic Rayleigh scattering, there is a distinct need to remove the interference. Traditionally, expensive double or triple monochromators were used to remove the excess inelastic light, however, modern Raman spectrometers are now more commonly fitted with holographic filters that remove interfering peaks and increase the accuracy of the analysis (Bartick 2002).

The accuracy of Raman spectroscopy in identifying particular molecules is predominately based upon the truism that each unique compound will have a unique vibrational spectrum. This

spectrum is dictated by the number of chemical bonds present, and the strength of the bonds (Chalmers, Edwards et al. 2012). The complex structure of most illicit substances, including that of cocaine and amphetamines, create distinct, and largely unique spectral profiles, allowing the identification of drugs of abuse to be a relatively simple task. Accurate identification is often a simple task of comparing collected samples from specimens with a digital library of reference spectra and standard spectra (Das and Agrawal 2011). While there will naturally be similarities between families of synthetic drugs with similar structures, such as 3,4-methylenedioxy-methamphetamine (MDMA) and cathinones, studies into the accurate identification of reference and seized samples have shown this similarity to be only a minor and ineffectual issue (Stewart, Bell et al. 2012).

Similarities between Raman and Infrared spectroscopy can be drawn, with both being vibrational spectroscopic methods, however it is known that the two techniques provide complimentary information. While the Raman shift peaks measured are based upon the change of electron polarisation, infrared spectra are obtained from incident light that is absorbed as a result of increased vibration in molecular dipole moments. This vital difference in technique means that the complimentary information can be obtained from samples. For example, strongly polar bonds, such as those found in carbonyls, appear far weaker in a Raman spectrum than in an infrared, while skeletal bands, such as unsaturated hydrocarbons will show far stronger in the Raman spectrum than in an infrared. By using the two techniques together, it is possible to achieve a complete vibrational profile of a chemical structure.

While the techniques together can produce a complimentary and more comprehensive identification of many compounds, a singular technique is often adequate in analytical analyses. There are known advantages to using Raman spectroscopy over infrared spectroscopy, with the most often cited being minimal requirement for sample preparation, convenient analysis of a solute in water, and the ability to sample through glass and plastic materials without interference (Bartick 2002). These are only a few examples indicating the most practical advantages of Raman spectroscopy, which have led many spectroscopists to believe that Raman spectroscopy may possibly render infrared analysis obsolete in forensic casework.

2.3 Sampling Techniques & Experimental Considerations

Historically, experimental methods involving Raman scattering have always shown great potential for the analytical investigation of illicit substances. However, in the early stages of their inception, these methods often ran afoul of issues that diminished their effectiveness and use in practical applications. Problems regarding low signal levels, overwhelming fluorescence emissions, and a lack of higher power laser sources with variable wavelengths meant that many experimental considerations had to be developed and understood if the best possible results were to be obtained. It is these experimental considerations that will be examined and detailed in this chapter, along with an explanation of why their optimisation is paramount in the development of any successful Raman spectroscopic method.

Of critical importance, is that the sampling techniques and experimental considerations of a method be adaptable and applicable to a wide range of possible variances. Differences in circumstances, whether that be stable conditions within a forensic laboratory, a dynamic

environment such as a clandestine laboratory or crime scene, as well as variations in sample forms, sizes and morphologies, all cause interferences that must be considered and accounted for.

With the Raman Effect being predominantly a weak scattering process, successful measurements rely upon an efficient sampling geometry and collection optics (Hendra 2002) (McCreery 2000). One of the most prestigious and often cited advantages of Raman spectroscopy, is that there is minimal sample handling and preparation required for successful analysis of a sample, particularly in comparison to that of infrared spectroscopy (Smith and Dent 2005) (Edwards and Chalmers 2005). A second, and less stated advantage however, is that since glass is a relatively weak Raman scatterer, samples can easily be mounted, contained, and held in place by glass cuvettes, capillaries, containers, or simple microscope slides, enabling secure and easy examination of a variety of samples (Smith and Dent 2013). This greater degree of freedom enabled in typical Raman spectroscopic methods offers a distinct advantage over other forensic techniques. Similarly, water is also known to be a relatively weak Raman scatterer, meaning that many water-based liquids, and samples contained within such liquids, can be easily analysed without the need for complicated extraction procedures or pre-treatment prior to examination.

While these advantages in containing and mounting samples for examination are effective and important, there are a number of additional considerations that must also be taken into account to achieve meaningful, representative, and high quality Raman spectra. These factors can ultimately control the level of quality obtained from a single measurement, and include factors such as the laser power, excitation wavelength used, and differences in the relative band intensities found within spectra (Socrates 2004).

The intensity of any band within a Raman spectrum is dependent upon the laser power used to obtain it, and for Stokes scattering, it is also proportional to the wavelength of the excitation laser used. In the absence of any fluorescence or resonance effects, the lower the wavelength of the excitation laser, the more intense a sample's Raman spectrum will be (Smith and Dent 2005). The result of this relationship, is that by using a lower excitation wavelength, more intensive and optimised series of spectra can be obtained, thereby creating more accurate results for both identification and quantification. A study by Sands et al. best illustrated the effects of utilising a lower excitation wavelength. Results from the study into the detection of narcotics revealed that not only did a 244 nm excitation laser enhance the band intensities of the spectra when compared to higher wavelengths, but it also significantly reduced fluorescence from samples of impure heroin and cocaine, allowing for a far greater level of accuracy to be obtained throughout the experiment (Sands, Hayward et al. 1998).

Another prominent effect regarding the excitation wavelength used is that fewer compounds absorb strongly at wavelengths longer than 750 nm, which aids in greatly reducing fluorescence emissions from samples (Hargreaves 2011). Due to this effect, the most commonly employed wavelengths for Raman spectroscopic analysis are generally 786 nm and 1064 nm, however commercially available instruments are commonly constructed with either a 780 nm or 830 nm excitation wavelength. Typically, the use of 785 nm excitation lasers are recommended for accurate experimental results, as it has been shown to give optimal balance between a longer wavelength reducing fluorescence emission, and a shorter wavelength providing more optimised Raman scattering (Tedesco and Slater 2000).

While the wavelength used in Raman spectroscopic analysis is important, so too is the appropriate application of the laser power. In absence of other experimental considerations, a greater laser power will result in a more optimal signal to noise ratio and a cleaner overall spectrum. However, the use of a higher laser power and density can lead to damaging results. If the laser power is set too high at the point of focus on the sample, degradation can occur, usually in the form of burning, dehydration, or polymorphic phase transformation (Hargreaves 2011). This potential destruction of samples can have catastrophic consequences in sensitive forensic investigations, or analyses where only a small sample mass is available.

A final experimental consideration remains in a spectrum's relative band intensities. A recorded single-beam Raman spectra is, in fact, a convolution of the sample's unique Raman spectrum and an instrument's response function, rather than an exact reading of the sample itself (McCreery 2000). The particular response function of an instrument will be dependent upon many instrumental components and variables, meaning that the relative intensity bands within a recorded Raman spectrum of the same sample will likely differ markedly when recorded on separate instruments. While not paramount to the success and accuracy of an experiment, this consideration must be taken into account, signifying that some differences between reference spectra and experimentally obtained spectra should be expected, but also showing that standards and samples should always be examined on the same instrumentation for accurate quantitative analysis.

While these experimental considerations can all be adhered to and referenced to produce the most accurate and optimised possible results, there is another series of considerations within the

sample and sampling methodologies used that must also be taken into account. These considerations include fluorescence effects, polarisation and orientation of the sample, and possible self-absorption of the sample.

The emission of fluorescence by a sample remains the greatest obstacle to successful Raman spectroscopic analysis of illicit and counterfeit drugs. Often, high concentrations of bulk samples have a low absolute level of Raman scattering, which commonly results in problematic level of fluorescence being emitted. This means that samples which would, under normal circumstances not be regarded as fluorescent can still have significant fluorescence backgrounds when subjected to analysis by Raman spectroscopy, in which high intensity excitation, good light collection efficiency, and sensitive detectors effectively create extremely sensitive fluorescence spectrometers. What is more, while the target compound and any possible excipients might have low fluorescence yields, the smallest trace of fluorescent impurities can still cause problems.

Theoretically, removing the fluorescing impurities would remove any issue, however the practical implementation of this theory requires extensive, and costly, clean-up procedures that are often too impractical to employ. For this reason, several alternative methods have been described, including variation of the excitation wavelength used, or by using enhanced Raman spectroscopic methods such as Spatially Offset and Surface Enhanced Raman spectroscopy. One further approach has also been described in the use of pulsed excitation and gated detection. The use of Kerr gated fluorescence rejection in studies of street cocaine samples was found to be incredibly effective, yielding excellent quality spectra with greatly reduced fluorescence, however with such a high cost in building and implementing the systems, and the overall

complexity of their use, the method is yet to be either widely or commercially implemented (Bell, Burns et al. 2000) (Littleford, Matousek et al. 2004).

Polarisation and the orientation of the sample and instrument will also have a dramatic effect on the quality of the spectra obtained during an experiment. The many optical components within a Raman spectrometer, particularly the sensitive gratings, can induce a degree of polarisation anisotropy into the system, which can result in a number of differences in the relative band intensities between spectra (McCreery 2000). Similarly, effects induced from the molecular orientation within the sample will also bring about marked differences in the relative band intensities between subsequent spectra. For a truly optimised method to be employed, both these polarisation and orientation effects must be taken into account and minimised as best as possible, including the use of a polarisation scrambler within the spectrometer, or by simple rotation of a sample between consecutive measurements to randomise the generated orientation effects.

Of equal concern to these effects is the sample size and possibility of self-absorption of the sample. The sample size able to be examined in Raman microspectroscopy can be as small as ca. 1 μm^3, and while this can be beneficial for certain detection and identification studies, it can also introduce a false representation of the sample's composition. Furthermore, with Fourier Transform Raman spectroscopy, the analysis of aqueous solutions can suffer from self-absorption in measurements, occurring when the absolute frequency of a particular Raman band coincides with a NIR absorption band within the sample, leading to selective attenuation of the Raman scattering (Everall 1994).

The various experimental considerations to be reviewed are not solely limited to sampling and spectral acquisition. The use of data pre-processing prior to the application of chemometric systems is known to have a large effect on the quality of the spectra analysed, resulting in large difference in the final quantitative values calculated. Currently, three common data pre-processing methods exist, namely; Cosmic Ray Removal, Noise Filtering, and Normalisation (Renishaw 2006), however various more steps are often similarly employed.

Cosmic rays are high energy particles that can randomly impact upon the charge coupled device detectors commonly used in Raman spectroscopy. When this occurs, a spectrum will exhibit additional, unrelated sharp peaks that can obscure and alter the final spectrum obtained and adversely affect a chemometric model. These additional cosmic ray features are usually removed by performing additional spectral accumulations, subsequently taking the average of each recorded spectra data point. While effective, this method is time consuming, and so alternatively the method of Nearest Neighbour Comparison can be utilised, providing faster processing while maintaining band structure integrity.

Noise filtering uses principal component analysis reconstruction to remove data variance not attributed to real or significant data within the spectra. The use of this technique means that filtered data will have significantly lower noise, resulting in beneficial chemometric processing and accuracy in predicted values. This technique is an essential step for the analysis of illicit drug samples, where higher levels of impurities and fluorescence will usually create significant noise in a spectrum.

A final pre-processing step commonly seen as a necessity is normalisation. Due to local variations and disturbances that can result from Raman spectroscopy experiments, the aim of normalisation is to remove intensity variations not arising from compositional changes in the sample (Renishaw 2006), and attempting to correct for scaling effects of all the variables while separating and retaining the properties of interest from those arising from interfering systematic errors.

If all the aforementioned experimental and sampling considerations are noted and accounted for, Raman spectroscopy will enable accurate, sensitive, and discriminatory identification and quantification of a multitude of drug samples in a variety of matrices with little or no interfering fluorescence emission or other effects.

2.4 Applications in Illicit Drug Detection & Quantification

The last several decades of technological and methodological advancements paved the way for a myriad of studies relating to the application and successful utilisation of Raman spectroscopy for the detection, identification, and quantification of illicit drugs of abuse and illicit substances. Studies and research by prominent academics such as Ryder, Hargreaves, Eliasson, Matousek, and Chalmers, to name just a few, have been instrumental in providing reliable and scientifically accurate evidence into the accuracy, sensitivity, specificity, and versatility of Raman spectroscopy, and have been highly valuable in championing its use and further applications in forensic analysis of illicit substances and drugs of abuse.

Raman spectroscopy's ability to provide rapid, non-destructive and unambiguous identification of samples with only the most minor of sample preparation or adulteration means that the technique has great potential in many forensic toxicological practices (Salzer 2012). In theory, and in practise, Raman spectroscopy has been shown to be useful as a screening method identifying illicit drugs of abuse in both individual and bulk samples, as a safe identification method for drugs and precursor chemicals in clandestine laboratories, and as a method for the in situ screening of smuggled and trafficked drug samples (Chalmers, Edwards et al. 2012).

Further laboratory based Raman spectroscopic methods and instrumentation increase the overall range of advantages that are not commonly present in other analytical techniques, including an optimised signal-to-noise ratio through the use of cooled, charged-coupled device detectors, high resolution from footprint spectrographs, automated sampling, and a rapid production of results due to the minimal amount of sample preparation required prior to analysis (Chalmers, Edwards et al. 2012). One further advantage that is present both for laboratory analysis of samples and in situ investigations is the ability to identify substances through the use of digital library comparison. The correct identification of a substance is based upon the molecular structure and characterised by a unique vibrational spectrum. By using an expansive digital library of collated standard spectra and corresponding known identities of compounds, direct comparisons with the spectrum of an unknown sample and a known standard can be made, allowing for simple and accurate identification. A secondary advantage of using a digital library, is that quantification using relative band intensities is also possible, allowing for greater determination of a substance and it's possible hazards (Chalmers, Edwards et al. 2012).

The powerful classification ability of Raman spectroscopy not only allows for the identification of illicit substances, but it has also been shown to be capable of distinguishing the type of drug present in a sample, such as whether a substance is cocaine hydrochloride (the more common powdered common) or freebase cocaine. This differentiation is possible by comparing relative band intensities present within a sample's spectrum, allowing for a highly thorough and complete analytical investigation to be carried out (West and Went 2011).

With Raman spectroscopy's ability to non-destructively detect and identify drugs of abuse in both homogenous and heterogeneous samples, particularly down to the nanogram and pictogram ranges, it is a technique of great importance to customs and law enforcement agencies (Chalmers, Edwards et al. 2012). This ability to detect even the most miniscule of samples, along with the minimal amount of sample preparation required for successful analysis, makes Raman spectroscopy one of the premier techniques for first-pass analytical screening and identification in a number of forensic and toxicological scenarios. Similarly, with the ability to capture unique characteristics in digital spectra, the majority of illicit substances, precursors, and explosives can be easily identified and differentiated.

Although the sampling size required for Raman spectroscopic analysis is very small, there is a distinct limit. Typically, the minimum size of samples is in the order of 1x1x5 μm, equivalent to a sample mass of only 5 pg (Chalmers and Griffiths 2001). It is the ability to narrowly focus the lasers, typically to between 10-100 μm, though reportedly to as low as 1 μm, that allows the identification of complex, microheterogeneous samples to be easily possible (Bell, Beattie et al. 2004). Furthermore, with an extensive catalogue of laser wavelengths and detector types

available, Raman spectra of suspected samples can be obtained throughout the range of 400 to 4000 cm^{-1}, which is the usual range in which Raman active normal modes of vibration for most organic molecules and drugs of abuse will appear, but it is also possible to record Raman spectra to much lower wavenumbers, allowing for complex heterogeneous mixtures to be fully analysed. These two impressive features and variabilities mean that great potential for the examination of both individual components and complete complex mixtures.

The potential of these advantages has been fully utilised in the advent of Composition Profiling; an analytical technique of great importance and prominence that can provide highly detailed information of a complex sample, allowing particular elements to be distinguished from other similar specimens, as well as enabling discrimination and determination of drugs, possible excipients, and exact ratios of the drug to it's possible excipients (Chalmers, Edwards et al. 2012). The benefits of composition profiling are well documented and immense. By allowing exact matches between different samples to be accurately attributed to a common origin and supplier, linkages between drug distribution networks can be identified, traced, and utilised by law enforcement agencies. An experimental study documented by Bell and Burns et al in 2000 demonstrated the effectiveness of Composition Profiling, documenting periods where law enforcement agencies were successful in seizing shipments of illicit substances, and using composition profiling to illustrate the presence of a greater commonality in the constitution of seized samples, indicating a wider distribution chain than previously anticipated (Bell, Burns et al. 2000). Since the study, a number of important experimental studies have been put into place using composition profiling, with the technique now being embedded into routine examination methods within forensic laboratories (Chalmers, Edwards et al. 2012).

Of special interest in this route of forensic investigation is the ability for modern Raman spectroscopy to detect and identify a suspicious substance that is held or concealed within a number of mediums. It has been noted in previous reviews that Raman spectroscopy provides the ability to record spectra of seized pharmaceutical samples that are encased either within evidential bags or their original containers. This process can occur either in a laboratory or at the scene of the seizure, thereby eliminating the need for a sample to be transported, opened, and handle in a qualified analytical library with no apparent loss of spectral quality (Eliasson and Matousek 2007). As well as allowing for in situ examination of samples, this process also has the advantage of being a more efficient process, reducing the cost and processing time, and alleviates any possible questions over the integrity of the methodologies applied and the preservation of evidential material. There are two main techniques capable of achieving quality results in this manner. The first, Spatially Offset Raman Spectroscopy (SORS) is an emerging technique that has gained increased focus of late due to its rapidity, ease of use, and the successful trials of the INSIGHT100; a table-top container-screening device used at security checkpoints in airports, government buildings and other passenger hubs (Loeffen, Maskall et al. 2011). The second method has come to be known as Depth Profiling, and is applicable to optically transparent samples, in which the composition of a mixture can be determined as a function of depth by successively focusing the excitation laser deeper into the sample matrix, and in doing so, recording depth-characteristic spectra (Everall 2000). The specific requirements, considerations, and accuracy of both these techniques will be discussed in later chapters of this report.

One final note on the suitability of Raman spectroscopy for the detection and identification of illicit substances is the ability to overcome the interference generated from fluorescence emission. The varying excitation laser wavelengths applicable in Raman spectroscopy, typically those of 785, 830, and 1064 nm, allow for a plethora of samples, particularly those which include complex mixtures or coloured matrices, to be easily analysed without the need for expensive equipment or potentially destructive sample preparation methodologies.

As detailed, Raman spectroscopy clearly has a profound number of practical advantages that make it a first choice technique for the rapid, non-destructive detection and identification of drugs of abuse, counterfeit pharmaceuticals, and explosives, but it is also capable of accurate quantification as well. It is already known that Raman scattered band intensities are, to a first approximation, linearly proportional to the number density of species responsible for the band (Chalmers, Edwards et al. 2012). From this simple relationship it can be seen that the normalised band intensities, or the relative height of area ratios, obtained from a samples Raman spectrum, can then be measured and used for quantification. The increasing advancements in technology have provoked the coupling of Raman spectroscopy systems with multivariate data analysis techniques, so that full spectra, and regions of spectra, can be accurately and autonomously identified, measured and quantified.

The employment of modern chemometric software and programming enables the development of complex quantitative calibrations rapidly after usual Raman spectroscopic examination, and can further provide visual classifications of a component's presence, as well as being able to discriminate between individual sample types within a set of similar samples. These powerful

advantages have led to the quantitative analysis of quality and counterfeit pharmaceutical dosage forms to become a widely accepted practise, however it is only in the recent years that the same has occurred for drugs of abuse (Sasic and Ekins 2007).

Traditionally, methods for quantitative analysis of samples have always been more complex than for identification alone. Typical quantitative analysis methods often involve complicated sample preparation and the use of potentially dangerous internal standards to correct for possible changes in signal intensity from small variations in experimental parameters. The use of chemometric software is a sophisticated way of circumventing these problems, ensuring that the most accurate possible results are obtained.

In complex mixtures, such as those typically found in street drug samples where additives and adulterants have been used to bulk the drug, it is vital that spectra which reflect the entire sample's composition are obtained, ensuring that minimal, if any, subsampling occurs (Chalmers, Edwards et al. 2012). The small focal objective used in a typical Raman probe means that the spectrum recorded for a single point in a specimen will often be microheterogeneous in contrast to the overall composition. While this factor may be useful for the identification of a single constituent in an overall more complex sample, it will often cause significant issues when trying to acquire data that accurately represents the overall sample composition.

There are a number of effective methods for overcoming this erroneous sub-sampling effect, however most require either extensive sample adulteration or significantly expensive equipment. One of the simplest methods, is to inspect a larger variety of positions within the sample matrix,

thereby improving the standard deviation in the measured signal by increasing the number of independent points interrogated (Bell, Beattie et al. 2004). For visible and far-red measurements, other methods also exist, such as commercially available fibre optic probes which are specifically designed to probe a large area of a sample and reduce sub-sampling issues while maintaining efficiency, however the majority of these probes are costly and have currently found limited application (Wikstorn, Lewis et al. 2005).

An alternative approach for circumventing sub-sampling effects within heterogeneous solids has been devised by Katainen et al in previous experimental research, however it necessitates the dissolving and adulteration of the sample. In the study, solid mixtures of amphetamine sulfate were dissolved into an aqueous acid solution, creating a homogenous sample, with a fixed amount of sodium dihydrogen phosphate added as an internal standard (Katainen, Elomaa et al. 2007). While this method allowed for the negative effects of sub-sampling to be eliminated, and ultimately enabled the amphetamine content of each mixture to be measured, the need to dissolve the solid samples prior to analysis greatly reduces the prominent advantages of using Raman spectroscopy, and it also requires adulteration of the sample and parcel which would undo the work championed in this research.

Katainen's study does illustrate one important consideration when developing quantitative methodologies. Quantification of the amphetamine content of each solid was calculated by either directly recording the ratio of peaks heights corresponding to the drug and the internal standard, or indirectly by constructing a multivariate partial least squares calibration model. While both

methods were shown to give results of sufficient accuracy for routine forensic casework, there are known and distinct advantages to the use of the more sophisticated multivariate technique.

The development of modern multivariate techniques has largely made the traditional, manual calibration based methods of quantification almost obsolete. Chemometric techniques allow for a large number of Raman spectral data to be analysed autonomously and simultaneously, extracting useful trends from a multitude of complex variables with greater accuracy and efficiency than manually possible. Similarly, chemometric methods are capable of easily analysing the entirety of a spectrum, and not simply individual Raman bands, so that every small change within collected spectra can be fully considered (Renishaw 2006). Despite the increased work load associated with generating a chemometric system, it offers the main advantage of a lower inherent error being present in the final information, thereby making all calculated results more accurate, as well as quicker and simpler to calculate (Renishaw 2006).

The use of multivariate data analysis methods to aid and improve the quantification of substances of abuse has been a critical advancement in the success of Raman spectroscopic methods. A vast array of varied processing methods exists, and while each has been proven to be successful, there are two methods that most commonly draw focus. Principal Component Analysis (PCA) and Partial Least Squares Regression (PSL-R) are the most commonly used methods that have been successfully used in the quantification of drugs of abuse, yielding rapid, accurate results in a number of prominent studies, notably by O'Connell, Ryder, and Durkin et al, whose studies serve as strong advocates for their use (O'Connell, Ryder et al. 2010) (Durkin, Ediger et al. 1998). One study of true relevance is that of Fenton, Tonge et al who showed promising results

for using partial least squares in the quantitative analysis of simulated illicit street drug samples (Fenton, Tonge et al. 2011).

The underlying method behind PCA and PLS regression is the creation of a calibrating model from a set of spectra obtained from various known concentrations, along with a second set of spectra taken from samples of known concentrations, which are used to validate and test the constructed model. In both methods, the initial stage of creating and validating a calibration model is the most crucial, as this is the stage in which the relationship between the spectra and the component concentrations are established (Haaland and Thomas 1988). It is from this relationship that predictions of unknown concentrations are calculated, and so the upmost accuracy when engineering the reference samples is crucial.

In order to utilise either of the multivariate techniques effectively, and to ensure that the maximum possible accuracy in later predictions is achieved, it is common practise to employ the use of pre-processing methods (Chalmers, Edwards et al. 2012). The use of the pre-processing techniques prior to undertaking any form of multivariate analysis has become a critical stage in most research projects, enabling reductions or removal of variances and outliers with data sets that appear to be irrelevant or unnecessary. With the success of PCA and PLS regression based upon the accurate establishment of a direct linkage between spectral peaks and known concentrations, it is critical that these variances be removed so they do not introduce damaging inaccuracies into the constructed model. The ability to reduce and remove these variances to increase the overall accuracy of calculations is an integral reason why these modern chemometric techniques have superseded manual quantitative methods.

A final, and extensive example of the accuracy and usefulness of these multivariate data analysis methods was performed by A.G. Ryder, G.M. O'Connor and T.J. Glynn in 1999 on cocaine, heroin, and MDMA mixed with simple foodstuffs (Ryder, O'Connor et al. 1999). In the study, Partial Least Squares Regression was used to identify and quantify the illicit substances, with detection of the drugs shown at levels of ca. 10% by mass. Additionally, analysis of data collected from a series of twenty mixtures of cocaine and glucose, of concentrations from 0-100% by weight of cocaine, gave a calibration model with a root mean square error of prediction (RMSEP) of only 2.3% overall. Extension of the experimental method to ternary mixtures of cocaine, caffeine, and glucose gave similar results, with a calibration model constructed with only a RMSEP of 4.1% overall. Further extension by Ryder to eighty-five samples diluted with several different combinations of materials showed that when PCA was utilised while restricted to only the most intense peaks in the obtained Raman spectra of pure drugs, discrimination between cocaine, heroin, and MDMA mixtures was easily possible, even with only 2-3% of the original spectral data used in the analysis (Ryder 2002).

Though a decade old, the results obtained in these studies provided powerful justification for the use of both Raman spectroscopy and multivariate analysis methods. Furthermore, the reliance on specific sampling methods, data pre-processing techniques, and the continued prevalence of principal component analysis and partial least squares regression, serve to prove how modern Raman spectroscopic methods can be effectively utilised in modern forensic analysis. Through these observations alone, it is clear why Raman spectroscopy has become a prominent technique for the detection, identification, and quantification of various drugs of abuse.

Chapter Three - Spatially Offset Raman Spectroscopy

3.1 Background

Although conventional Raman spectroscopy is able to offer a vast range of practical advantages over other analytical and spectroscopic techniques, limitations such as lower sensitivity and poorer spatial resolution created a need for more sophisticated, enhanced, and specialised Raman techniques. In the past two decades, several advanced techniques have been developed, with one of the most prominent and practically important new methods being that of Spatially Offset Raman Spectroscopy (SORS).

The origins of spatially offset Raman spectroscopy can be found in early subsurface studies into diffusely scattering samples. These studies date back to the mid 90's, with confocal Raman microscopy and time-resolved Raman spectroscopy used in probing a wide variety of different media, including notable work by J. Wu & Y. Wang et al. and C. J. H. Brenan & I. W. Hunter into suspensions of polystyrene spheres and milk respectively becoming benchmark studies for the emerging techniques (Wu, Wang et al. 1995) (Brenan and Hunter 1996).

With these early studies came a deeper understanding of the effectiveness of the time-resolved Raman approach, with its ability to isolate the Raman spectra of deep layers proven substantially. However, the complexity of the required instrumentation, and the high peak intensities associated with short-pulse lasers remained stoic obstacles to the techniques' mainstream acceptance and wider application (Matousek and Morris 2010). Research into overcoming these issues ultimately created the first instance of spatially offset Raman spectroscopy, as the focus

shifted away from the temporal properties of diffusely scattered photons, and instead addressed the spatially offset characteristics.

From this intense focus and research, the first SORS method was born, with the first initial demonstration reported in a 2005 journal article by P. Matousek & I. P. Clark et al., who investigated a two-layer sample composed of poly(methyl methacrylate) (PMMA) and trans-stilbene powder (Matousek, Clark et al. 2005). In this study, a simple two-layer sample composed of a 1 mm thick PMMA powder layer on top of a trans-stilbene powder sublayer was analysed throughout a series of different spatial offsets, the results of which can be seen in Figure 3 below.

A conventional Raman spectrum was initially obtained with zero spatial offset, while subsequent introduction of a non-zero spatial offset was seen to lead to a rapid decrease in spectral contributions from the PMMA surface layer. With an acquisition time of 100 seconds for each spectrum, and with an average laser power of 12 mW, it was found that for a spatial offset of 2 mm, the surface-to-subsurface relative Raman intensity was successfully diminished by an order of magnitude (Matousek, Clark et al. 2005).

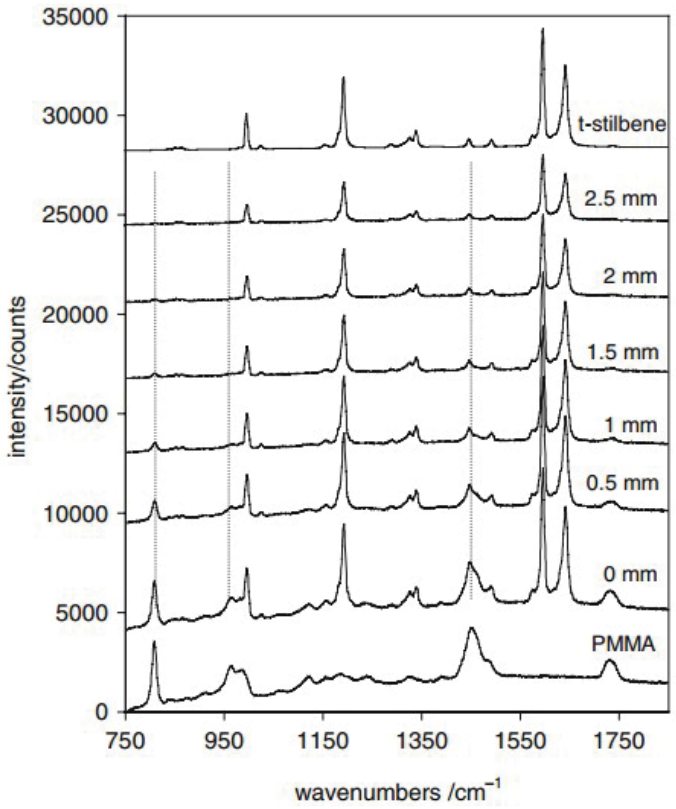

Figure 3: A series of SORS spectra collected from the two-layer system of PMMA and trans- stilbene powder, shown at different spatial offsets. The top and bottom spectra are standards of trans- stilbene and PMMA respectively for comparison, with all spectra offset for clarity (Matousek, Clark et al. 2005, Sasic 2008).

In 2006, a further variation of the successful SORS method was proposed by a collaborative research team led by P. Matousek at the Rutherford Appleton Laboratory in Oxfordshire (Matousek 2006). The new technique, named Inverse SORS, was found to permit greater depths of samples to be interrogated than was previously possible with conventional SORS, owing largely to an increase in sensitivity through the elimination of spectral distortion. Additionally, inverse SORS was also noted to exhibit far greater flexibility and adaptability, allowing for on-the-spot tailoring of experimental conditions to a sample (Matousek 2006).

Since the establishment and success of both methods, many subsequent applications for the SORS method have been proposed, including non-invasive Raman spectroscopy of bones (Schulmerich, Dooley et al. 2007), counterfeit pharmaceuticals (Eliasson and Matousek 2007), and various security screening processes (Eliasson, Macleod et al. 2007), including the successful creation and implementation of Cobalt's RapID and Insight100 range in many airports across the United Kingdom. Further research into new technologies and possibilities has also served to increase the accessibility and accuracy of base SORS methods, with greater enhancement of its already capable qualities made possible through the more contemporary Surface Enhanced Spatially Offset Raman spectroscopy (SESORS), a highly sensitive method that has been used to measure spectra through various thicknesses of bone (Sharma, Ma et al. 2013).

3.2 Theory & Practical Geometries

SORS is seen as a crucial new technique for the deep probing of sealed bottles, packaging materials, tissue samples, and a plethora of other biological and chemical samples. Its ability to counteract many of the obstacles of traditional Raman spectroscopy has made it an invaluable step forward for the interrogation of diffusely scattering media. While the underlying scientific principles behind the formation and collection of spectra from a sample are the same as in conventional Raman spectroscopy, there are a series of unique phenomena that enable the success of SORS.

The key principle behind spatially offset Raman spectroscopy technique is based upon the collection of a series of Raman spectra from the surface regions of a sample that are set distances

away from the point of illumination of the laser (Matousek 2006). Raman spectra collected in this way will be seen to exhibit a variation in relative intensities between the contributions from the surface and subsurface layers. These relative contributions can be numerically processed to yield the pure Raman spectra of each individual sub-layer (Matousek, Clark et al. 2005).

In the SORS technique, monochromatic light from a laser source will fall upon the sample, penetrating it with an exponentially decaying intensity to depths of up to a few centimetres (Olds, Jaatinen et al. 2011). As the photons propagate throughout the sample, their original straight trajectory from the laser source will be quickly converted to a range of sideways scatters, which will eventually result in complete randomisation of the photons' pathways through the sample (Das, Liu et al. 1997). Provided that the surface layer (the sample's packaging) is adequately thin, some of the propagated photons will reach the concealed, subsurface compound that is held within the container. When this has occurred, many of the photons will have been displaced sideways from the point of origin into the sample, creating a larger volume of diffuse light within the sample (Matousek, Clark et al. 2005). On average, the photons that are back-scattered from within the sample towards the container wall will emerge from the sample with a greater degree of sideways scattering due to their return journey to the surface. Therefore, it can generally be seen that the deeper a photon has travelled into a sample, the further it's offset from the initial point of illumination will be, and the more spectral information it will have collected. Collection of photons from greater spatial offsets will then tend to capture Raman photons that will have originated from a greater depth within a sample, thereby revealing a greater spectral profile of the concealed sample's sub-layers (Matousek and Morris 2010).

While the majority of excited photons scattering from the sample will tend to be elastic, Rayleigh scattering, with the light remaining at the original laser wavelength, a small percentage will be inelastic, Raman scattering. Consequently, careful collection of the inelastic Raman scattered photons at increasing offset will yield a bias towards the Raman signal of underlying layers. The Raman photons originating from the surface layer of a sample will also tend to decay rapidly with increasing offset from the point of illumination, predominantly as they have had less opportunity to travel sideways via scattering and path randomisation (Olds, Jaatinen et al. 2011).

These characteristics of scattered photons and spatially offset collection enable relatively pure spectra of a concealed subsurface to be obtained through a scaled subtraction. By completing a scaled subtraction of the initial and spatially offset position, namely, the spatially offset spectrum (containing information of the container wall and contents) minus the spot spectrum (which predominantly contains information of the container), a simple spectrum of the concealed compound can be obtained (Matousek, Clark et al. 2005).

For a simplistic two layer sample, which is most commonly found in the case of a container and its contents, scaled subtraction of the spectra acquired at two different spatial offsets, such as the zero and non-zero spatial offsets, will cancel the residual surface component to such a degree that it will satisfactorily render the pure subsurface spectrum (Matousek, Clark et al. 2005). However, for more complex multi-layered samples, the use of multivariate statistical data analysis techniques, such as Band Target Entropy Minimisation (BTEM), multivariate curve resolution (MCR), or Parallel Factor Analysis (PARAFAC) is often required to yield optimum

results (Buckley, Kerns et al. 2014). In both cases, the processes of obtaining and differentiating spectra can be automated, increasing the efficiency, accuracy, and rapidity of a chosen method.

The above method is not the only geometry that has enabled the collection of spot and SORS Raman spectra. Two additional methodologies are currently also in use, with each offering their own advantages and detriments.

The first alternate method is that of Inverse SORS, whose geometry was first introduced in 2006 and was founded upon utilising a ring-shaped source of illumination, rather than the conventional displaced spot illumination described in SORS (Matousek 2006) (Schulmerich, Dooley et al. 2006). Raman light in an inverse SORS geometry is collected through a central point, with a group of tightly packed fibres at the centre of the probe by binding their signals on a charge-coupled device (CCD) chip into a single spectrum (Matousek 2006). The laser probe beam is brought onto the sample in the form of a ring centred around the collection zone; leading to a complete reversal of the conventional SORS setup where Raman spectra are collected from rings while the laser is delivered at the centre of the probe.

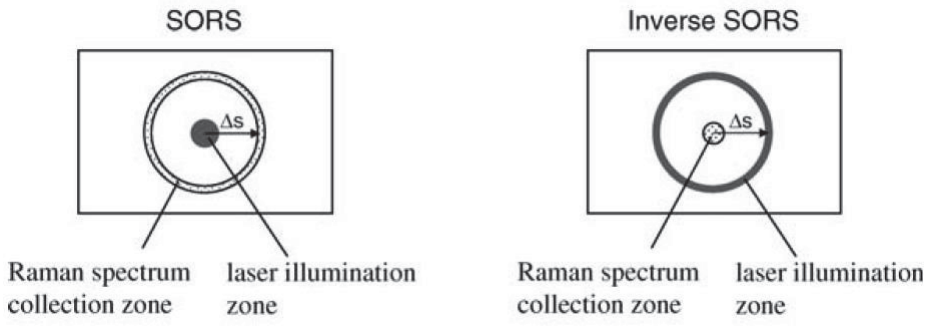

Figure 4 - Schematic diagrams of conventional SORS and Inverse SORS geometries, where Δs is the distance between the collection and illumination zones (Matousek 2006).

In inverse SORS, the spatial offsets required can be generated and varied simply by changing the radius of the ring-illumination zone, which can be easily established through the inclusion of an axicon optical element positioned at different distanced from the sample (Mosier-Boss, Lieberman et al. 1995). By using an axicon to create a laser ring of illumination, an arbitrary number of spectra of different spatial offsets can be subsequently collected by simply altering the distance of the axicon from the sample. This allows for a single Raman spectrum with a SORS spatial offset equal to the ring radius to be collected and averaged.

With inverse SORS comes the potential to overcome the spectral distortions that are inherent with SORS instrumentation, while also allowing the excitation light to be spread over a larger area, thereby facilitating the use of higher laser powers and reduced acquisition times (Olds, Jaatinen et al. 2011). A further advantage of Inverse SORS is its simplicity and suitability for retrofitting on existing Raman microscopes as an 'add-on' feature. In such a case, there is only one main requirement for the system; that the laser beam delivery path to the sample be altered to enable a ring illumination. This allows for the Raman collection system, if fibre based, to remain unaltered (Matousek 2006).

A third and final geometry for SORS can be described as Tilted SORS. This methodology is accomplished simply by adjusting the angle of the laser beam entering the sample, enabling a laser beam to intersect the Raman collection zone placed below the surface of a container, as depicted in Figure 5 below (Chalmers, Edwards et al. 2012). An early study by Eliasson et al. was successful in demonstrating that such a configuration with a fixed spatial offset of 10 mm, and a laser beam angle of 45°, could effectively probe a wide range of both diffusely scattering and transparent containers (Eliasson, Macleod et al. 2007).

The use of this tilted geometry can be made compatible with probing of transparent containers with the added benefit of suppressing fluorescence from with the packaging material. This occurs simply because the laser beam will intersect the container material spatially offset and out of sight of the Raman collection system. Furthermore, when presented with a diffusely scattering sample, the configuration behaves entirely as a SORS device, with the laser photons rapidly losing their original directionality to enable the randomised pathways required. However, it should be noted that if fluorescence originates from the probed medium, it cannot be eliminated by these means.

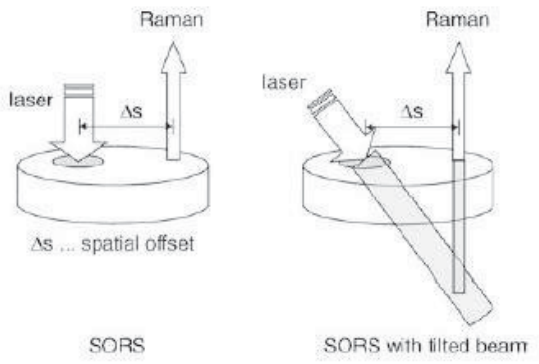

Figure 5 - Illustration of how tilting the incident laser beam facilitates simultaneous capability to probe transparent and diffusely scattering containers with a single fixed SORS geometry. (Chalmers, Edwards et al. 2012)

The general applicability and the selection of the SORS geometry is generally limited to the sample type being investigated. Samples that do not exhibit strong absorption, and samples that do not exhibit excessive fluorescence originating from the contents itself are generally optimal for the technique. For both of these restrictions, their effects can generally be reduced or eliminated by probing further using laser excitation in the near-infrared region of the spectrum (Chalmers, Edwards et al. 2012). In practical, experimental settings, the effects of fluorescence can be minimised by operating the SORS system with either a 830 nm or 785 nm laser excitation wavelength, thereby minimising the degree of exciting fluorescing electronic states while still permitting the use of effective CCD detectors. In specialised situations where fluorescence persists, it is possible to move even longer laser excitation wavelengths of 1064 nm and above, which can still yield beneficial results, as demonstrated by Hopkins et al. in their investigation of chemicals through physical barriers (Hopkins, Pelfrey et al. 2012).

3.3 Experimental Considerations

As well as the common experimental considerations and sampling techniques that must be considered for conventional Raman spectroscopic methods, a successful inverse micro-SORS method must include the careful consideration and optimisation of many unique experimental parameters, such as the refraction pattern of the axicon lens utilised, diameter of the laser ring established, as well as the optimum focal point and working distance of the optical elements within the system. Secondary considerations involving the choice of laser excitation source, and the experimental and pre-processing methods applied, will also create drastic changes in the quality of results obtained. These considerations, along with their effects are discussed below.

3.3.1 The Axicon

In a micro-SORS assembly as described in Figure 6 below, the axicon lens is arguably the centrepiece of the method. The 'fundamental' axicon system, as it is often described, consists of a combination of a focusing lens, such as those commonly found in microscope objectives, and a positive axicon lens, which will work together to produce an annular ring focus (Dickey 2014). Placement of the axicon close to the focusing lens will enable this annular focus due to the rotational symmetry of the system, with a focused ring of light produced upon the surface of the sample. It follows then, that the diameter of the ring will be linearly dependent upon the distance of the axicon from the sample (Matousek 2006). A desired ring size can be obtained simply by varying the distance of the axicon lens from the sample, either manually or by using a controlled positioning stage.

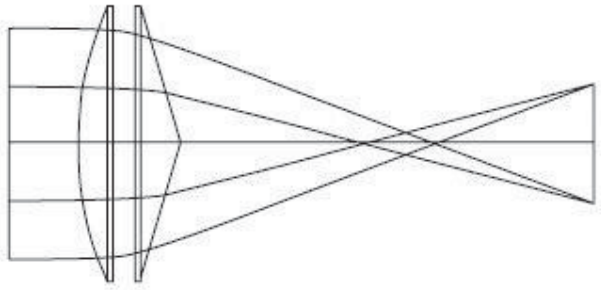

Figure 6 - A two-dimensional schematic detailing annular ring formation with a focusing lens and a positive axicon positioned after the focusing lens.

The radius of the ring formed can have a marked effect on the sensitivity and accuracy of the method being utilised. It has been previously shown by P. Matousek & I. P. Clarke et al. how the quality of the SORS spectrum obtained changes with the amount of spatial offset. As the lateral offset between the Raman collection point and the point of probe beam incidence (given by the radius of the ring) increases, there is a noticeable depreciation in the intensity of the Raman signals from the surface layer of a sample relative to the signal of the contents (Matousek, Clark et al. 2005). However, it is also noted that if the lateral offset is too great, there is notable depreciation of the Raman signal from the contents as well, and so an optimum offset must be found. This point of optimal performance will be dependent upon the base angle of the axicon being utilised, along with the initial radius of the excitation beam, and the distance from the axicon to where separation of the beam into a ring occurs.

One interesting point of reference however comes from the work of J. R. Maher and A. J. Berger, who studied the determination of ideal offset for SORS. In their work, it was found that while the SORS ratio of the signal from the concealed substance to the surface layer monotonically increases with spatial offset, the signal-to-noise ratio (SNR) does not. Furthermore, the pair

illustrated that there exists a specific spatial offset that yields the best SNR for signals originating from the bottom layer (the concealed substance) of a two layer sample. Accordingly, it was shown that a spatial offset closer to 0 mm produced an optimal SNR for strong Raman bands, while weaker bands required a greater spatial offset , suggesting that specific, optimal offset exist for different matierals (Maher and Berger 2010). Importantly, it should be stated that the analysis presented by Maher and Berger assumes that the illumination power and the collection area are both constants, independent of spatial offset.

A further point of interest for the axicon system illustrated is the depth of focus utilised when capturing Raman spectra from a concealed substance. While variation of the ring radius in an inverse SORS measurement can produce varying results, so too can the variation of the focal distance of the system. For conventional Raman spectroscopy, a defocused system has been shown to produce a substantial degree of relative ratio change between surface and subsurface layers in simple two-layer systems (Eliasson, Claybourn et al. 2007).

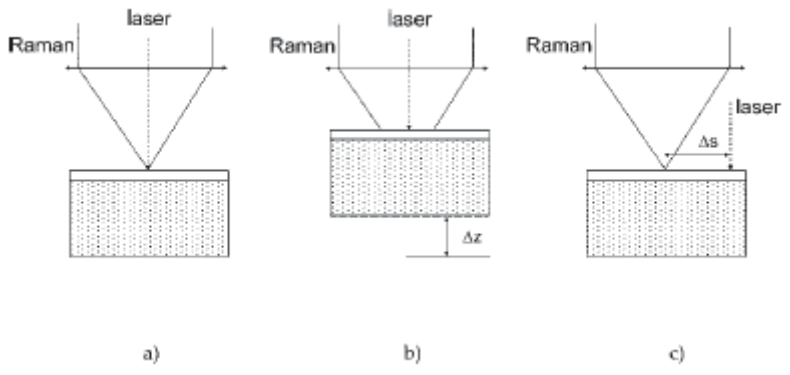

Figure 7 - Schematics of conventional backscattering Raman approach (a), the defocused Raman concept, where Δz indicates the displacement of the sample from the object plane (b), and the standard SORS method where Δs indicates the spatial offset (c).
(Eliasson, Claybourn et al. 2007)

In the study by Eliasson, Claybourn and Matousek, it was seen that simply locating the sample 12 mm closer to the Raman collection lens produced more favourable results, and while the results were not as clear as those obtained from a comparative standard SORS system with 5 mm offset, their observations provide an interesting potential for inverse micro-SORS methods. In an inverse micro-SORS system where the distance between the axicon and the sample's surface remains fixed, the focus and accuracy will depend upon the working distance of the microscope objective used; that is, the distance from the focusing lens to the sample's surface which will produce the sharpest possible image. Potentially then, defocusing an inverse micro-SORS system in a similar way to that described in Eliasson, Claybourn and Matousek's work should produce even greater results.

To establish the best possible degree of defocusing, the objective of the microscope system, the focal point, and the working distance must all be accounted for. On modern microscope systems, the level of enhancement of a sample will depend almost solely upon the objective used. A basic microscope objective is classified based upon its specimen magnification and its numerical aperture (NA) (Laikin 2006). The magnification power of the microscope is a simple term detailing the level of magnification achievable, with the greater power relating to a greater degree of magnification. The second value, the NA is a dimensionless number that characterises the range of angles over which the system can accept or emit light (Smith 2000). These two features are crucial in determining the useful microscopic range, depth of focus, and effective working distance of the system being employed.

While commonly given on the microscope objective being utilised, the NA of a system can be easily calculated using the equation below (Murphy 2001);

$$NA = n\,Sin\,\theta$$

Where n is the refractive index of the medium between the sample and objective, for air this is simply 1, and θ is equal to the half angle of the cone of specimen light accepted by the objective lens. It is seen from this equation, that the larger the half angle, the greater the NA of an objective will be. An interesting consequence of this, is that the greater the NA, the lower the depth of focus of a system, that is, the thickness of the optical section along the z-axis within which objects, such as samples being interrogated, are in focus. This relationship can be best expressed in the equation for the calculation of the Depth of Focus (Z) shown below (Murphy 2001);

$$Z = \frac{n \cdot \lambda}{NA^2}$$

Where n is the refractive index of the medium between the sample and objective, λ is equal to the wavelength of light in air, and NA is the numerical aperture of the objective lens. With the NA as the denominator, it can be seen that a greater NA produces a reduced depth of focus, which in turn limits the space in which an axicon lens can be placed to achieve the SORS effect. Careful consideration of the optimum NA and magnification is then twofold; while a greater power of magnification and NA will produce more sensitive, accurate results, its limited depth of field limits the size of the optical element which can be used to produce the required ring of excitation light. A compromise must therefore be found to achieve the greatest possible results, one which

allows for effective use of an axicon lens with the most optically appropriate microscope objective.

To help assess an appropriate objective, and the level of defocusing possible, the working distance of an objective can be considered. The working distance of a lens is a known distance, and dictates absolute distance from the front lens to the closest surface when in sharp focus, and so the appropriate working distance will indicate the vertical limits in which an optical element, such as an axicon lens, can be placed. Generally, the working distance of an objective will be noted upon the objective itself, and can be highly specific to the type and make of microscope objective being utilised, however one governing rule is that a greater NA will have a smaller working distance (Smith 2000). For the development of an optimised method, it is therefore better to consider the lower NA objectives first.

While these considerations are of critical importance for the microscope object, they need not be applied to that axicon lens. In the two component lens system, such as that encountered with the converging (convex) lens of a microscope object and an axicon, it can be shown that while the radius of the laser ring produced will be determined by the base angle of the axicon, the focal length of the system will be determined predominately by the converging lens (Veloso, Chuaqui et al. 2005). The reason for this effect can be shown in Figure 8 below, a two dimensional illustration of the refraction patterns occurring along with approximations of the focal points present for the system (Depret, Verkerk et al. 2002).

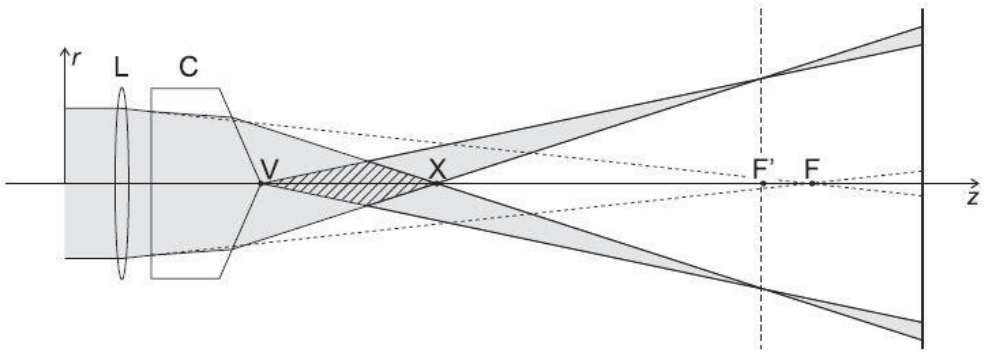

Figure 8 - Schematic representation of a converging beam passing through a converging lens, at L, followed by a positive axicon, at C. The vertex of the axicon is illustrated by V, with the point of first beam divergence into the ring form shown at X.

In a paper by Dépret, Verkerk, and Hennequin, (Depret, Verkerk et al. 2002), they use the above diagram to illustrate the effects of an axicon lens on a collimated beam. In the diagram, the focal point of the convergent lens is shown at F, while the optimal focal point of the ring from the axicon is found at F'. These two focal points are found to be approximately equal, allowing for careful focusing of the convergent lens and microscope object to be sufficient for effective use of the axicon lens.

At this optimum location, where F is found to be approximately equal to F', a ring radius of optimal focus (R_o) will be produced in accordance with the equation given below.

$$R_o = (n-1)(f-d)$$

Where n is the refractive index of the axicon, *f* is the focal length of the convergent lens, d is the distance between the two lenses, and α is the base angle of the axicon (Depret, Verkerk et al.

2002). In most practical realisations, including in Raman spectroscopic applications, the incident beams used are often produced by a laser, and thus are considered to be Gaussian beams. As the transverse expansion of a Gaussian beam is theoretically infinite, all the quantities in the above equation become indefinite. However, for large incident beams, those whose width is far greater than their wavelength, the geometrical approach described is seen to remain a good approximation (Depret, Verkerk et al. 2002).

While the above equation, and the noted focal points enable easy optimisation of experimental assemblies, it does introduce three more considerations into the parameters. As shown, calculation of the ring radius requires knowledge of the base angle of the axicon, the material it is composed of, and to some extent, the width of the incident laser beam.

The base angle of the axicon used in a particular experimental assembly can have a marked effect on the produced radius and focal point of the ring. As expressed in the equation below, the angle at which an incident beam of light is deviated from z-axis (θ) is largely dependent upon the base angle and the refractive index of the axicon utilised (Zhang 2008).

$$\theta = \sin^{-1}(n \sin \alpha) - \alpha$$

Where α is the base angle and n is the refractive index of the axicon. It can be seen that with an increase in the refractive index of the material, a noticeable increase in the degree of refraction is observed. Similarly, the same increase in the angle of refraction is noted with an increase in the base angle of the axicon. Together, and as independent factors, both these parameters can have a

marked effect on the size of the ring produced, with a greater value of θ producing a wider possible radius over a set distance. With base angles commonly ranging from 0.5° to 20°, and with a variety of materials and coatings including BK7 glass and UV fused silica available commercially, the choice of appropriate characteristics can be critical. For example, the use of an axicon with greater refractive index and less acute base angle can yield favourable results by allowing for a larger ring radius to be generated within a smaller available working space.

3.3.2 The Laser Excitation Source

A final important characteristic that should be considered when selecting the optimum conditions for SORS measurements is the width of the laser beam utilised. In a micro-SORS method, the incident laser on the lens system will be shaped by the microscope objective, with the spot diameter entering the system defined by the wavelength of the light, defined by λ, and the numerical aperture, NA, of the objective utilised. The laser spot size, given as a diameter, d, is then calculable using an approximation as an airy disk, and the following expression (Zoubir 2012).

$$d = \frac{1.22 \cdot \lambda}{NA}$$

The use of this expression correlates with two important experimental considerations highlighted in the previous chapter on conventional Raman spectroscopy, namely the laser excitation wavelength used, and the laser power.

It is known that the observed intensity of any band within a Raman spectrum is dependent upon the laser power involved (Liang, Tse et al. 1993). In the absence of other considerations, a higher

excitation laser power will lead to a better, more refined signal to noise ratio and a cleaner spectrum. However, if the laser power density used is too high at the point of focus on the sample, degradation of the sample matrix can occur in the form of burning, dehydration and polymorphic phase changes (Hargreaves 2011). In the case of an inverse SORS method, the potential for degradation of the outer layer of a sample remains an important experimental consideration, and care must be taken to use a laser power and density appropriate for the matrices being tested.

In the absence of fluorescence and resonance effects, the wavelength of the excitation laser used in analysis will also have a marked affect upon the quality of the Raman spectrum obtained. Notably, the lower the wavelength of the excitation laser, the more intense a sample's Raman spectrum will be (Smith and Dent 2005). Practically, a lower wavelength has been shown to produce favourable results, with a reduction in fluorescence and enhanced resonance effects intensifying the Raman bands observed when using a 244 nm excitation wavelength in the detection of narcotics (Sands, Hayward et al. 1998).

Another noticeable trend with the wavelength used, is that fewer compounds absorb strongly at longer wavelengths of above 750 nm, which leads to noticeably reduced fluorescence in initial readings (Hargreaves 2011). It is for this reason that two of the most widely used wavelengths range between 785 nm and 1064 nm. Typically, the choice of a 785 nm wavelength is recommended for optimal experimental results, with this wavelength producing the most favourable balance between minimising fluorescence emission and maintaining accurate Raman scattering from the C-H fingerprint region (Tedesco and Slater 2000).

3.3.3 The Experimental Procedure

The choice of instrumentation, lens, and laser settings are not the only parameters that need to be considered. Specific changes in the number of acquisitions, spectral accumulations, exposure time, and the selection of a specified wavenumber range will all affect the quality of the spectra obtained from a sample.

The various instrumental parameters, including the number of accumulations and acquisitions completed when collecting a sample's Raman spectrum have all been shown to have a marked difference on the quality of the results obtained. Increasing the number of accumulations is a simple, yet effective technique for reducing the random noise inherent with a Raman spectrum (Lewis and Edwards 2001). To achieve the technique, the number of accumulations required is determined by the operator, with the software and instrumentation then proceeding to successively accumulate the desired number of spectra, adding each spectrum to an accumulating buffer on a pixel-by-pixel basis. In general, random noise will be greatly reduced by the square root of the number of spectra that are summed together (Lewis and Edwards 2001).

Additionally, the number of CCD acquisitions used in an experiment can also greatly improve the noted signal to noise ratio of the results. Increasing the integration time by combining the electrons from repeated acquisitions leads to an enhanced signal with greatly reduced noise (McCreery 2005) While both these techniques will aid in the collection of more sensitive and accurate spectra, they do drastically affect the run time required, reducing speed and efficiency.

A further technique for increasing the quality of a Raman spectrum is to increase the exposure time. Lengthening the exposure time allows for a prolonged integration time for each pixel within the computed spectrum, thereby improving the signal to noise ratio generated. Increasing the exposure time is now common practice, allowing for far better spectra to be obtained from weak Raman scatterers, while helping to maintain some of the efficiency that Raman spectroscopy offers (Wieboldt 2010)**.** It should be noted however, that the use of a longer exposure time does not enhance the Raman signal generated; it will only reduce the noise present.

Control of the aperture is another key parameter that has critical importance within inverse SORS methods. The aperture controls how much Raman signal is allowed to pass into the spectrograph and onto the detector, ultimately controlling the spectral resolution achievable. While in some Raman microscope systems, the use of a smaller aperture will enable confocal operation of the instrumentation, it is best in inverse SORS methods to use a larger aperture, thereby allowing for the collection of the further displaced Raman signals (Matousek 2006). In practicality, smaller apertures of between 10-25 μm will yield the highest rated spectral resolution of an instrument, while larger apertures of between 50-100 μm will give results with slightly degraded spectral resolution. Often, the slight loss in spectral resolution from the use of a larger aperture is insignificant, however experimentation with various aperture sizes is recommended for obtaining optimum results.

A final important parameter when collecting Raman spectra is correctly defining the spectra range to be analysed. The typical working range for infrared spectra is between 650 and 3500

cm^{-1}, however the standard spectral range for Raman spectroscopy often reaches well beyond this range. Typically, it is best to collect spectra over a range of 200 to 4000 cm^{-1}, to ensure that all possible vibrational bands are accounted for.

The most important region for Raman spectroscopic analysis is the defined 'fingerprint region', which extends from 400 to 1800 cm^{-1}, and encapsulates the majority of vibrational bands. For many qualitative and quantitative applications, this range is often seen as sufficient; however, there are noted vibrational bands that predominantly occur outside of this region. Below 400 cm^{-1}, vibrations from heavier atoms such as organic halogen compounds and metal oxides commonly occur; while above the 1800 cm^{-1} limit, C-H stretches, hydroxide and amine stretches, and nitrile bands occur. To preserve time and efficiency, a smaller spectral range can then be employed once a complete Raman spectroscopic profile has been witnessed.

3.3.4 Data Pre-Processing Methods

Although the experimental parameters selected during the collection of Raman spectra is of vast importance, there are a number of pre-processing methods than can be applied after collection of the spectra to increase the quality of the final results. Data pre-processing is an important preliminary step in the analysis of spectroscopic data, as it allows for the reduction of interference effects arising from such factors as variability in particle size, morphological differences, undesirable optical effects, detector artefacts, and differences in Raman scattering coefficients (Sasic 2008).

These powerful corrective techniques include Cosmic Ray Removal, Truncation, Smoothing, Normalisation, Baseline Correction, De-Trending, and the use of Standard Normal Variate (SNV) processing. The order in which these processes are applied is also an area of careful consideration, and while some rules are present that serve as guidelines for their application, experimentation is often required to achieve optimal results.

Cosmic rays are high energy particles from outer space which interact with atoms and molecules in the Earth's atmosphere. If a cosmic ray interacts with a CCD detector, it will generate a false signal in the shape of a very sharp peak in the spectrum (Croke 1995). This sharp peak will be unrelated to the spectrum of the sample being analysed, and so has the potential to obscure and alter final identification and quantification data, particularly when using chemometric processes. Thankfully, processes such as Cosmic Ray Removal give the ability to remove these interfering cosmic ray peaks, enabling a higher degree of accuracy to be retained.

Spectral truncation is the simplest, yet arguably most effective pre-processing procedure available. It allows for the shortening of collected spectra to regions of specific interest, such as the fingerprint region. By shortening a spectrum to an area of known importance, unrelated variables and noise can be eliminated and baseline variations in the selected region can be simplified. For the task of quantification, truncation will often result in a simpler series of data points, which often leads to a more robust model.

Smoothing is a similar technique that allows for the reduction of noise that is potentially associated with the recorded spectrum. Its use has become common practise due to the advent of

complex smoothing algorithms, which rely upon the fact that spectral data is assumed to vary somewhat gradually when going from spectral data point to data point, while noise associated with the spectrum typically changes very quickly. When a rapid change indicative of noise within the spectrum is noted, the algorithm will replace the unexpected value with an estimated value from the surrounding data points. While efficient, care must be taken when applying smoothing algorithms to avoid alteration of the true Raman signal. Overly extensive smoothing, for example, will result in a "smearing" of the Raman peaks, altering their height and/or width. Additionally, small shoulder peaks might be lost, potentially creating additional inaccuracies that will hinder identification of a sample (Dieing, Hollricher et al. 2010).

As well as noise and cosmic rays, most spectroscopic techniques will feature scaling differences that arise from path length effects, scattering effects, source and detector variations, and other general instrumental sensitivity effects (Martens and Naes 1992). Sample normalisation is an effective pre-processing technique that attempts to correct these small aberrations by identifying some aspect of each spectrum which should be essentially constant from one sample to the next, and then correcting the scaling of all variables based upon this characteristic, while retaining the properties of interest. Normalisation also helps to give all spectra an equal impact upon any multivariate models formed, thereby diminishing the risk of severe multiplicative scaling effects altering the contribution of a spectrum to a constructed model, which could potentially result in a loss of accuracy.

Another important function in data pre-processing is baseline correction. Raman and infrared spectra are often affected by intense and irregularly shaped baselines due to contributions from

fluorescence, scattering, or other phenomena (Siesler 2014). To aid in the removal of these effects, typical baseline correction, based on either linear models or complex mathematical functions can be performed, which serve to retain the important features of a spectrum, while correcting only the linearity of the baseline (Naes, Isaksson et al. 2002).

A final two processes of note are Detrending and Standard Normal Variate (SNV). These techniques work hand in hand to reduce and remove non-linear trends, multicollinearity, baseline shift, and curvatures in spectroscopic data. The detrending process calculates a baseline function as a least square fits of a polynomial to the sample spectrum; as the polynomial order increases, additional baseline effects are removed, generally to the trend of 0 Order: offset; 1st Order: offset and slope; 2nd Order: offset, slope and curvature. The combination of detrending with SNV, allows for the further removal of multiplicative interferences such as baseline shift (however SNV-corrected spectra may still be affected by baseline curvature). To ensure removal of this effect, detrending is predominantly performed using a second-order (or higher degree) polynomial. Importantly, the use of these techniques does not disturb or disrupt the shape of the collected Raman spectra, allowing for accurate identification to still be possible.

While these pre-processing methods will all provide favourable results, there is noted and prominent variation in the quality of results dependent upon the order of pre-processing techniques used. While there are no set laws to follow, various studies have lent their weight to produce a favourable order of pre-treatment.

Baseline correction is known to produce favourable results when completed after techniques which remove noise, such as smoothing, so that the baseline will be better defined and can be corrected more accurately (Siesler 2014). Furthermore, baseline correction methods should also be performed in advance of normalisation methods. Similarly, detrending and SNV processes are best completed prior to normalisation; predominantly so long time variations which bear little influence on the shape of a spectrum can be removed more effectively. It has also been recommended that detrending and SNV operations should be performed before baseline correction, allowing for the spectrum to take the most linear form possible (Huang, Romero-Torres et al. 2010).

Truncation of spectral data to the specific region of interest is best achieved as a preliminary pre-processing operation, largely so that subsequent operations are more closely focused on one specific area of interest. The shortening of a spectrum prior to any other pre-processing, enables the creation of simpler, more robust models which are free from variability associated with excipient peaks and microheterogeneity differences. Furthermore, it has been shown that in Raman data with fluorescence interference, pre-processing methods such as detrending and SNV are far more effective when applied to shorter spectral regions, which strongly advocates the use of truncation early in the analysis.

By taking into account these points, guidelines to the best theoretical processing method can be constructed. Initially truncating the spectra to an area of importance, commonly to the fingerprint region found between 400 cm^{-1} and 1800 cm^{-1}, followed by careful smoothing should allow for a more specified, less noisy spectrum. Continuing with detrending and SNV processes should then

allow for enhanced reduction and removal of non-linear trends, multicollinearity, baseline shift, and curvature from the data, allowing for final baseline correction and normalisation to provide an optimised series of spectral data.

3.3.5 Spectral Subtraction

A key component in all spatially offset Raman spectroscopy methods is the subtraction of the two collected spectra to yield a relatively pure spectrum of the concealed subsurface (Olds, Jaatinen et al. 2011). To achieve this end , the collected spectra must be either scaled and then subtracted from each other, or processed using multivariate decomposition methods involving similar data manipulation operations (Matousek 2006).

For inverse SORS, the general method of data treatment is subtraction of the spot measurement, collected through conventional Raman spectroscopy, from the ring measurement, which will be enriched with subsurface information (Cletus, Olds et al. 2011). This simple method has been found to be incredibly effective at isolating a pure spectrum for concealed substance, with proven use in studies led by W. J. Olds (Olds, Sundarajoo et al. 2012), M. Bloomfield (Bloomfield, Loeffen et al. 2010), and N. A. Macleod (Macleod, Goodship et al. 2008) testifying to its accuracy.

While accurate, it has been noted that spectra collected in this way will exhibit small distortions due to imaging imperfections present at some level within the spectrograph, and while the adulterations can often be eliminated or compensated for, their complete removal is practically impossible (Matousek 2006). The presence of these inherent inaccuracies limits the sensitivity of

conventional SORS techniques, reducing the method's ability to recover weak Raman signals from deep layers of a sample. An additional problem also arises from small variations in the pixel sensitivity of the CCD detectors. This problem can be seen in the subtraction of two identical Raman spectra imaged on different CCD tracks; even though the subtraction would produce a flat line residual, noise-like features would still exist along the line, with amplitudes potentially exceeding those of photon shot noise brought about by the detected signals (Matousek 2006). While most of these instances can be numerically corrected, they still represent an additional undesired complication.

In Matousek's initial study into the effectiveness of Inverse SORS, a paracetamol tablet acquired over the counter was analysed through a white water-drainage PVC pipe that was 2 mm thick. It was found that although the Raman spectrum of paracetamol was recovered with sufficient quality to determine is chemical identity, the Raman spectrum was littered with large artefacts stemming from imperfect subtraction of the collected spectra (Matousek 2006). While these differences were far more pronounced in the conventional SORS results, their presence in both models indicated an inherent issue.

Despite this, the simple methodology of scaled subtraction of the ring spectrum from the spot spectrum has continued to great effect, with various pre-processing methods applied to enhance the obtained results. Inverse SORS data treatment such as scaling, background correction, normalization, and polynomial baseline correction are now commonplace (Olds, Sundarajoo et al. 2012, Bloomfield, Matousek et al. 2013). This method has also been shown to be effective for

defocused geometries, with B. Cletus et al. using it to great effect in a 2011 study into concealed substance identification (Cletus, Olds et al. 2011).

3.3.6 Chemometric Methods

The use of chemometrics in spectroscopy has been widespread in recent years, with the application of mathematical and statistical treatments for qualitative and quantitative means now commonly used in analytical studies. Two of the most common techniques, are that of Principal Component Analysis (PCA) and Partial Least Squares (PLS), which both serve to analyse a series of spectral data and elucidate accurate qualitative and quantitative information. As an unsupervised learning technique, PCA is seen to reduce the dimensionailty of multivariate data, such as a series of Raman spectra, and to maximise the variance along each component to enable more efficient qualitative discrimination (Beebe, Seasholtz et al. 1998). PLS on the other hand, aids in the development of prediction models within multivariate data, which facilitates the quantitative analysis of samples (Ryder, O'Connor et al. 1999). While both methods allow for important information and results to be generated, it is PLS that will be the sole focus of this section, as its ability to produce accurate quantitative information is far more pertinent to the research at hand.

The use of PLS methods can be traced throughout many modern Raman spectroscopic methods, beginning with Ryder et al. in 1999, who used the technique to quantify narcotics concealed within solid mixtures (Ryder, O'Connor et al. 1999), to the more recent study by Eliasson et al. in 2008, who quantitatively assessed the contents of pharmaceutical capsules (Eliasson, Macleod et al. 2008). The application of PLS has also seen positive results in SORS measurements, with Olds et al. using PLS regression to construct models capable of predicting the

concentration of acetaminophen and phenylephrine hydrochloride with a root mean square error of prediction of only 3.8% and 4.6% respectively (Olds, Sundarajoo et al. 2012).

Like most multivariate analysis methods, PLS relies upon the assumption that the relationship between spectral response and concentration follows the Beer-Lambert law. In the presence of external information, generally a known concentration, PLS can be used to build regression models that can quantitatively predict the concentration of unknown samples (Macleod, Goodship et al. 2008). While generally only a minor issue, this assumption that the Raman shift spectra of pure materials will not change when they are mixed together or dissolved has been shown to fail, with the pure signal shapes exhibiting small differences, even for the same concentration (Lei, Li et al. 2012).

This unavoidable issue is generally caused by a combination of instrumental factors, such as variations in laser power or wavelength, optical train variations, and irreproducible sample placement, as well as a litany of sample related factors such as variations in structure and the presence of dyes and adulterants (Giles, Gilmore et al. 1999). Although robust, there is a secondary problem faced when applying PLS regressions models, in that a traditional model will generally over-fit to a data set when samples are limited, which will greatly reduce more widespread application of a generated model (Lei, Li et al. 2012). In order to combat these issues, a larger sample size is generally recommended, allowing for a more comprehensive prediction to be generated, although at the expense of time and efficiency.

3.3.7 Sample Considerations

Although SORS enables the ability to acquire chemically specific spectra of substances concealed behind barriers of polymers, paper, and glass, there are some materials that still prove to be formidable obstacles for the technique. Various samples of thick cardboards, including the more traditional brown and grey cardboards, and thicker corrugated cardboard samples have been shown to be incompatible with current SORS methods, as well as metallic containers that are impenetrable to light (Olds, Jaatinen et al. 2011, Bloomfield, Matousek et al. 2013).

For other materials, there are a notable series of characteristics that will affect a sample's susceptibility to current SORS methods. The thickness of sample, along with the density, opacity, colour, and the ability to fluoresce will all have critical impact upon the quality of spectra obtained and the effectiveness of any method.

It has been previously shown that spatially offset Raman spectroscopic methods produce favourable results with samples that are highly scattering and arranged into a thick layer, largely because the photons collected during the spatially offset measurements are generated from deep within the sample (Matousek, Clark et al. 2005). This effect shows that it is therefore beneficial to extend the underlying sample depth by increasing it's thickness, thereby enabling maximal Raman signals to be produced and collected.

In the case of SORS techniques that utilise a near infrared (NIR) laser light, the penetration depth of the excitation light can be in the order of a few centimeters, depending upon the scattering, absorption, and transmission characteristics of the sample and so the importance of using a

sufficiently thick sample matrix can be critical for optimal results to be produced and collected (Matousek, Clark et al. 2005).

Furthermore, it can be seen that when a sample is thinner, the amount of material which is able to contribute to Raman scattering is reduced, and so there will be a greater transmission loss of the excitation light through the sample. This effect was noted by W. J. Olds et al. when probing an envelope using a backscattered collection geometry, where the signal collected from the thin layer of concealed acetominophen was noted to be relatively weak (Olds, Jaatinen et al. 2011). In contrast, it was also noted that a greater signal was collected from a thicker sample layer, which enabled successful identification of the acetominophen through more formidable barriers, such as a padded postbag and an opaque plastic bottle. Although only the thickness of the thinner layer of acetominophen is given in the study (as 1 mm), it can still be seen that the thicker sample would have allowed for greater generation of Raman photons, creating a stronger overall signal.

Similar to the effects of the thickness of a sample is the effects of a sample's specific density. While more densely populated matrices are known to produce stronger Raman signals, as there will be a greater production of Raman photons from the more densely packed substrate, this enhanced backscattering can have both advantageous and detrimental concequences. Solid samples will generally give good quality Raman spectra due to their high structural density and instense backscattering (Sasic 2008), and so it can be expected that if the concealed substance being interrogated was densely packed, then optimised results could be collected. However, the same effect applies to the packaging concealing the drug of interest, where a more intense Raman spectrum could obscure vital information.

W. J. Olds et al. noted the effects of varying sample density in a 2012 study into the non-invasive, quantitiative analysis of drug mixtures (Olds, Sundarajoo et al. 2012). In the study, it was found that containers with thicker walls, or higher density polymers were far less penetrable to incoming excitation light and outgoing Raman photons. As a result, the spatially offset measurements collected from these containers contained markedly weaker spectral contributions from the concealed substance. Conversely, thinner and less densely packed containers were found to permit incoming excitation light and outgoing Raman photons far more, and so more favourable spectra were produced (Olds, Sundarajoo et al. 2012)**.**

For thicker and more densely populated packaging, such as heavy plastics and cardboards, the reduced contributions from the concealed substance and an increased uncertainty and noise, will undoubtedly affect the accuracy of any qualitative and quantitative methods developed. Consequently, it would be advisable that samples be prepared into dense, thick layers when possible, and noted that thinner, less dense packaging materials would produce the most accurate results.(Sasic 2008)

A second influence of a sample's density is its resulting opacity. Diffusely scattering media are commonly characterised by their opacity (or the minimal degree of transparency), which is a direct result of the density of populated particles present (G., JR. et al. 1984)**.** A more densely populated matrix will often be opaque, with the greater particle population preventing the passage of light through the sample, conversely, a more sparsely populated matrix will often

appear either transparent or translucent, with light being able to pass between the particles in the sample more easily.

In the case of opaque samples, the propagation of photons will result in multiple scattering, and as a result, the sample will appear opaque and render objects behind the sample non-discernable (Lewis and Edwards 2001)**.** These opaque and turbid samples will be much more difficult to measure due to the reduction in the excitation energy penetrating the sample, and an increased amount of light being reflected. While little can be done to change the opacity of a selected packaging material, it is important to note that darker, more opaque samples will present a more formidable obstacle for anaylsis.

Two final, and arguably most influential sample characteristics are the colour and potential for fluorescence. Generally, the applicability of SORS is limited to samples which do not exhibit strong absorption, such as dark containers, and samples which do not exhibit strong fluorescence (Chalmers, Edwards et al. 2012). Dark coloured samples are notorious in most spectroscopic techniques for being difficult to analyse, and the issue persists for SORS measurements. Most black plastics contain large amounts of carbon as a blackening pigment, and with carbon being an efficient absorber of near-infrared (NIR) light, it makes analysis far more problematic (Olds, Jaatinen et al. 2011). A consequence of dark samples absorbing the excitation laser light is that the resulting heating effect will often cause irreversible degradation of the sample (Loadman 1999). Some progress in the interrogation of dark samples, particularly dark glass which is notorious for being highly fluorescing, has been made in recent years. Eliasson et al. reported in 2008, a displaced Raman spectroscopic technique, built upon the theory of SORS to detect

cocaine that had been dissolved in rum to an estimated detection limit of ~ 9 g per 0.7 L (Eliasson, Macleod et al. 2007). By introducing the displaced excitation laser beam into the bottle at an angle, so that its focal point was established within the bottle, the fluorescence from the dark glass could be suppressed, while generation of Raman photons within the collection volume could be achieved without hindrance.

The problem of fluorescence eclipsing useful spectral data can still persist with coloured samples when using a NIR light source, particularly in the case of brightly coloured materials and some oxidatively degraded polymers (Loadman 1999). Again, progress has been made to reduce the impact of fluorescence, with Matousek and colleagues having reported the successful use of SORS and transmission techniques to retrieve Raman spectra from a range of off-the-shelf cold and flu tablets and capsules of varying colours (Eliasson and Matousek 2007, Yu, Xie et al. 2014)**.** The use of an inverse SORS technique with a 1 mm diameter spot and an 827 nm laser source produced favourable results of the active pharmaceutical ingredients and excipients without undesired noise, proving that the interfering fluorescence signals could be effectively suppressed using SORS methods (Eliasson and Matousek 2007). Furthermore, Olds et al. reported the successful interrogation of an antibiotic tablet (amoxicillin and flucloxacillin) with a darkly colored shell, retained inside its blister pack, using the inverse SORS geometry and a current-stabilized 785 nm diode laser (Olds, Jaatinen et al. 2011).

The use of a higher wavelength excitation laser is crucial to the suppression of fluorescence, and so the use of either 785 nm or 830 nm wavelengths in any SORS system is now viewed as essential. In some extreme cases where fluorescence persists, the use of even higher

wavelengths, such as 1064 nm, is also recommended. Unfortunately, while the use of a higher excitation wavelength will yield favourable results in some cases, it will still not permit the interrogation of metallic containers (Chalmers, Edwards et al. 2012).

If all the aforementioned experimental, instrumental and sample considerations are noted and accounted for, the application of SORS should enable the accurate and discriminatory identification and quantification of a multitude of drug samples concealed within a variety of matrices with little or no interfering fluorescence emission or other undesirable effects.

3.4 Applications in Illicit Drug Detection

The use of conventional Raman spectroscopy in the detection, identification, and quantification of illicit drugs has been well documented in the past, and is gradually becoming accepted as an integral part of modern, practical forensic investigations. The use of SORS however, is currently limited, largely due to the relative adolescence of the technique.

What has been shown so far is that the technique is an effective means for the non-invasive characterisation of the internal contents of containers; capable of analysing samples held within a variety of opaque and transparent materials. While its use in the detection, identification and quantification of concealed drugs of abuse is limited, there are a number of persuasive studies that strongly relate the techniques potential.

An initial study into inverse SORS by P. Matousek in 2006 gave definitive evidence of the technique's capabilities. In the study, inverse SORS was used to analyse paracetamol tablets hidden beneath 2 mm thick white polyvinyl chloride (PVC) pipes, samples of a 1 mm outer-layer

of PMMA powder on top of a 2 mm trans-stilbene powder layer, and the non-invasive monitoring of brown paper envelopes containing sugar. In all cases, the inverse SORS method applied was found to successfully, and accurately, identify the concealed substance, while also having the added benefit of inhibiting the fluorescence noted in conventional Raman spectroscopy.

In addition, the study also highlighted the potential for inverse SORS to non-invasively recover Raman spectra of active ingredients within pharmaceutical capsules and coated tablets, a process that would be supremely beneficial in the analysis of illicit substance. One year later, P. Matousek, along with C. Eliasson performed another intensive study, focusing on counterfeit pharmaceutical tablets and further demonstrating the potential of SORS for the detection of drugs of abuse in packaging such as plastic blister packs and opaque, white plastic containers (Eliasson and Matousek 2007).

In the same year, a detection method based on SORS was developed by C. Eliasson, N. A. Macleod, and P. Matousek for the detection of cocaine concealed inside transparent glass bottles containing alcoholic beverages (Eliasson, Macleod et al. 2007). This new technique, coined Displaced Raman Spectroscopy used the same principles of SORS, and was able to detect cocaine with good signal-to-noise ratio from a ~300 g solution of adulterated cocaine (noted to be 75% pure) within a 0.7 L brown bottle of rum. Impressively, the detection limit of the technique was estimated to as low as 9 g of pure cocaine with 0.7 L of rum, equivalent of ~0.04 M of the illicit drug.

In 2008, another study by M. D. Hargreaves et al. demonstrated the ability of portable Raman spectroscopy and benchtop SORS techniques to rapidly identify real and fake ivory samples. The developed SORS technique was then further shown to be able to identify ivory concealed in plastics, paints, varnishes, and cloth, proving the methods effectiveness and superiority over the conventional Raman spectroscopic methods (Hargreaves, Macleod et al. 2008). Macleod and Matousek et al. furthered their work with SORS in the same year by completing a study into the applicability of the technique for monitoring the depth of optically thick layers within turbid media. In their work, it was found that the deep penetrative capability of SORS was able to characterise significantly thicker layers than was currently possible with conventional Raman spectroscopy. Furthermore, it was also shown that the incorporation of depth information into a SORS experiment as an additional dimension allowed the pure spectra of each individual layer to be resolved through the use of three-dimensional multivariate techniques, with accuracies comparable to that of a simpler two-dimensional analysis. A specific focus upon the use of Principle Component Analysis (PCA) and Partial Least Squares Regression (PLS) for two-dimensional samples, and Parallel Factor Analysis (PARAFAC) for three-dimensional samples was noted (Macleod, Goodship et al. 2008).

Two years later, SORS was shown to be able to effectively discriminate between the spectrum of a concealed substance, and the spectrum of opaque, coloured plastic containers and glass bottles that were several millimetres thick. The extensive study by M. Bloomfield et al. illustrated SORS effectiveness against samples such as polypropylene, high density polyethylene, polyethylene terephthalate, polystyrene, as well as green and brown glass, all ranging from 1 to 4 mm in thickness. The importance of this study is twofold, firstly, it proved that SORS is capable of high

chemical specificity in detecting concealed substances within opaque plastic and glass containers, without any prior knowledge of the sample, and also that SORS could obtain significantly cleaner Raman spectra of concealed material than is possible with conventional backscatter Raman spectroscopic methods, a key feature that permits the identifications of concealed materials with a higher confidence level (Bloomfield, Loeffen et al. 2010).

In 2011, B. Cletus and J. Olds et al, while working at the Queensland University of Technology, took a step forward, developing an inverse Spatially Offset Raman Spectrometer capable of non-invasively identifying packaged chemicals from a distance. The new method was found to accurately identify samples of acetaminophen concealed within high density polyethylene container placed at 30 cm from the collection optics. The research was not only a step forward for the technique, but also created the distinct potential for concealed hazards to be safely and remotely investigated (Cletus, Olds et al. 2011).

B. Cletus and J. Olds et al. were again instrumental in 2012, with their further research into the possibility of non-invasive, quantitative analysis of drug mixtures hidden within containers using SORS and multivariate statistical analysis (Olds, Sundarajoo et al. 2012). In the study, three component mixtures consisting of the target drug, either acetaminophen or phenylephrine hydrochloride, with two diluents (glucose and caffeine), were created at a range of concentrations from 5% to 100%. After conducting SORS analysis, principal component analysis (PCA) was performed to reveal trends within the data, with partial least squares (PLS) regression then performed to construct models and predict the concentration of each target drug. It was

found that the PLS regression models were able to predict the concentration of acetaminophen in the validation samples with a root-mean-square error of prediction (RMSEP) of 3.8% and the concentration of phenylephrine hydrochloride with an RMSEP of 4.6%.

A successful display of the quantitative potential of SORS was a critical step for the universal acknowledgement and widespread acceptance of the method. With the work of B. Cletus and J. Olds et al. able to demonstrate the effectiveness of SORS coupled with multivariate statistical techniques, numerous applications were demonstrated, including the monitoring of the degradation of pharmaceuticals, forensic investigations into counterfeit drugs, and the analysis of illicit drug mixtures which may contain multiple components (Cletus, Olds et al. 2011).

Successful development of a spatially offset Raman spectroscopy method was achieved with a 1064 nm excitation laser by R. J. Hopkins et al. in 2012, who demonstrated the detection of chemicals through physical barriers such as containers. The use of a longer wavelength in the experimental proceedings allowed for issues with fluorescence from target chemicals to be overcome, while retaining the many benefits of the SORS techniques for through-barrier detection (Hopkins, Pelfrey et al. 2012).

Further emphasis was placed upon the use of multivariate systems for complex multilayer samples with Buckley and Kerns et al. demonstrating the use of Band-Target Entropy Minimisation (BTEM), Multivariate Curve Resolution (MCR), and Parallel Factor Analysis (PARAFAC) in the decomposition of spatially offset Raman spectra of human bone transcutaneously in vivo (Buckley, Kerns et al. 2014). The results obtained were found to be

highly positive, indicating the potential for a highly successful quantitative SORS method. Matousek and Bloomfield et al. also continued research into spatially offset Raman spectroscopic methods in 2013, demonstrating a new approach for the verification of incoming raw materials through packaging in pharmaceutical manufacturing. In their study, acquisition times of less than 10 seconds were used with a SORS related method to accurately identify common pharmaceutical materials through a range of frequently used packaging, including translucent plastics, paper sacks, and coloured glass bottles. With the exception of metallic containers and cardboard drums, it was found that all tested packaging materials proved to be amenable to the technique, illustrating the widely applicable viability of the method (Bloomfield, Matousek et al. 2013).

Another interesting demonstration of SORS, and its increased accuracy over conventional Raman spectroscopy, was conducted by Zhang et al. midway through 2013. In the study, the action mechanism of how spatially offset Raman spectroscopy can effectively detect the medium concealed in the non-transparent bottle was analysed, along with showing off the increased detection depth and applicability of the SORS method over conventional Raman spectroscopic methods (Zhang, Zhang et al. 2013).

In more recent years, a new micro-SORS method was detailed by Z. Di and B. Hokr et al. This method, aimed to overcome the major SORS limitation of required knowledge of the optical properties of the medium being a necessity to translate an offset into a sample depth (Di, Hokr et al. 2015). In their research, the various benefits of performing SORS with micron offset distances, as opposed to the more typical millimetre offsets commonly used were illustrated,

along with Monte Carlo simulations to demonstrate that their obtained results depended less on the scattering coefficient of the material. Importantly, the new method produced great potential and provenance for SORS instruments coupled with microscopes for the analysis of small, complex samples.

The idea of a non-invasive micro-SORS method was further applied for the analysis of thin painted layers of sculptures and plasters by Conti & Colombo et al., who showed the techniques ability to reveal the chemical makeup of most layers (Conti, Colombo et al. 2015). While the study is not explicitly related to the analysis of illicit drugs, pharmaceuticals, or powders, the demonstration of the technique's ability to non-invasively, and non-destructively, analyse individual paint layers is an impressive credential for further SORS development and study. Conti et al. reported another study into the effectiveness of the micro-SORS methods by applying it successfully to non-invasively detect the presence of thin, highly turbid layers within polymers, wheat seeds, and paper (Conti, Realinia et al. 2015). Both of these studied served to illustrate the wide range of applications that SORS and micro-SORS methods can accomplish.

One further feasibility study indicated that SORS methods are capable of interrogating substances concealed in clothing, opening up the potential for the screening of mail and individual people (Siesler 2014). In the study, SORS was used to measure ordinary white caster sugar that was hidden under several layers of fabric. The fabric used was an ordinary kitchen cloth, which was 0.2 mm thick, chequered in white and pale greens, pinks, blues, and yellows. From the study, it was found that the Raman spectrum of sugar could be clearly identified in the SORS spectra for up to four sheets of fabric, with a spatial offset of 5 mm.

Overall, the past decade has presented numerous examples of SORS accuracy, adaptability, and the vast range of applications in which it can be superior to conventional Raman spectroscopic techniques. While the majority of the studies outlined are not specific to the identification and quantification of illicit drugs, they provide powerful and promising foundations for research in that area.

Chapter 4 - Chemometric Processes

In recent years, there has been a growing trend of combining Raman spectroscopic methods with chemometric processes in an effort to elucidate greater information from spectra measurements. Several groups have previously experimented with the forensic and pharmaceutical benefits of combining processes such as Principal Component Analysis (PCA), Partial Least Squares Regression (PLS-R), and Multivariate Curve Resolution (MCR) to uncover hidden patterns within spectral data, and to identify pure components of mixed samples. In this study, the three aforementioned processes were used to great effect, with this chapter detailing the processes and methodologies behind each model.

4.1 Principal Component Analysis (PCA)

PCA has quickly become a go to chemometric method for any investigation involving Raman spectroscopy. Its use has been examined and championed by several prominent research groups, particularly when interrogating counterfeit drugs such as Viagra (Veij, Deneckere et al. 2008), Cialis (Kwok and Taylor 2012) and anti-malarial tablets (Veij, Vandenabeele et al. 2007), and more illicit samples such as simulated street drugs (Noonan, Tongue et al. 2009) and studies of classified mixtures of illicit drugs (such as cocaine, heroin, and MDMA) alongside numerous cutting agents (Zoubir 2012).

Following the introduction of PCA at the beginning of the twentieth century by Pearson and Hotelling, the technique has been used in many different disciplines including agriculture, biology, chemistry, climatology, demography, and many others. It is a linear method, meaning that the transformation between the original data and the new lower dimensional representation

is a linear projection. While the techniques' main purpose is dimensionality reduction, it is also an effective method for exploring the relationships between variables (Demsar, Harris et al. 2012).

PCA is regarded as an exploratory technique which uses eigenvectors to extract the significant variation of a multivariate data matrix. It is designed to reduce a large number of variables while simultaneously eliminating various noise contributions, and as such, it has become a natural addition to Raman spectroscopic examinations. The cornerstone of any PCA model lies in the careful determination of the appropriate number of principal components; if too few components are selected, then important information will be lost, while too many components will mean that excess noise is incorporated into the model (Demsar, Harris et al. 2012).

Although this research utilises CAMO's Unscrambler X software to identify the optimal number of components, a secondary method is found in examining the percentage of variance that is explained by each principal component. Plotting the percent of the explained variance or accumulated eigenvalues against the principal component provides a relatively straightforward way of determining how many principal components should be kept, with the optimum number of principal components shown at the point where the curve of this graph levels off (Kwok and Taylor 2012)**.**

When dealing specifically with Raman spectra, PCA can be used to extract information from complicated spectra because it removes redundant variables and noise interference, making it possible to isolate the important information from a spectrum that originally appears to be

unintelligible (Noonan, Tongue et al. 2009). Furthermore, PCA has been used in the past to try to remove some of the effects of fluorescence (Eliasson and Matousek 2007), allowing for more detailed information to be glimpsed.

4.2 Partial Least Squares Regression (PLS-R)

The Partial Least Squares Regression method is gaining importance in many fields of chemistry, including analytical, physical, clinical chemistry and even industrial process control, which all benefit from the use of the method (Geladi and Kowalski 1986). The pioneering work of PLS-R was completed in the late 1960's by H. Wold, who used the technique in the field of econometrics, with S. Wold and H. Martens then applying the method to chemical applications (Wold et al. 1982).

One of the most common quantification processes used to aid in the use of spectroscopic methods, PLS-R has been applied fluently in recent years to give accurate quantitative results, with notable studies and academics advocating its use when dealing with real and simulated illicit drug samples (Fenton, Tonge et al. 2011).

Simply stated, PLS-R works by constructing a calibrations model from a set of spectra collected from known concentrations, allowing for a relationship between observed spectra and component concentrations to be defined (Haaland and Thomas 1988). From this relationship, an estimated value of unknown component concentrations can be calculated through the use of complex algorithms, such as the NIPALS algorithm.

One of the most extensive studies completed was into the use of multivariate data analysis methods to identify and quantify drugs of abuse in complex mixtures of various types. Initial work in 1999 on cocaine, heroin and MDMA mixed with foodstuffs, showed that it was possible to detect the presence of drugs at levels down to ca. 10% by mass (Ryder, O'Connor et al. 1999). Additionally, partial least squares analysis of data from a series of 20 mixtures of cocaine and glucose (0-100% concentrations by weight of cocaine) gave a calibration model with a root mean standard error of prediction (RMSEP) of 2.3%. When this work was extended to ternary mixtures containing cocaine, caffeine and glucose, the concentration of cocaine could be predicted with a RMSEP of 4.1% (Ryder, O'Connor et al. 2000). Further extension to 85 samples diluted with several different materials showed that when principal component analysis was restricted to the most intense peaks in the Raman spectrum of the pure drugs, discrimination between cocaine, heroin, and MDMA mixtures was possible even though only 2% or 3% of the original spectral data was used in the analysis (Ryder 2002).

4.3 Multivariate Curve Resolution (MCR)

Another innovative chemometric process, Multivariate Curve Resolution has become popular in recent studies for the resolution of multiple component responses in unknown, unresolved mixtures (Jaumot, Gargallo et al. 2005).

MCR works by resolving a multi-component system into individual, pure components. In general, the process involves the decomposition of a data matrix that contains the responses of a multi-component system into a product of two matrices, with each containing either the pure

component information in the row and column directions of the original data matrix (Kwok and Taylor 2012). When applied to spectroscopic data, MCR is capable of defining the relative concentrations and spectral profiles of the pure components respectively, allowing for relatively pure components to be identified.

In order to obtain the resolved components, a number of algorithms are available. One of these algorithms is Alternating Least Squares (ALS), an iterative least square process used to minimise the least square errors of row and column directional matrices simultaneously. This process continues until a pre-defined convergence criterion is reached (Gaubert, Clement et al. 2016). Importantly, no prior information is needed for MCR-ALS, ensuring it's use and relevance in multiple fields that involve unknown compositional matrices.

Chapter 5 – A Modern Age of Drug Dealing

5.1 Digital Markets & Postal System Trafficking

The number of cases relating to the seizures of narcotics or psychotropic substances in 2013 was 51,381, which was significantly higher than for 2012, when this total stood at 43,771 cases (WCO 2013). This increase was in the region of 17%, and was indicative of the commitment by Customs services to combat drug trafficking more effectively, enhanced by a greater understanding of control techniques. It was also a strong indication of the true reality of criminal organizations' commitment to pursue the production and trafficking of narcotics and psychotropic substances, for which the diversification of the delivery routes and the innovative products coming on the market are genuine causes for concern and require constant vigilance and adaptation by the inspection services.

An increase in seizures was found for cannabis, khat, psychotropic substances and cocaine, in varying proportions throughout 2013, however this trend tended to be downward for opiates. In addition, new forms of drugs flooding the markets posed, and continue to pose, major problems in identification and interception for enforcement agencies, especially as they are primarily traded via the Internet and conveyed by postal or express mail services (WCO 2013). The order of the means of transport used in 2012, was found to be mirrored in 2013, with a single difference noted, that the postal and express mail system far outstripped all other means of transport, with 41% of total seizures in 2012 and 45% in 2013 (WCO 2013).

In 2013, the WCO reported approximately 2,000 interceptions by mail of only cocaine, involving a total of nearly three tonnes of the substance. A more comprehensive illustration of the postal system as a major trafficking channel can be found in Operation Sky-Net, a 2012 initiative carried out by the WCO in 2012, in cooperation with Chinese Customs. The operation demonstrated the potential of this means of transport for trafficking narcotics and precursor chemicals.

More than 941 parcels containing drugs or precursor chemicals were seized in the course of Operation Sky-Net, which targeted postal and express mail channels. The operation was carried out over the course of 49 days, between the 10th of September and 28th of October 2012, with the participation of 68 WCO Members, five WCO Regional Intelligence Liaison Offices and the active support of INTERPOL. Alarmingly, Operation Sky-Net resulted in the discovery of over 9.5 tonnes of illicit products, including cocaine, heroin, opium, methamphetamines and anabolic steroids. A total of 167 kg of cocaine was detected in the short amount of time Operation Sky-Net was in place (WCO 2012).

The results of Operation Sky-Net are mirrored by Australia's own domestic market. The postal system is the most frequently used channel for cocaine trafficking. Between 2000-1 it accounted for over 70% of all cocaine detections at the border, and that amount that increased to 94.1% of all detections in 2012-13 (Jevatovic and ACC 2014).

Shipping small volumes of cocaine through the postal system is not a new trend, and early examples of the practise can be seen as far back as the early 20th Century. In the 1920's, the sale

and shipping of cocaine was considered legal, and Hoffman Le Roche, one of the largest cocaine and heroin producers and exporters would commonly ship various quantities of the drug worldwide. However, after the adoption of the Hague Treaty in 1925, and the Geneva Treaty of 1931, such transactions were then considered to violate international law. In response, it became common practise for small shipments of the drugs to be sent through the post, while larger quantities would often be sent in purposefully mislabelled crates (Karch 2005).

Since these early days, the practise has remained relatively simple and increasingly frequent. There have been numerous reports in the UK of brazen drug pushers shipping quantities of cocaine through gaols, with an average of two packages containing illegal drugs being intercepted by security staff every day (Traynor 2015). Elsewhere in the UK, international supply chains smuggling cocaine through the post system have only recently been discovered. One such examples is that of Kenneth Oranyendu, who was behind a large scale, transatlantic scheme in which kilograms of cocaine were shipped in everyday items, such as children's books and photocopier cartridges. Reportedly, Oranyendu's supply chain was active for nearly three and a half years before it was discovered. It is known that 23 packages were sent in the scheme; with the majority of these not intercepted (Osuh 2014).

Far from being limited to the United Kingdom, reports of cocaine trafficking through the postal systems are just as frequent in the United States. One particular example from Pennsylvania is that of Jose Eduardo Garcia De Quevedo. Originally from Puerto Rico, Garcia de Quevedo received a package containing approximately 300 g of cocaine with a street value of $30,000 shipped through the mail from Texas. The discovery was only found due to the use of a police

informant (Carr 2012). Another prominent example involved the smuggling of cocaine to New York by dressing up the illicit drug as colourfully wrapped children's birthday presents. Shipments covered in pink birthday wrapping paper, held within gift bags, and accompanied by stuffed toys, notably an Olaf doll from the Disney movie 'Frozen', and a Minion doll from the 'Despicable Me' franchise. Investigators seized five packages, each containing a kilogram of cocaine, equal to a combined street value of $225,000 over a two week span (Tracy and Paddock 2015).

In Australia, the practise is arguably just as prominent. In 2005, cocaine worth almost half a million dollars was posted into Australia in 39 individual envelopes. Sent from the United States, the envelopes were collected from Bondi Beach post office, and contained a combined 2.5 kilograms of the drug (AAP 2005). On a smaller, but more prolific scale, a 41 year old man was also apprehended in 2008 when police seized fourteen parcels containing a combined weight of 1.01 kg of cocaine on route to him. Twelve of the parcels were carried by Australia Post, while international courier DHL delivered the other two (Morrison 2013).

More recently, Australian authorities have estimated that 94% of intercepted cocaine packages enter the country via parcel post (Hurley 2014). A reason for this increase in prominence is likely due to the growing number of people in Australia that have abandoned traditional channels for buying illicit drugs in favour of purchasing them on online Darknet markets such as the now defunct Silk Road.

Although e-commerce on the dark web only started around 2006, illicit drugs were among the first items to be transacted using the internet, when in the early 1970's, students at Stanford

University and Massachusetts Institute of Technology used the ARPANET to coordinate the purchase of cannabis (Power 2013). Popularisation of the World Wide Web and e-commerce in the 1990's enabled illicit transactions to be more widely accessible, and it wasn't long before web-based drugs markets began to launch. One of the very first of its kind was The Hive, an information sharing forum for practical drug synthesis and illegal discussion which launched in 1997.

In the early 2000's, early cybercrime and carding forums such as ShadowCrew experimented with drug wholesaling on a limited scale, and this soon gave birth to dedicated online markets (Hoffmann 2015). The Farmer's Market opened in 2006 as Adamflowers, and served to connect and mediate transactions for buyers and sellers of illicit substances through extensive use of Hushmail, and encrypted email service. In 2010, the website moved to a hidden site on the Tor network, where it became "like an Amazon for consumers of controlled substances" (Goodin 2012). The Farmer's Market generated revenue through commissions based on the size of each purchase. An estimated three thousand people across all fifty states of the U.S. and throughout 34 other countries made transactions, and according to estimates by the Drug Enforcement Administration (DEA), the site processed about $1 million between 2007 and 2009 (Goodin 2012).

The site allowed for several forms of payment including cash, PayPal, Western Union, Pecunix, and I-Golder, which ultimately led to its demise in April 2012. Law enforcement agencies were able to trace payments, and the site was closed, with several operators and users arrested as a result of Operation Adam Bomb (Schwartz 2012).

Silk Road was the first pioneering marketplace to implement both Tor and Bitcoin escrow. Founded by Ross Ulbricht under the pseudoname 'Dread Pirate Roberts' in February of 2011, it became the gold standard for Darknet markets. In March 2013, Silk Road had approximately ten thousand products for sale by vendors, of which 70% where drugs. Later, in October 2014, there were 13,756 listings for drugs, grouped under the headings of stimulants, psychedelics, prescription, precursors, other, opioids, ecstasy, dissociatives, cannabis and steroids/PEDs. Most products bought and sold on Silk Road were delivered through the mail, with the site's seller's guide instructing sellers how to vacuum-seal their products to escape detection. At its height, Silk Road had over 100,000 active buyers, completing more than 5000 transactions a week and worth an average of more than $100 per transaction (Ormsby 2012).

Silk Road was finally shut down by the Federal Bureau of Investigation (FBI) in October 2013, but its prominence was quickly reasserted by a greatly increased number of shorter-lived markets. From late 2013, new markets were being launched with relative regularity, and Silk Road itself was reborn as Silk Road 2.0, run by the former site's administrators and the Agora marketplace (Greenberg 2013).

November 2014 saw the instigation of Operation Onymous. Executed by the FBI and the UK's National Crime Agency, the operation led to the seizure of 27 hidden sites, including the new Silk Road 2.0 and twelve smaller markets and individual vendor sites. Agora was one of the largest Darknet marketplaces to avoid Operation Onymous, and as of April 2015, had gone on to

be the single largest overall marketplace, with more listings than Silk Road at its height (Greenberg 2014).

Currently, the exact number of Darknet marketplaces that deal in the sale of illicit drugs is unknown, but more than fifty live markets have currently been identified (DeepDotWeb 2013). What is apparent is that with every closure, the security and technology employed by surviving marketplaces is increased. In 2015, there have already been great strides in market diversification and further developments around escrow and decentralisation that ensure payments are more difficult to track. With greater security, strengthening anonymity, and increasing use it's clear that the sale and purchase of drugs through these digital marketplaces is the future of narcotics dealing. This future will undoubtedly mean an increased reliance upon the global postal systems as unwitting traffickers, and stresses the importance of new detection methodologies.

Chapter Six – Method Development

The studies previously mentioned in this paper, along with a plethora of new and emerging research, present a valuable source of information regarding the appropriate and effective use of spectroscopic instrumentation, excitation wavelengths, sampling considerations, and data pre-processing techniques. The focus of this chapter is the development of the optimised inverse SORS method that will be used, describing each consideration and its selected parameters, along with justification of their characteristics and inclusions, as well as an overview of the research completed throughout this project.

For all experimental work, a Renishaw inVia Raman Microscope coupled with a Leica DM2500M microscope, Renishaw charge coupled device (CCD) detector, and Philips SPC1030NC webcam were used. A Renishaw 785 nm, near infrared diode laser with 1200 l/mm grating was used for all measurements, and all spectra were collected using the WiRE 3.4 software. CAMO's The Unscrambler X software was used for all chemometric processes, while OMNIC 8.2 Spectral software by Thermo Scientific was used for the identification of collected spectra.

6.1 Method Development – Identification of Atropine

6.1.1 Analysis of Optimised Parameters

6.1.1.1 Microscope Objective

The Leica DM2500M microscope used during the experiment had the capability to provide magnification at 5x, 20x, and 50x objectives (with numerical apertures of 0.12, 0.40, and 0.75 respectively). Each of the objectives were known to have their own advantages and

disadvantages that would affect which provided optimal results. The lower 5x objective allowed for quick and simple focusing, and would allow for a larger diameter laser to probe the sample. This increased laser thickness would have the advantage of reducing any subsampling effects, but would also increase the distance required for a beam to diverge and form a ring. A further disadvantage of the smaller objective, is that it would reduce the observable detail of each spectrum collected. Conversely, the 50x objective would provide more accurate measurements, and the smaller laser beam diameter would enable a finer ring to be produced in a shorter amount of space.

To ensure the quality of the results being obtained, a test examination of pure atropine under all three objectives was made. As can be seen in Figure 9 below, when the sample, positioning, and laser power (500 mW) were kept constant, the 50x objective produced the most intense peaks, while the lower 5x objective produced a clearly visible, but less intense atropine spectrum.

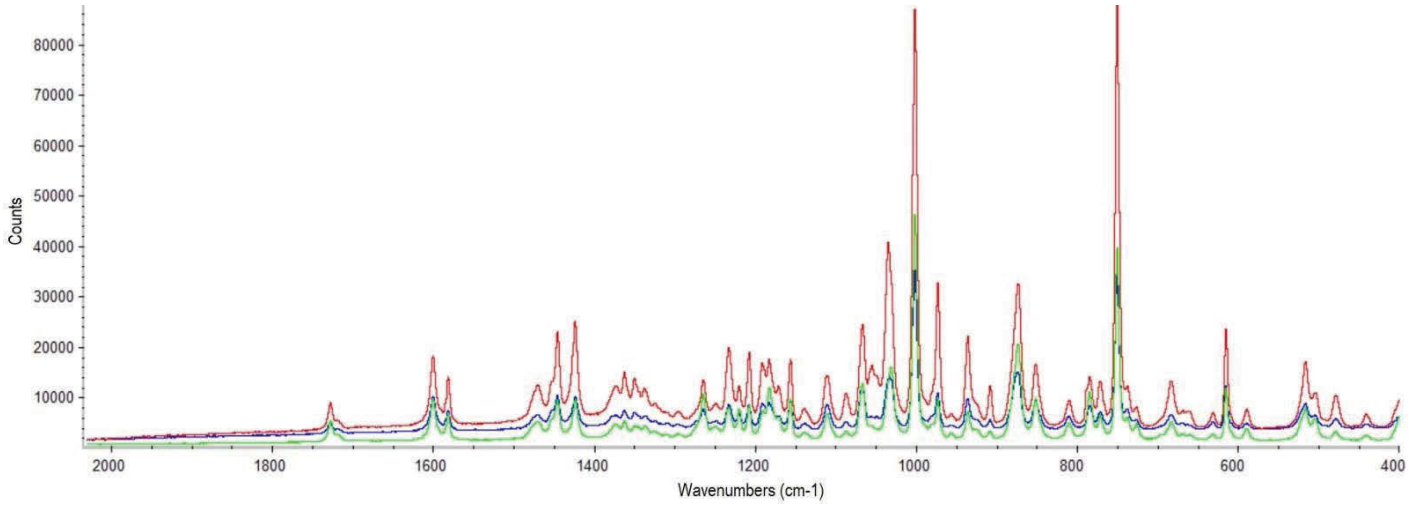

Figure 9 - Comparison of atropine spectra obtained from 5x objective (light green), 20x objective (blue), and 50x objective (red).

These results indicated that use of the 50x objective would produce the optimum results during testing. This would be true, if not for the reduced working distance experienced when using a greater level of magnification that made it an impossibility. It was found that in order to maintain sufficient focal depth while accommodating the axicon and its mount system, only the 5x objective could be used. In this instance, the additional accuracy and specificity that would be gained from the higher objective had to be sacrificed in order for the SORS technique to be viable.

6.1.1.2 Excitation Laser Wavelength

Another crucial parameter that had to be examined was the laser wavelength utilised. Three wavelengths of 633 nm, 785 nm, and 1064 nm were examined for their suitability by comparing spectra collected from a pure sample of atropine at each wavelength. In each case, the laser power and additional parameters were kept as consistent as possible. As shown in the collected spectra presented in Figure 10 below, all three excitation wavelengths were highly similar in their ability to accurately examine atropine. Noticeably, the 1064 nm wavelength did show reduced peak specificity and greater noise along the baseline, however it was still acceptable quality to determine the identity of atropine.

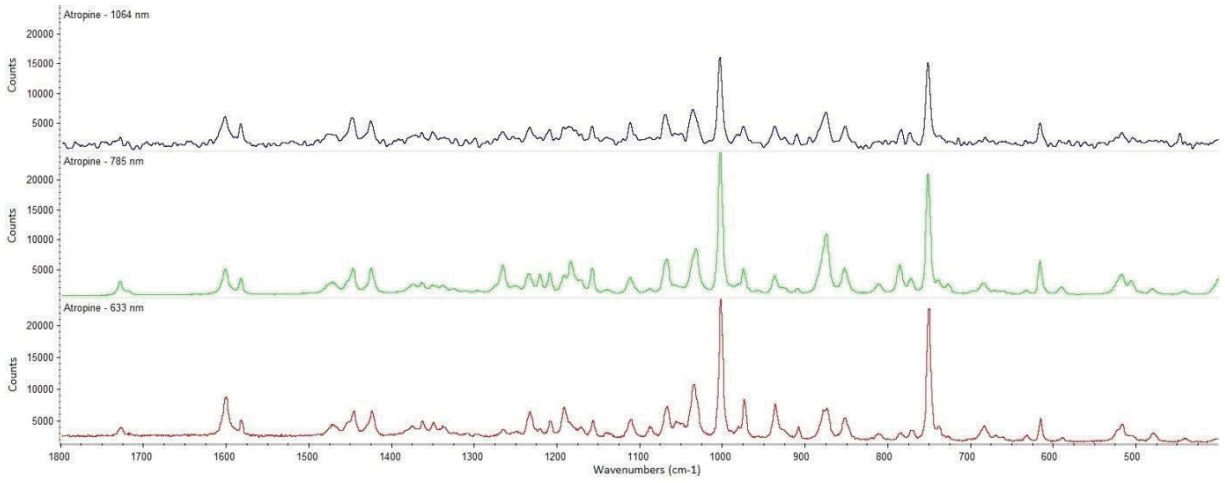

Figure 10 - Comparison of atropine spectra collected at excitation wavelengths of 1064 nm (top), 785 nm (middle), and 633 nm (bottom).

A second series of tests involving the three excitation wavelengths was completed using a plain white envelope, one of the more common packaging types that were encountered as a smuggling matrix in the literature. The results of this testing, as illustrated in Figure 11 below, indicated that only the 785 nm wavelength was suitable for further testing.

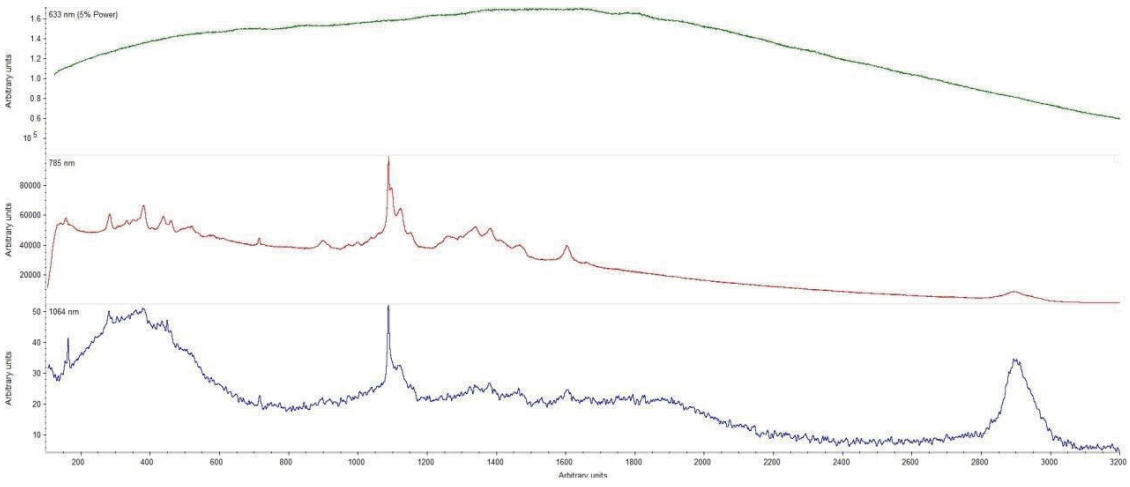

Figure 11 - Comparison of spectra collected from a plain white envelope at excitation wavelengths of 1064 nm (bottom), 785 nm (middle), and 633 nm (top).

As can be seen, the 633 nm laser wavelength produced an overwhelming amount of fluorescence, even at the 5% (~25 mW) power level that is shown above in Figure 11. Comparison of the remaining two excitation wavelengths indicated that while the 1064 nm diode laser had captured adequate peaks from the envelope without overwhelming fluorescence, the level of noise present in the baseline was far greater than that found in the 785 nm laser. For that reason, the 785 nm excitation laser was found to provide the best results, and so was selected for use in the remainder of the study.

6.1.1.3 Laser Power

The available range of 1% to 100% laser power was examined to review the various effects of the laser power on the quality of the spectra obtained. A series of spectra were collected from a pure standard of atropine, with all settings and focus kept constant, while the laser power was varied. The results of this examination are shown below in Figure 12.

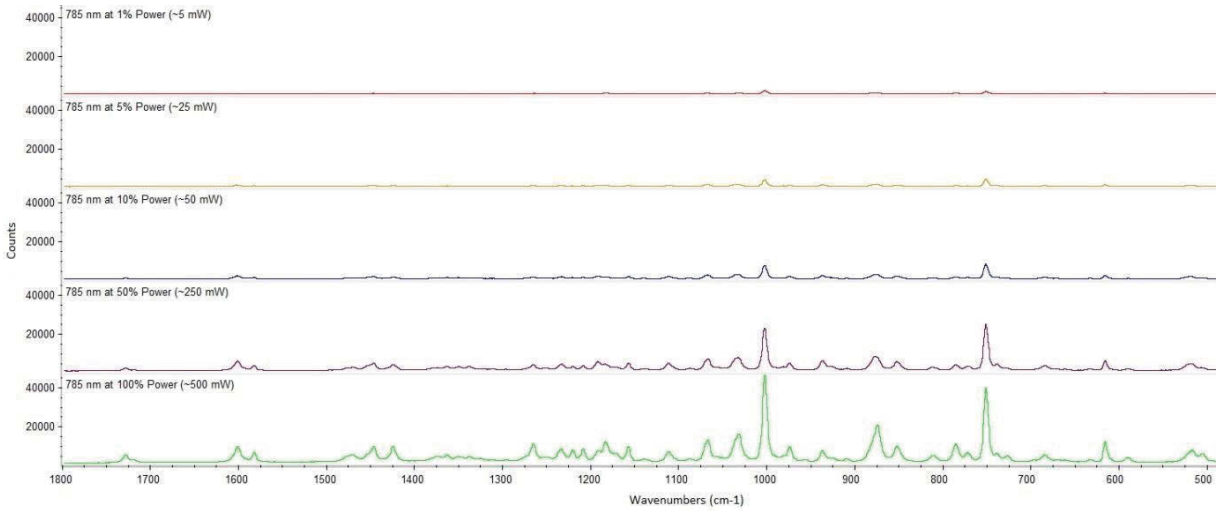

Figure 12 - Comparison of a changing laser power on the spectrum of pure atropine.

The results obtained largely reflect the observations previously found by Liang, Tse et al., with the greater laser power generating an increased intensity within the Raman spectra (Liang, Tse et al. 1993). Use of the maximum laser power in all experiments was noted to give optimised results, however early experiments using LDPE and newspaper showed that this strategy was not always appropriate. Sample degradation, particularly burning or melting of the packaging material was found to be a relatively common occurrence when using 100% laser power, as the laser power density was far higher than the materials could withstand. In an effort to subvert this damaging effect, a laser power of 50% was instigated as the default setting for each examination, with the laser power percentage then lowered if thermal degradation occurred.

6.1.1.4 Spectral Range & Other Programmable Parameters

The spectral range over which data is collected can greatly enhance the level of information gathered during analysis. To ensure that no important spectral data from either the atropine standard or packaging materials were initially omitted, a range of 120 to 4000 cm^{-1} was utilised for all SORS and conventional Raman measurements. Five spectral accumulations were collected to enhance the quality of each spectrum, and a ten second exposure was utilised.

The use of greater number of accumulations, increased exposure time, and the interrogation of a wider spectral range of wavenumbers proved little advantage and served only to increase the run time of each analysis.

6.1.1.5 Focus of the Raman Microscope System & Axicon Position

Obtaining the optimum focus on a sample is known to produce a more accurate spectrum when utilising Raman microscopy, particularly when attempting to quantitatively examine a sample (West and Went 2011). A seemingly contradictory effect has been noted when exploring depth profiling and a defocused system in the interrogation of simple two-layer systems. For a conventional Raman microscope, Eliasson et al. has shown that a defocused system can produce a substantial variation in the relative ratio between surface and subsurface layers, often serving to enhance the signal from the subsurface space (Eliasson, Claybourn et al. 2007).

Although this practice produces less clarity with slightly more noise, the favourable results Eliasson et al. observed could potentially be used to optimise the method at hand. To examine this potential, a series of measurements were taken involving a sample of atropine concealed beneath a plain white piece of paper. As in the nature of inverse micro-SORS systems, the distance between the sample and the axicon in all measurements remained fixed, while the change in focus was achieved by varying the distance of the microscope objective and the sample. Spectra were collected at the point of optimum focus for a conventional Raman system, and then at distances of -10, -5, +5 and +10 mm (where a negative value indicates movement of the microscope objective towards the sample, and a positive value indicates movement of the microscope objective away from the sample).

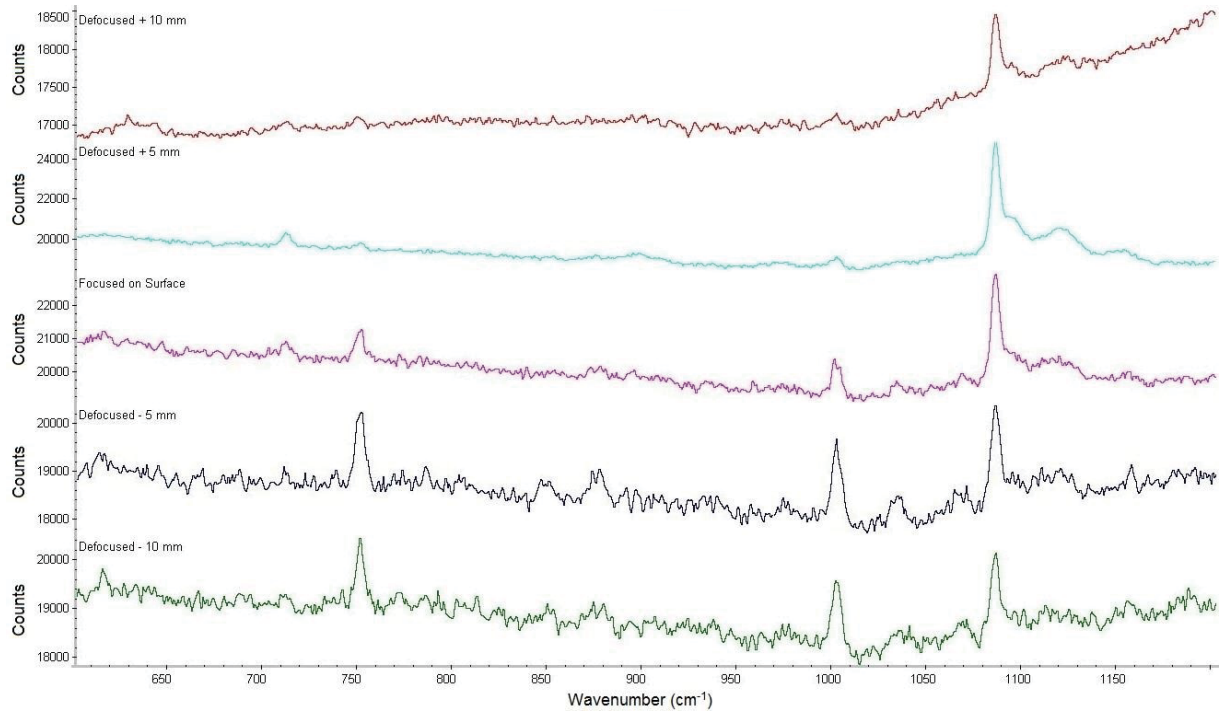

Figure 13 - Comparison of Raman spectra collected from a two-layer sample of atropine concealed underneath plain white paper. Each spectrum collected at the differing focal points noted.

As can be seen in Figure 13 above, reducing the distance between the sample and the microscope objective both increased the prominence of the peaks at 750 cm^{-1} and 1000 cm^{-1}, which are characteristic of atropine, but also reduced the large peak at 1086 cm^{-1}, which is representative of the calcium carbonate found exclusively in the office paper.

By focusing the SORS micro-system approximately 10 mm inside the samples being questioned, an enhanced spectrum, where the atropine signals are intensified and the packaging's signals diminished, can be obtained. Secondary examination of this trend using additional samples such as high density polyethylene (HDPE) and paper envelopes of varying colours further confirmed these observations, and aligned the defocusing practice as a constant element in the finalised method.

The optimal position of the axicon lens was found to be largely dependent on the focus of the microscope objective. As described by Dépret, Verkerk, and Hennequin, (Depret, Verkerk et al. 2002), maintaining a close distance between the microscope objective and the axicon will ensure that the focal points of both lenses are approximately equal. This meant that once focused upon the sample of the packaging, and then defocused inwards by 5 mm, aligning the axicon and objective closely would help to ensure optimal focusing was completed and enhanced results collected.

This theory was examined, and was found to hold firm; as with increasing distance between the microscope objective and the axicon, there was increasing fluorescence from the backscattered light, and a reduction in the visibility of peaks associated with the concealed atropine sample.

6.1.2 Axicon Characteristics

The axicon lens purchased from Eskma Optics was crafted from borosilicate glass Schott BK7, which is an extremely common crown glass used in precision lenses. This material was selected as borosilicates contain approximately 10% boric oxide, have good optical and mechanical characteristics, and are highly resistant to chemical and environmental damage. Another important factor was the materials clarity, and its minimal absorbance of wavelengths within the visible range and down towards 350 nm. These characteristics would ensure the production of a clean laser ring, without any major obstructions or absorptions. It would also aid in reducing the possibility of small changes in the axicon with use, ensuring repeat measurements remained as reliable and accurate as possible.

The lens selected featured a 25.4 mm diameter, and had a 175° apex angle (with base angles of 2.5°). While a more acute apex angle would cause greater refraction to occur, a more obtuse apex angle was eventually selected as it was the most easily obtained and cost effective.

6.1.3 Sample Characteristics

While the ideal parameters for both the laser and axicon can be researched, observed, and generally chosen to suit a particular purpose, the characteristic of each sample are set, with little to no freedom to vary their structures while maintaining the integrity of each parcel. With this in mind, a degree of testing was done on various packaging types in the aim of better understanding the obstacles faced.

6.1.3.1 Thickness of Sample Layers

As noted when reviewing the available literature, SORS measurements can be greatly enhanced through the use of a thick sample layer, as the thicker layer will enable more photons to be transmitted from the concealed sample and collected by the detector. This observation was tested using samples of atropine arranged in layers of varying thicknesses, from 2.5 mm to 5.0 mm, 7.5 mm, and final 10.0 mm. Each atropine sample was concealed beneath a 0.8 mm thick piece of HDPE.

As can be seen in Figure 14 below, the prominent peak from the HDPE at approximately 1300 cm^{-1}, relating to the cumulative effects of CH_2 twisting (Sato, Shimoyama et al. 2002), remains at a relatively constant level of intensity at 20,000 counts. Meanwhile, the samples of atropine

show an increasing intensity with increasing thickness. A comparison of the peaks at 750 cm^{-1} and 1000 cm^{-1} revealed that the 2.5 mm thick atropine sample had intensities of only 14,500 and 15,000 counts respectively, while the 5.0 mm thick samples held intensities of approximately 19,500 and 20,000 counts respectively. Above this thickness, there was minimal improvement of the signals, with both the 7.5 mm and 10.0 mm thick samples of atropine registering intensities of just over 20,000 counts for both peaks.

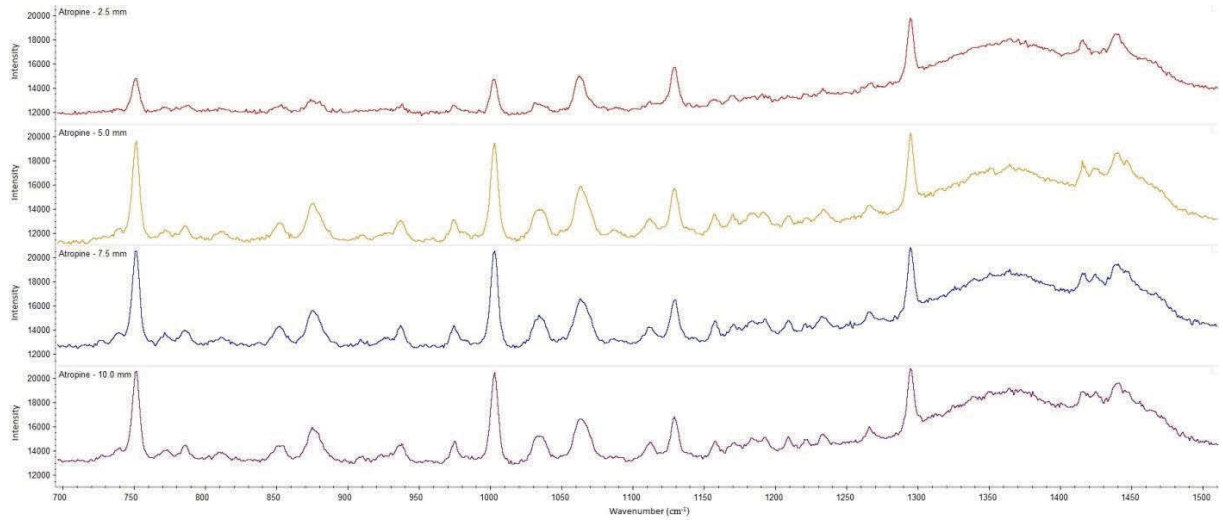

Figure 14 - Comparison of SORS spectra collected from samples of atropine beneath a piece of HDPE. Atropine thicknesses, 2.5 mm (red), 5.0 mm (yellow), 7.5 mm (blue) and 10.0 mm (purple).

Importantly, this series of testing revealed that by using a sample of atropine, measured to 5 mm in thickness or greater, a more enhanced SORS spectrum of the concealed sample can be revealed.

The same effect on the layer's thickness was noted to occur for the sample packaging, and the observations previously noted in the literature were mirrored in a further series of tests relating to the thickness of the packaging concealing the substance of interest. In these experiments, a

sample of atropine, at constant thickness of 5.0 mm, was concealed beneath layers of plain office paper (at a thickness of 0.15 mm per sheet) and packing foam (at 0.556 mm per layer), independently.

In both constructs, increasing the number of layers of the packaging, thereby increasing the thickness, resulted in diminished signals from the concealed atropine, and greater prominence of signals originating from the packaging. These effects can be seen in Figures 15 and 16 below, in which the peaks at 750 cm^{-1} and 1000 cm^{-1} grow weaker with subsequent layers of either packaging.

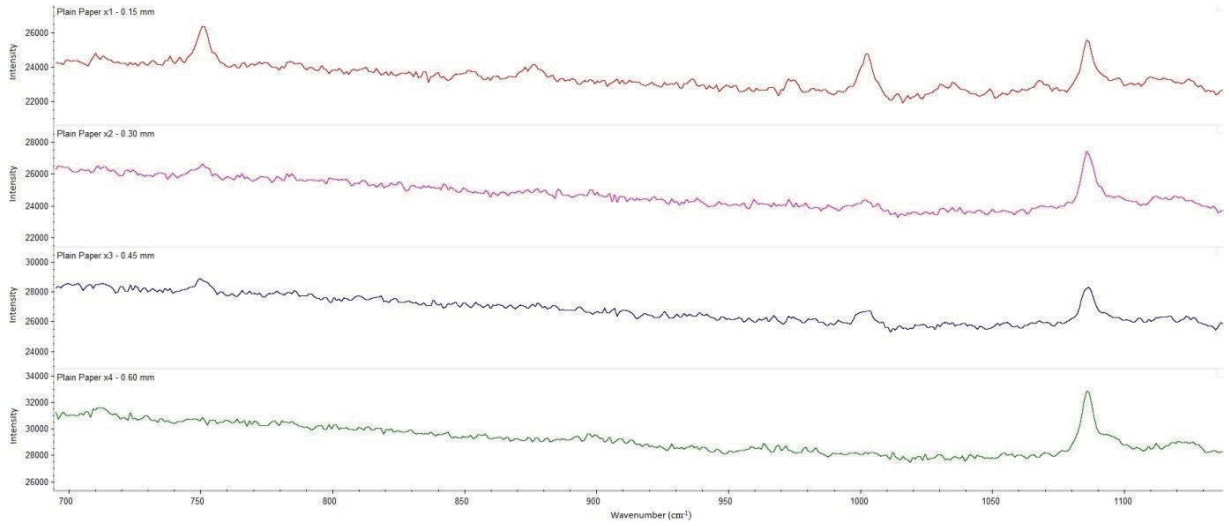

Figure 15 - Comparison of SORS spectra collected from a 5.0 mm thick sample of atropine concealed within increasing layers of 0.15 mm white paper. The spectra in order of increasing paper layers, where 1 layer is shown in red, 2 layers in pink, 3 layers in navy, and 4 layers in green.

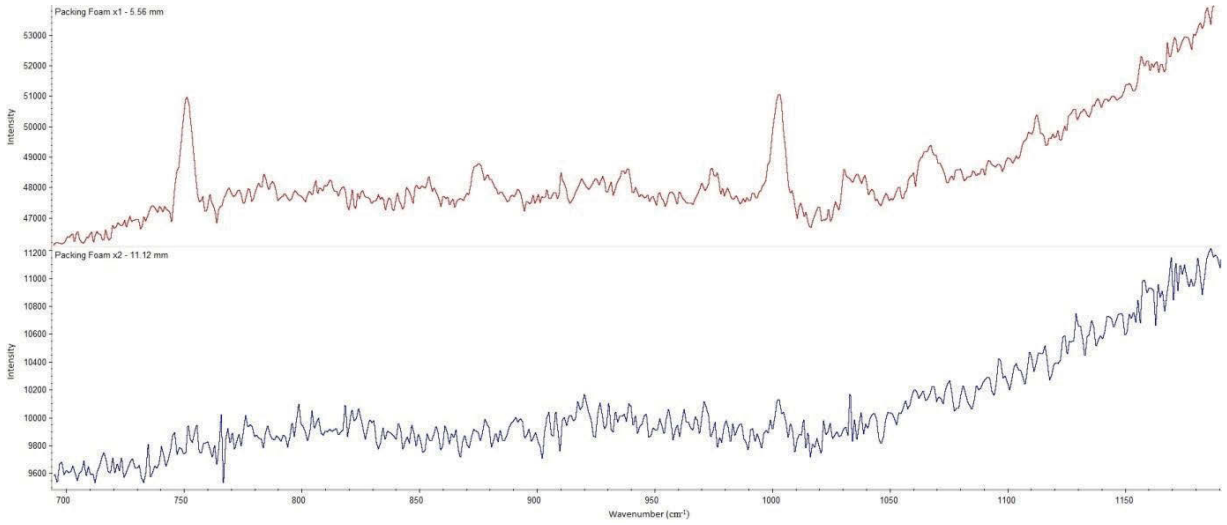

Figure 16 - Comparison of SORS spectra collected from a 5.0 mm thick sample of atropine concealed within increasing layers of 5.56 mm packing foam. The top spectrum in red is representative of 1 layer of foam, while the blue spectrum is 2 layers.

While it is clear from these examples that the thickness of each layer in a sample has a dramatic effect on the spectra obtained, the greatly different thicknesses of the paper and packing foam, and the varying intensity of atropine signals in the results obtained indicated that the successful application of the SORS method was not dependent on thickness of layers alone, but also on the density, colour, and transparency of the packaging type.

6.1.3.2 Density of Packaging Types

As a large number of the packaging types to be examined were paper and cardboard based, a rough estimation of each sample's area density was calculated in grams per square meter (GSM). While a direct comparison of identical packaging materials with different densities was not possible, a comparison between samples of white HDPE and LDPE was.

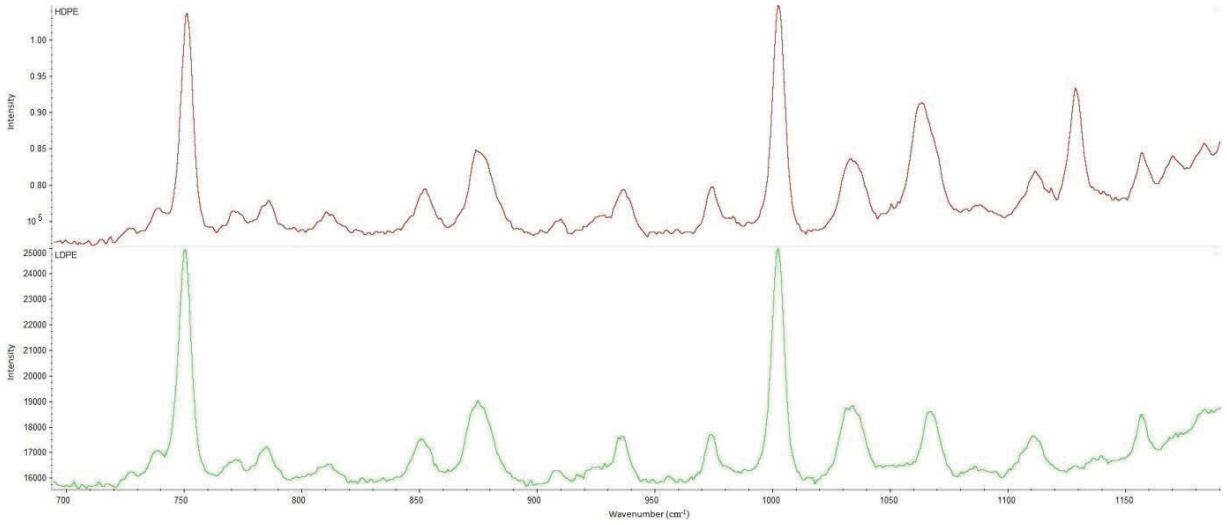

Figure 17 - Comparison of SORS spectra collected from atropine concealed beneath HDPE (top) and LDPE (bottom).

As seen in Figure 17 above, there is a noted increase in signal intensity for the atropine peaks at 750 cm^{-1} and 1000 cm^{-1} in the spectrum correlating to the sample involving the HDPE. When comparing the calculated GSM values, it was noted that the HDPE held a much higher value, with approximately 654.10 g/m^2, while the LDPE was only 111.52 g/m^2. These results mirrored the previous findings in Figures 15 and 16, where the denser packing foam (GSM of 101.76 g/m^2) was far more penetrable than the paper (GSM of 81.16 g/m^2). Evidently, the density of the packaging was not a major influence on the susceptibility of a packaging type to the SORS method.

6.1.3.3 Transparency of Packaging Types

One observed difference between the HDPE and LDPE samples, and the paper and packing foam samples, was the transparency of packaging types. In both cases, the more easily penetrable sample was the least opaque. These results matched the theory uncovered in the literature, where

opaque and turbid samples were said to be much more difficult to measure due to the reduction in the excitation energy penetrating the sample, and an increased amount of light being reflected.

6.1.3.4 Colour of Packaging Types

One of the remaining phsyical characteristics of the packaging that also had to be examined was the effect of the sample's colour on the spectrum obtained. Conventional Raman and SORS methods are known to be limited by dark, strongly absorbing samples, and so the interrogation of black and dark packaging was known to be difficult.

A final series of experiments were conducted to investigate the various effects of different coloured papers using a Micador 'Create It' Art Pad that featured ten distinct colours, Black, Blue, Brown, Green, Orange, Pink, Purple, Red, White, and Yellow. Each of the spectra were taken using conventional Raman spectroscopy with a spot focus under 20x objective and 785 nm excitation laser. All samples tested also had identical area densities of 80 g/m^2; ensuring that the only variable in each measurement was the colour of the sample. The resulting spectra, along with the laser power used to capture each individual spectrum are shown in the appendix.

As can be seen, the typically darker colours of black and brown produced minimal, defineable peaks, as the majority of the laser light was absorbed by the paper. This same effect was also noted with the black LDPE sample.

Interestingly, the slightly lighter colours of purple, blue, and green did transmit defined peaks, but a much lower (≤10% laser power) had to be utilised to minimise the overwhelming

fluorescence that occurred with higher settings. The remaining, lighter colours of orange, pink, red, white, and yellow emitted no fluorescence and produced useful spectra at 50% laser power, the highest possible setting applicable without causing damaging degradation of the packaging type.

6.1.3.5 Fluorescence of Packaging Types

For conventional Raman spectroscopy, fluorescence has continued to be a major barrier to the interrogation of many samples. It had been mentioned in many research articles that fluorescence could be minimised by using a displaced geometry, as done in most SORS methods. To compare the effects of SORS with conventional Raman spectroscopy, a final experiment was conducted in which a 5.0 mm thick sample of atropine was concealed beneath brown paper, a packaging type known to exhibit fluorescence. Both mock parcels were examined using 100% laser power, with the results shown in Figure 18 below.

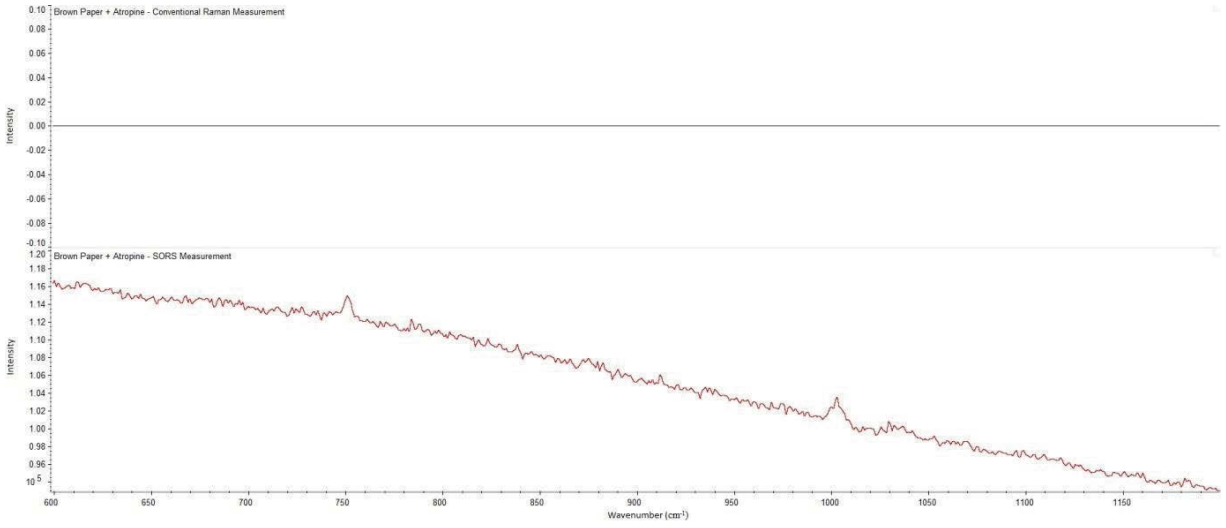

Figure 18 - Comparison of the relative levels of fluorescence obtained when examining a sample of atropine concealed beneath brown paper with conventional Raman microscopy (top) and the developed SORS method (bottom).

When considering the spectra obtained, it is immediately clear that the SORS methodology greatly reduced the obscuring effects of fluorescence, to the point where the atropine peaks at 750 cm^{-1} and 1000 cm^{-1} were visible. This last experiment pertaining to development of a micro-SORS method proved irrefutably that the new geometry had discernible benefits.

6.1.4 Mock Parcel Assembly

To ensure efficiency and easy recycling of the atropine powder, each 5g sample was kept within a thin, wallet sized Ziploc bag made of polyethylene plastic resin. This bag was used so that the powder would not disperse and be lost between changes of the packaging material, and to ensure that a thick layer of the atropine could be maintained. The Ziploc bag was found to have a simple and non-interfering Raman spectrum, making it an ideal vessel to hold the concealed powder.

Furthermore, the transparency of the bags ensured minimal absorption of the excitation laser, while the small thickness would help reduce any issues with permeability of the laser light.

To emulate a complete package concealing the atropine, strips of each material were wrapped around the Ziploc bag, ensuring the top and bottom of the sample were covered in a single layer of the packaging. For materials such as the PVC and HDPE where this structure was not possible, a square cutting of the packaging was simply placed on top of the atropine filled bag, creating a simple two-layer sample (three if including the Ziploc bag).

These mock parcels were then positioned on the microscope stage, with the mounted axicon placed on top. This enabled quick transition between the conventional Raman spot measurements and the SORS ring measurements without disruption of the sample or instrumentation.

6.2 Method Development – Quantification of Atropine

An important step in the construction of each quantification model was the pre-processing and accuracy of the calibration spectra. Analysing each spectrum at a smaller spectral range was found to increase the accuracy of a created method, allowing for non-essential, and interfering peaks to be removed from the analysis while maintaining focus upon target peaks. To this end, all spectra were truncated to a range of 200 cm^{-1} to 1800 cm^{-1} prior to any further examinations.

Once truncated, a sequence of smoothing, normalisation, Standard Normal Variate (SNV) and detrending, and baseline correction was applied in an effort to remove local variations and disturbances from the experiment and Raman spectrometer, as well as to aid in the removal of non-linear patterns and to ensure that the baseline was set to a level intensity of zero counts.

Once completed, the corrected spectra were all examined as a line graph, with each concentration colour coded and examined to ensure a progressive rise in peak intensity with concentration.

These pre-processing stages not only allowed for the identification and removal of apparent outliers, but also ensured that only the most accurate and pertinent of spectra were used in the chemometric models. Once processed, the initial analysis was achieved by constructing a

PCA model from the spectra, thereby enabling each sample to be identified in terms of its base components.

After this stage, a Partial Least Squares (PLS) Regression model using the constructed known calibration samples, those of 0%, 10%, 20%, 40%, 60%, 80%, and 100% by weight of atropine (and diluted with baking powder) was completed, with related responses given for each concentration. The PLS Regression model was built using the NIPALS algorithm and full method validation. Once constructed, this model was used to predict the concentrations of the three validation samples, those of 25%, 50%, and 75%, all of which had previously undergone equivalent pre-processing methods and the inclusion of a reduction (averaging) phase, ensuring that the ten collected spectra combined to give a single, representative spectrum of each concentration and prediction.

6.3 Method Development – Analysis of Complex Mixed Samples

While comprehensive in nature, the preliminary identification and quantification methods dealt purely with single layer parcels, excluding the plastic bag in which the powders were held. To more effectively examine the capabilities of the developed SORS method, a series of complex powders were measured using atropine, baking powder, caffeine, and crushed aspirin.

In each of these samples, the quantity of the three adulterants was kept equal in each sample, while the amount of atropine involved varied, ensuring that all concentrations were easily made by weight of atropine. Each of these samples were then analysed using the same procedure as previously detailed, however due to time constraints only the following packaging types were

examined with the complex, mixed samples – LDPE, Australia Post PB3 padded bag, opaque polystyrene, white cardboard, and the PPS Plainface DL white envelope.

Once collected, a scaled subtraction was employed to reveal the spectrum of the underlying samples, while Principal Component Analysis (PCA) and Multivariate Curve Resolution (MCR) was then employed in an attempt to elucidate the pure component spectra.

It was the hope that this brief examination of more complex samples would appropriately demonstrate the overall power and specificity of both the SORS technique and the chemometric processes.

6.4 Method Development – Analysis of Complex Packages

A final stage in this research was to assess the overall effectiveness of the developed method when considering more complex, multi-layer packages. In theory, the addition of more layers and packaging types should not hinder the developed method, as the scaled subtraction aims to remove the influence of the surface layers, however, as seen, different packaging types, colours, and densities, can have a dramatic effect on the method.

To address this, six multi-layer packaging combinations were designed, each involving one or more of the most commonly found packaging types. These complex packaging types were analysed in the same way as previously mentioned, with the successive collection of a conventional and spatially offset spectrum.

Due to constraints with time, all combinations of the packaging types could not be examined, however six three-layer samples of varying combinations and packaging types were created, involving brown tape, bubble wrap, HDPE, LDPE, polystyrene, a padded bag, a white envelope, and white cardboard.

Combined into several three-layer packaging types, these materials enabled the upper limits of the developed method to be examined, as well as providing more insight into the various sample characteristics that would either enable, or impede, the method.

Chapter 7 – Proof of Concept Studies

Although the method developed during the course of this research was extensively based upon previously successful studies and experiments, it was deemed necessary to collect data that would substantiate the claim that an effective inverse SORS technique had been created. In aid of this point, a simple series of tests to examine the effect of the axicon on a monochromatic beam of light was devised. Furthermore, to ensure results in keeping with an inverse SORS method were obtained from the devised method, two previous studies by William L. Olds et al. (Olds, Jaatinen et al. 2011) were replicated, with a comparison of results enabling the effectiveness and application of the method to be examined.

7.1 The Axicon

Although the use of an axicon to convert conventional Raman spectrometers into functional inverse SORS geometries has been well documented, with various aforementioned papers acting as a testament to their use, working proof of its application in this study had to be shown. To illustrate this point on a safe and sufficiently large scale, a simple set up involving two parallel retort stands was devised.

In the arrangement, one retort stand was positioned to hold a 1mW micro laser pointer (Dick Smith, Model Number: XP0671), which produced a red, 650 nm laser beam through a simple push-button. The second retort stand was positioned parallel to the first, and held the axicon within its mount, attached to a six-inch-long, Ø 0.5-inch optical post (ThorLabs, Part Number:

TR6). Both the optical post and laser pointer were attached to the retort stands using retort clamps and boss heads.

With the laser pointer's activation button held down, it then projected the red laser beam through the axicon, projecting the refracted laser beam on to a plain white wall, which was then photographed.

The results of this simple investigation proved that the axicon could successfully create the refraction necessary to form a wider diameter laser ring for inverse SORS measurements. As can be seen in Figures 19 below, the axicon easily facilitated the necessary refraction, creating a ring several centimetres wider than the actual point focus of the unrefracted laser beam.

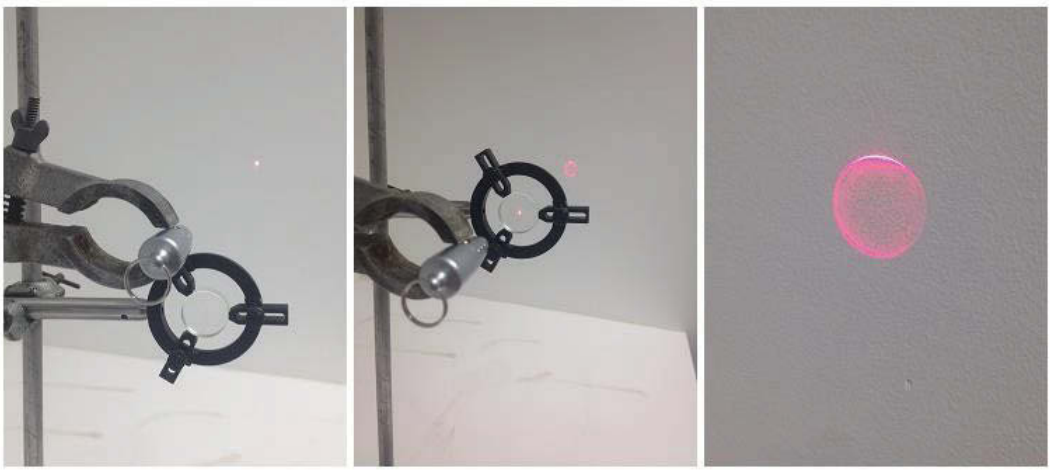

Figure 19 - Proof that the axicon used could facilitate the formation of a ring of laser light from a single point.

It can be seen, that while the ring itself is clearly apparent, it is not cleanly projected with some scattering or blurring of light creeping into the centre of the ring.

While this is of some concern, the appearance of this scattering can be viewed largely as negligible for a number of reasons. When comparing the laser used in this brief experiment to that used in the actual Raman analysis, it's clear that several key differences exist. The laser pointer used in the demonstrations was far less powerful (1 mW compared to the 500 mW capacity of the Renishaw laser), and was largely unfocused and likely uncollimated, making its divergence greater than that of the 785 nm infrared laser utilised in the experimental work. Furthermore, the overall laser quality found in the pointer is far reduced when compared to the 785 nm infrared laser, simply because their purposes are greatly different, and so a greater divergence from the laser pointer is to be expected. A final important note is also the greater distance used in the demonstration; for the experimental work, the laser source is constantly within 10 mm of the axicon and within 20 mm of the sample, while in the demonstration shown in Figures 20, 21 and 22, the laser pointer is approximately 50 mm from the axicon and almost 610 mm (2 feet) from the wall (Winburn 1989, Laufer 1996).

Taking these factors into account, it is easy to understand why a far lower degree of divergence would be expected from the 785 nm laser used in the analytical work, ensuring that a fully formed and focused ring would be presented during the experiment. Another way of viewing the apparent divergence as negligible is by considering the subtraction performed to obtain the final SORS spectrum. Any information collected by the diverged laser light would also be present in that of the conventional spot spectrum, as the spreading light tends towards the centre and reduces the spatial offset. In this case, the subtraction of the conventional, spot spectrum from the spatially offset spectrum would largely remove any real interference

7.2 – Testing the Method

With the axicon found to be functioning as predicted, it was also required to test the effectiveness of the devised method. In an effort to ensure that an inverse SORS method had been created, two previously published experiments by William J. Olds et al. (Olds, Jaatinen et al. 2011) were re-created so that the observed results could be compared as directly as possible. If the results proved to be highly similar, then the devised method could be considered to be successful. In each case, the experimental method was produced as faithfully as possible, with all changes noted and explained below. In both the original work and the recreations, a 785 nm laser was utilised, along with an axicon, allowing for an accurate comparison of the results to be made.

The first experiment involved a padded postbag and a concealed sample of barium sulphate powder. The package, along with the method of testing the package, is shown below in an excerpt from the paper by William J. Olds et al (Olds, Jaatinen et al. 2011).

"A padded postbag was probed with the SORS device. The postbag had a thick white paper exterior (a few hundred microns thick) and an inner layer of transparent bubble wrap which are together a few millimeters in thickness. This type of postbag has a sturdy, rugged construction and is commonly used to post items that require a strong protective package. A sample of barium sulfate powder, common filler in pharmaceutical preparations (~ 5 g in a small plastic bag, 1 cm depth), was placed inside and the laser was incident on the exterior of the postbag near the

position of the concealed sample. Spot and ring measurements were taken with ten, 5- second exposures. The spot measurement yielded significant fluorescence originating from the paper."

In the recreation, a similar postbag was acquired; however, the same make and manufacturer could not be confirmed. In both cases, the postbag was predominantly white, had a paper exterior and transparent bubble wrap interior, and was recorded to be 2.08 mm thick. A pure sample of Barium sulphate was obtained from BHD Chemicals, from which 5.0344 g of the compound was taken and concealed within a small, transparent bag made from polyethylene plastic resin. The sample was then arranged to meet the 1 cm depth requirement specified in the study, before being concealed within the padded bag.

Once this had been arranged, both the conventional spot measurement and the spatially offset measurement were collected using five, ten second exposures. This was differed from the original method; however, it was found to be a necessity as the WiRE software would not allow exposure times of less than ten seconds. In an attempt to reconcile this difference, the number of measurements was reduced, ensuring that each sample received a similar exposure time of fifty seconds in total.

The results from Willliam J. Olds' research, shown below in Figure 20, indicated considerable fluorescence from the post bag, as well as two peaks at ~ 985 cm^{-1} and ~1085 cm^{-1} in the 'Spot' measurement, and a dominant single peak at ~ 985 cm^{-1} in the 'Ring' measurement, leading to a scaled subtraction almost identical to that of the reference spectrum.

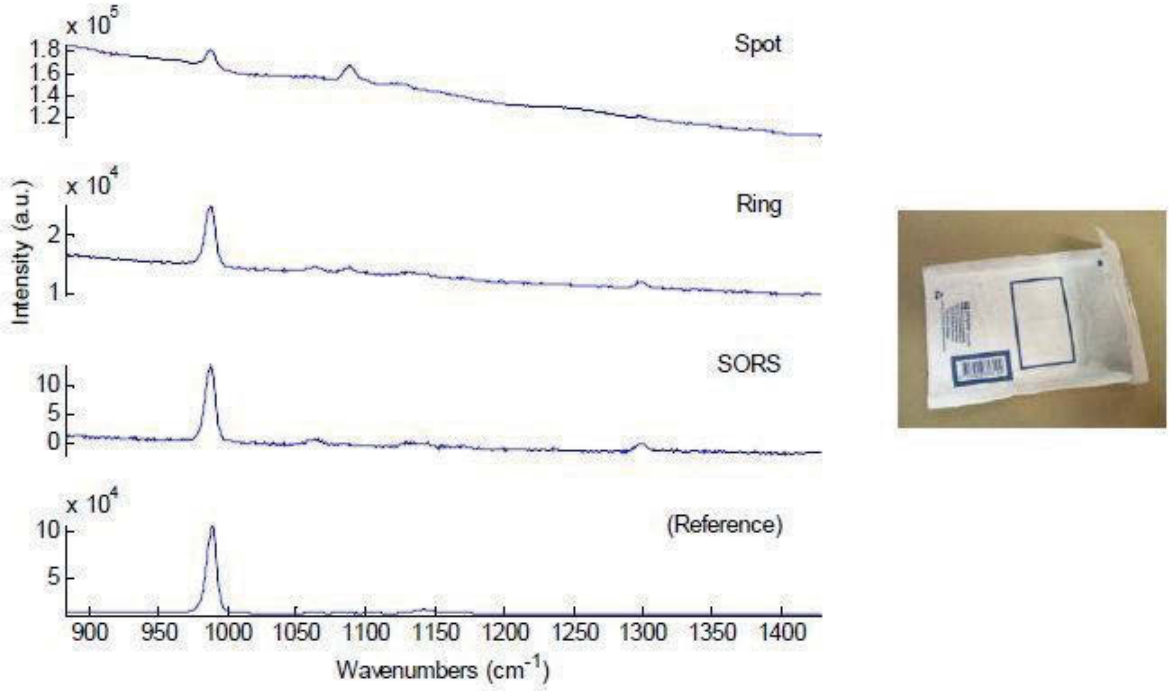

Figure 20 - Spectra obtained from the white postbag and barium sulphate sample in the original study by William J. Olds et al. (Olds, Jaatinen et al. 2011)

The results obtained from the re-enacted study (shown below in Figure 21) included a greater level of variation across the baseline and more significant peaks around 1085 cm^{-1} in the initial 'Spot' and 'Ring' measurements, however the final 'SORS' result was dominated solely by the prominent peak at ~985 cm^{-1} which was strongly identified as Barium sulphate with a quality of 84.30%. This peak also correlated with a previously reported spectrum of Barium sulphate (Harroun, Bergman et al. 2011), increasing the validity of the identification.

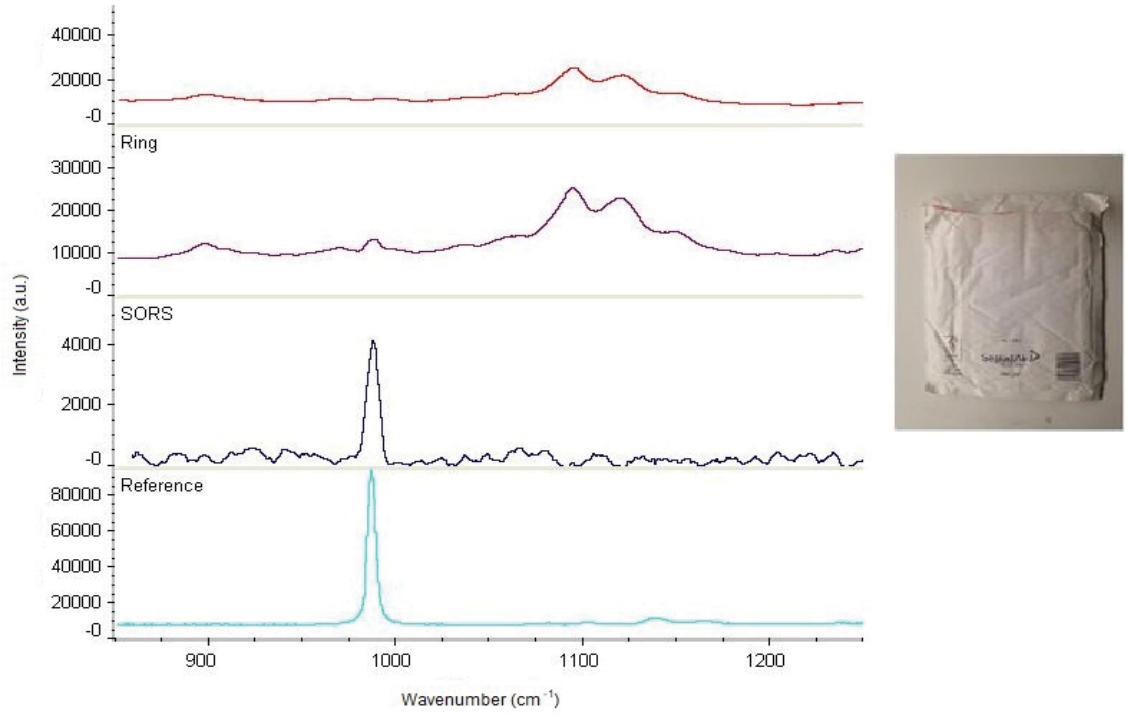

Figure 21 - Spectra obtained from the white postbag and barium sulphate sample in the re-enacted experimental work.

In the second experimental re-enactment, Olds et al. initially probed a yellow envelope containing a 1 mm-thick layer of acetaminophen, as referenced in the excerpt below (Olds, Jaatinen et al. 2011);

"...we probed a thick yellow paper envelope containing a 1 mm-thick layer of acetaminophen using transmission Raman. First the empty envelope was probed, giving strong fluorescence emission from the paper. Such a spectrum would be expected from a legitimate letter containing only paper. Once the drug was placed inside, however, a clear acetaminophen spectrum could be obtained through the envelope using the transmission geometry (5 x 1 second accumulations)."

Although there was a noted difference in geometry, and in the number and duration of accumulations utilised in the original study and the re-enactment, the results obtained were found to be highly comparable.

Both the original results from Old et al. (shown in Figure 22) and the observed results in the re-enacted study (Figure 23), with peaks corresponding to the acetaminophen appearing in both spectra around 1175 cm^{-1}, 1250 cm^{-1}, and near 1300 cm^{-1}, which also correlated with previously published reference peaks (Farquharson and Smith 2004, Qian and Chandler 2013). Furthermore, both spectra correlated with the reference spectra used, with the re-enacted study producing a correct identification of acetaminophen with a quality of 87.74%.

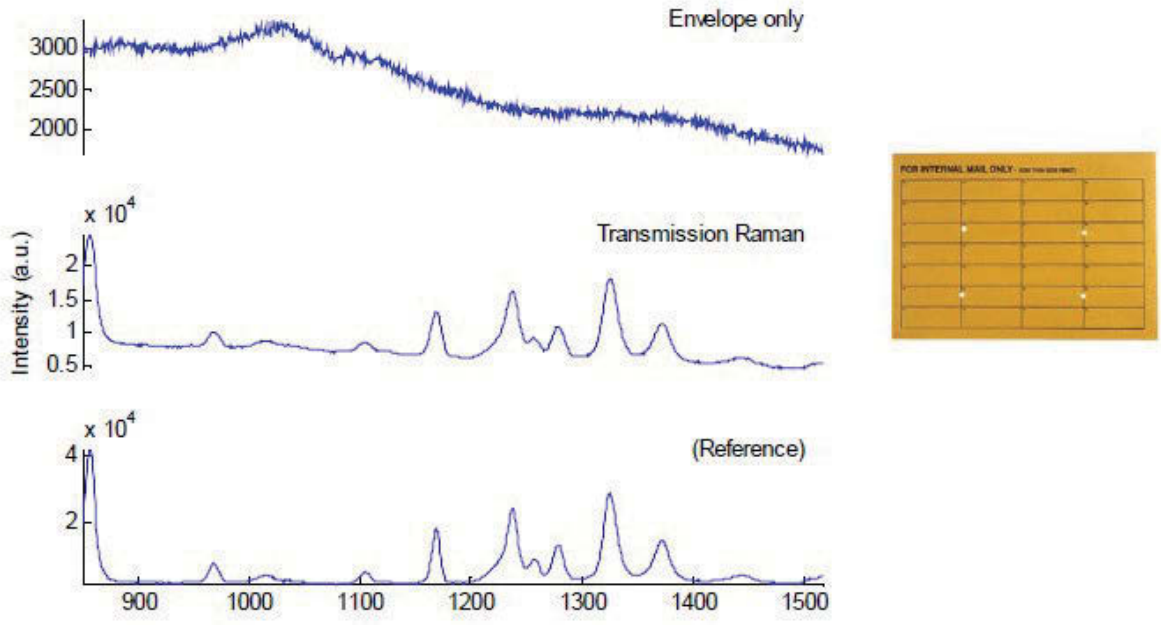

Figure 22 - Spectra obtained from the yellow envelope and acetaminophen sample in the original study by William J. Olds et al (Olds, Jaatinen et al. 2011).

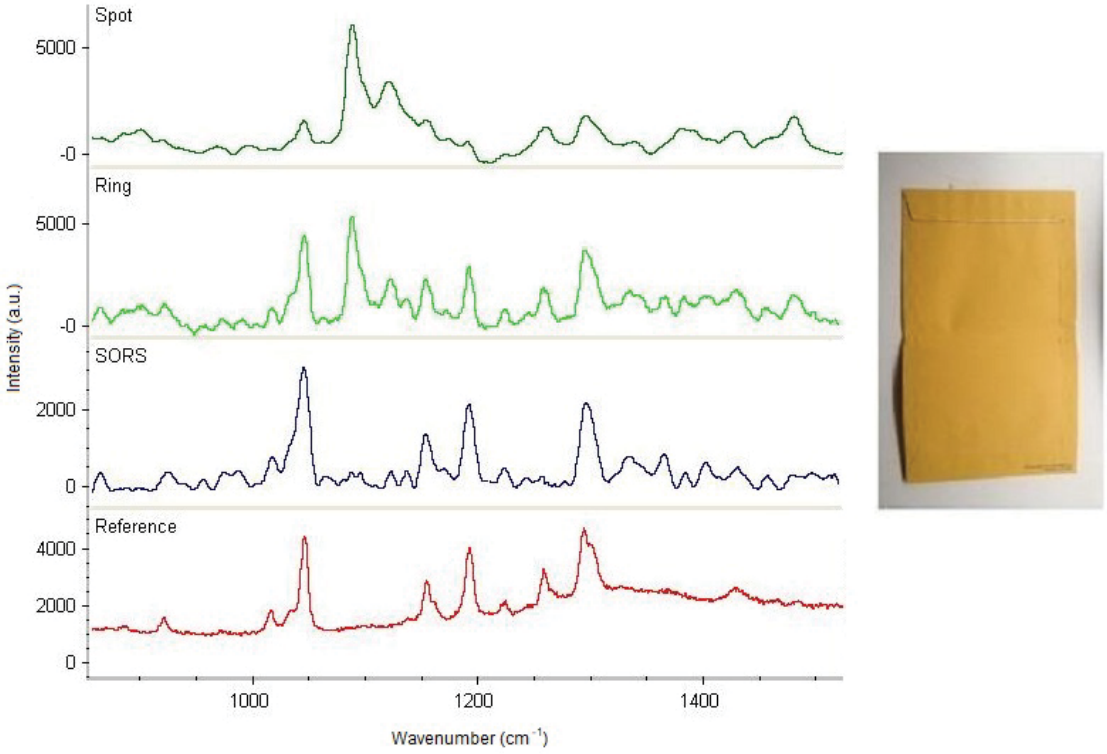

Figure 23 - Spectra obtained from the yellow envelope and acetaminophen sample in the re-enacted experimental work.

7.3 – Blind Tests

Not content with just confirming the effectiveness of the method through recreating previous studies, the method developed was also subjected to a series of 'blind tests' involving five envelopes and five unknown samples.

In each case, a plain white envelope was selected and labelled with a letter from A-E. A third and unrelated party then placed within each of the envelopes one of ten possible samples collected from a safe storage location. Each of these samples was designed to simulate a

concealed drug, and so all had the appearance of a simple white powder, however each sample differed in either concentration or composition. The ten samples included,

1. Baking Powder
2. Barium Sulphate
3. Homebrand Cake Mix
4. Crushed Aspirin Tablets
5. Atropine (Pure)
6. Atropine (75%) and Baking Powder (25%)
7. Atropine (50%) and Baking Powder (50%)
8. Atropine (25%) and Baking Powder (75%)
9. Caffeine
10. Acetaminophen

The envelopes, once filled with a sample, were sealed and returned for examination using the developed method, ensuring that no prior-knowledge of the samples' identity existed and making sure that the identification and quantification of the samples would rely solely on the accuracy of the method, and not on any bias of the examiner.

Each of the envelopes were examined in the same manner, with ten conventional and offset Raman spectra collected from various points on the envelope's surface. Each measurement was taken across the wavenumber range of 120 cm^{-1} to 4000 cm^{-1}, with two accumulations, a 10 second exposure time, and 50% laser power (250 mW) from a 785 nm excitation source.

With both the spot and spatially offset spectra collected, the WiRE software was used to smooth the spectra and adjust the baseline, before each spectrum was truncated to the wavenumber range of 120 cm^{-1} to 1800 cm^{-1}, then normalised to a maximum intensity of 25,000 counts to ensure the pairs of spectra were set to the same scale. The spatially offset spectrum was then corrected for any interference brought about by the axicon, before the two spectra were subtracted (SORS –

Spot). This revealed the isolated spectrum of the concealed powder which was identified using a database comparison.

To quantify the concentration of each compound, the collected spatially offset spectra were run through a partial least squares regression model built using known concentrations of atropine, with all predicted values noted down. The results of this blind testing, along with the actual identifications and concentrations of the unknown compounds are shown below in Table 1.

Table 1 – Results of the blind testing showing all envelopes and their predictions.

Envelope	Predicted ID	Predicted Conc.	Actual ID	Actual Conc.
A	Atropine	86.27%	Atropine	75.31%
B	Baking Powder	95.62%	Baking Powder	100.0%
C	Barium sulphate	42.99%	Barium sulphate	100.0%
D	Atropine	28.44%	Atropine	25.11%
E	Aspirin	16.59%	Aspirin	81.06%

The results of the blind testing were incredibly positive, revealing that all unknown samples were identified correctly without any false positives or false negatives recorded. Furthermore, the unknown samples hidden within envelopes A, B, and D were quantified within a reasonable margin of error, showcasing the abilities of the method. Regarding the remaining envelopes of C and E, the noted and distinctive difference in the actual and predicted concentrations can be attributed to the fact that a PLS Regression model built on atropine standards was used. Had the models been built using the spectra of Barium sulphate and Aspirin, it is expected that more accurate results would be obtained. Unfortunately, this test was not possible to complete due to a lack of time and materials.

Regardless of this small inconsistency, the re-enactments of experiments conducted by Olds et al. and the blind testing served to prove that the method developed was working exactly as predicted and with sufficient accuracy to continue further development and refining.

Chapter 8 – Powders & Packaging

While the elucidation of samples hidden within each package were the main focal points of this research, it was important to ensure that a thorough cross-section of all the available, potential packaging types was studied. Packaging commonly found in post offices and supermarkets were of keenest interest, with various tapes, padded bags, and papers being collected, however more novel items such as newspaper and plastics were also examined. Items such as glass and metals were ultimately removed from testing, owing to the multitude of research already published on SORS and glass, and the known fact that metals are impervious to the vast majority of spectroscopic techniques, or were not commonly used.

Furthermore, the samples which were hidden within the packages also had to be carefully selected. While real drug samples would have allowed conclusive statements on the methods effectiveness to be more easily made, the legality of obtaining such samples, and in great enough quantities was an unassailable issue. Instead, a promising substitute was selected, along with a variety of commonly used adulterants to help examine the full ability of the method.

8.1 Choice of Samples

8.1.1 Selection of Atropine

Due to the issues of legality, purity, and availability that surround cocaine hydrochloride, initial method development was achieved through the use of atropine. Atropine was found to be an ideal substitute, as its lower cost, relative ease of availability, and high structural similarity with cocaine allowed for an accurate simulation of results.

The noted similarity extends well into the structure of each compound, as seen below in Figure 24. As shown, the only differences in the structures of the two compounds are the additional ester group present in cocaine hydrochloride, and additional alkyl and hydroxyl groups present in atropine.

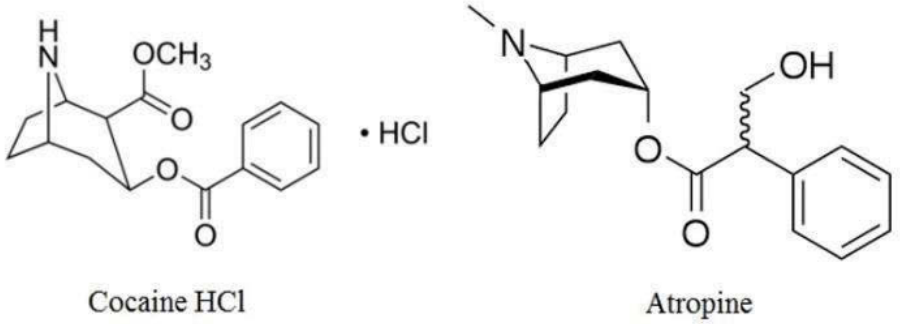

Figure 24 - The molecular structures of cocaine HCl and atropine.

Importantly, the similarity between the compounds is also strongly observed in their respective Raman spectra. It is known that the Raman spectrum of pure cocaine hydrochloride is found to have a number of characteristics that are essential to its identification (Ali, Edwards et al. 2009). These features include the benzoate ester (C=O) stretch that appears at ~1710 cm^{-1}, an aromatic ring (C=C) stretch at ~1595 cm^{-1}, ring breathing mode at ~1000 cm^{-1}, the pyrrolidine ring (C-C) stretch at ~866 cm^{-1}, and finally, the piperidine ring (C-C) stretch at ~785 cm^{-1}.

These features, specifically the ring breathing mode, the piperidine ring (C-C) stretch, and the aromatic ring (C=C) stretch are found to be equally present in the spectrum of atropine (Buckley, Kerns et al. 2014). These peaks allowed for the accurate and easy identification of atropine

within the more convoluted spectra of the target packaging materials, and made it highly likely that any developed model would be equally as accurate for cocaine hydrochloride.

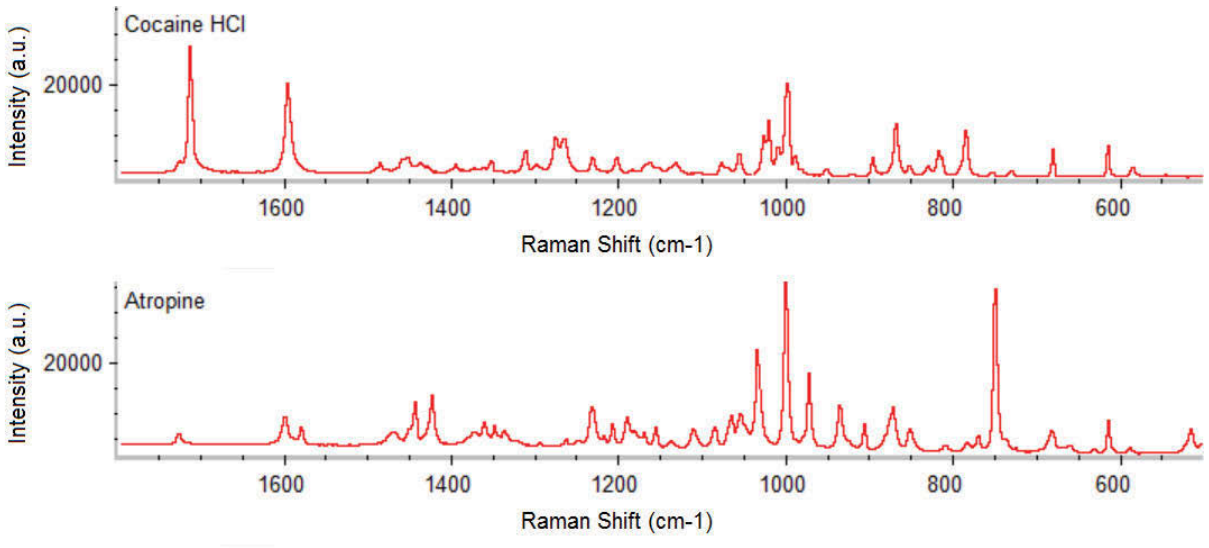

Figure 25 - The Raman spectra of cocaine HCl and atropine.

8.1.2 – Selection of Adulterants

To ensure samples of different concentrations could be constructed accurately, and to create more complex samples for interrogation, three basic powders were selected alongside the active pharmaceutical ingredient (API) of atropine. These three samples were Anchor brand baking powder, caffeine, and Coles' own brand Aspirin

Baking powder was primarily selected as it would allow for cheap, but effective large scale bulking of the atropine samples, while not producing many large peaks that would interfere with the spectra obtained from atropine. Furthermore, baking powder is commonly used in the drug trade to harmlessly increase the quantity of a drug, particularly in cocaine (Verster, Brady et al. 2012), making it a perfect choice as an adulterant in this research.

Predominantly baking powders are made up of corn starch, sodium bicarbonate and one or more acid salts, resulting in a simple spectrum of three distinct peaks at ~1250 cm^{-1} and ~1100 cm^{-1} resulting from CO_3 stretching, and lattice mode vibrations around 680 cm^{-1}, as can be seen below in Figure 26**.**

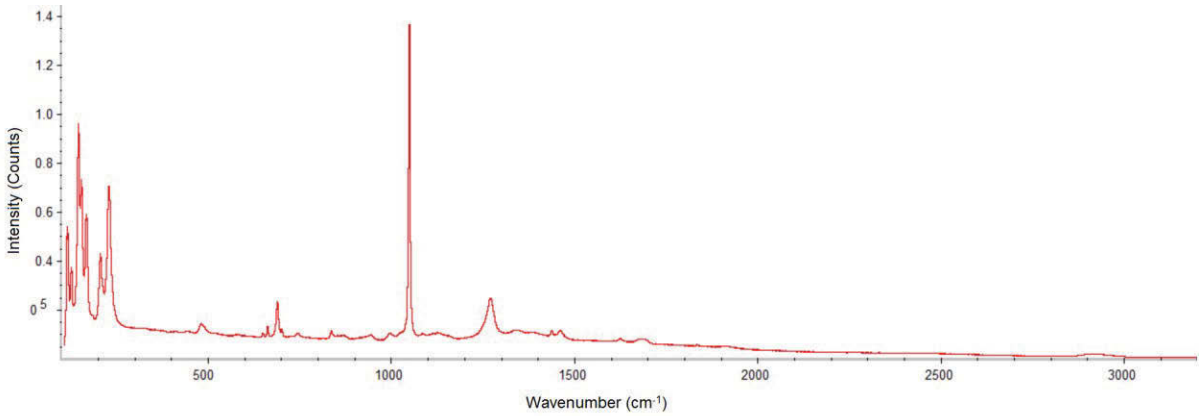

Figure 26 – Reference Raman spectrum of Baking Powder.

Caffeine was another prime choice as an adulterant in the study. It's inert nature, white colour, and powdered texture meant it could be used as a perfect, and visually indistinguishable adulterant, and as a standalone sample for examining the specificity of the devised method. Furthermore, caffeine has a long history of being used to cut and bulk illicit drugs such as cocaine, notably in South America (Brookshire 2015), but with growing prominence internationally (Mehta, Jain et al. 2004).

Pure caffeine was used throughout the study. With a far more complex Raman spectrum than baking powder, caffeine also acted as a more complex text of the devised method's ability to

differentiate peaks and identify more concealed target analytes. The more complex spectrum of caffeine is shown below in Figure 27, where notable peaks such as the imidazole ring at 1328 cm^{-1}, pyrimidine and imidazole rings (CH_3) at 740 cm^{-1}, pyrimidine ring (CNC and CH_3) at 555 cm^{-1}, and the pyrimidine ring (CNO and CH) at 483 cm^{-1} can be seen (Edwards, Munshi et al. 2005).

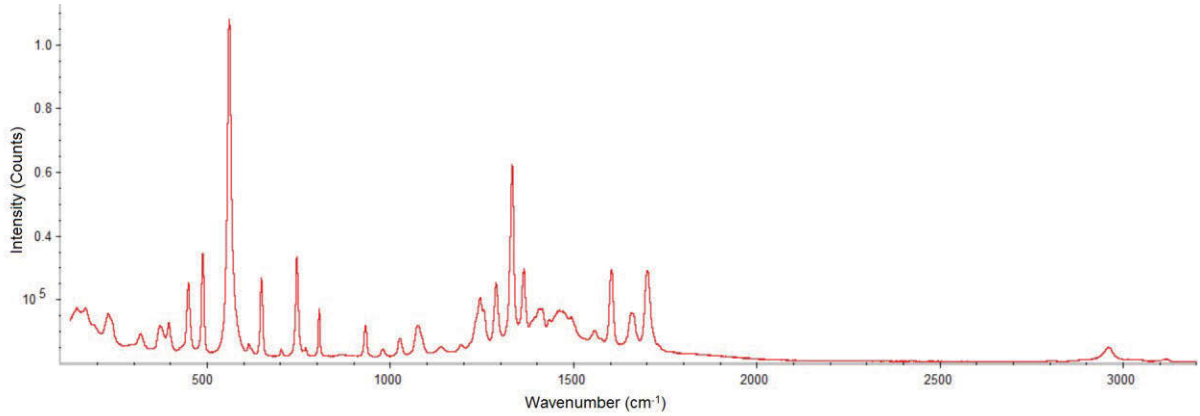

Figure 27 – Reference Raman spectrum of Caffeine.

Aspirin was another adulterant selected for its complex Raman spectrum and frequent use within the illegal drug trade. A common adulterant for many illicit substances (Esse, Fossati-Bellani et al. 2011), aspirin is also easily obtained over the counter, and generally appears as a white tablet or powder which can be used to bulk, adulterate, and cut a maelstrom of substances.

As seen below in Figure 28, the standard spectrum of aspirin revealed characteristics peaks at ~1000 cm^{-1} and ~1300 cm^{-1} , indicative of C-H vibrations, and aromatic C-H vibrations at ~810-860 cm^{-1} and 900-960 cm^{-1}, along with CO_2 rocking at ~615 cm^{-1}. Further peaks were also observed at ~1400 cm^{-1} and ~1625 cm^{-1} from C=C vibrations (Renganayaki et al. 2012).

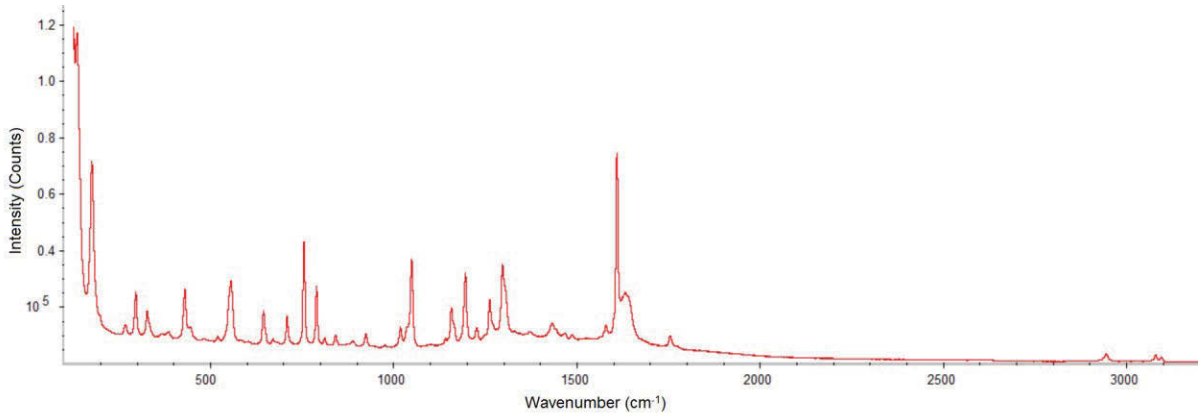

Figure 28 – Reference Raman spectrum of Aspirin.

8.1.3 Choice of Suspect Packaging Materials

The majority of the twenty-five packaging materials examined were selected based upon documented instances of use, while other samples were selected purely because they were easily available and commonly used in the construction of parcels.

A wide variety of packaging types were tested, with the exception of glass containers, bottles, and metallic boxes. The reason for their exclusion was predominantly based on the wealth of available literature testifying to their incompatibility with the SORS methods. Ultimately, the sample space tested included various coloured envelopes and papers, padded postal envelopes, plastic satchels, cardboards, and plastics.

The twenty-five selected packaging materials selected for analysis are shown below.

1. Australia Post Brand Bubble wrap
2. Australia Post PB3 Padded Bag
3. Australia Post Prepaid Parcel Post satchel – Small (500 g)
4. Australia Post brand brown packing tape
5. Australia Post brand clear packing tape
6. Black Low Density Polyethylene Satchel
7. Brown Cardboard
8. Brown Envelope
9. Generic bubble wrap (Coated in white LDPE)
10. Generic Padded Bag
11. Generic Padded Satchel
12. Generic Wrapping paper – Black & White pattern
13. Grey Cardboard
14. Newspaper (The MX)
15. PPS Kraft Paper – Brown
16. PPS Plainface DL White envelope
17. Packing Foam
18. Quill Coloured Envelope – C6 Orange
19. Reflex A4 White Paper
20. Semi-opaque High Density polyethylene square
21. Transparent polystyrene square
22. White Cardboard
23. White polystyrene square
24. White polyvinyl chloride tile
25. Wood Grain polyvinyl chloride tile

To ensure an analytical comparison of the results obtained, the weight, length, width, and thickness of all samples were measured using an analytical scale, rule, and digital callipers. From these measurements, the grams per square meter (GSM) of each packaging type were calculated using Microsoft Excel. The results of which are shown in the appendix.

Chapter 9 – Optimised Inverse SORS Method

From all the aforementioned experimentation, an optimised method for the successful detection and identification of concealed drugs using an inverse micro-SORS geometry was assembled. This method incorporated the optimised parameters observed during the method development phase of testing, as well as a streamlined method for the subtraction of the SORS and conventional Raman spectra that allowed for more rapid identification of the concealed sample's spectrum.

9.1 Sample Preparation

Within the experimental method, minimal sample preparation was required. Samples were prepared in accordance with previous work by A.G. Ryder et al. (Ryder, O'Connor et al. 2000), in which each sample was weighed and constructed to a pre-determined concentration by weight of target constituent. After weighing, the samples were ground together into a fine powder using an agate mortar and pestle, and then transferred and stored with a small, plastic Ziploc bag.

This process aided in maintaining integrity of the samples by minimising contamination, maintaining a simple and controlled method, allowing for sets of concentrations to be easily and efficiently produced, and increasing the sample homogeneity of the solid mixtures.

9.2 Detection & Identification

The Renishaw InVia Raman Microscope was set up in the traditional backscattering geometry, with the sample positioned beneath the microscope objective. Standard spectra of the unconcealed atropine, axicon, Ziploc bag and each of the twenty-five packaging types were first collected with spot illumination and the x50 microscope objective. All standard spectra were collected over a spectral range of 120 to 4000 cm^{-1}, with two spectral accumulations, 10 second exposure time, and using a 785 nm infrared laser with 1200 l/mm optical grating. While the spectrum of atropine was successfully collected with 100% laser power (500 mW), the variation in strength of each packaging type meant that individual laser powers had to be implemented to ensure accurate, but non-destructive spectra, free from fluorescence were collected. The various laser powers utilised were recorded in Table 2 below.

Table 2 – Record of laser power used for each tested packaging type.

Packaging Type	Laser Power (%)	Laser Power (mW)
Australia Post Brand Bubble wrap	50	250
Australia Post PB3 Padded Bag	50	250
Australia Post Prepaid Parcel Post satchel	50	250
Australia Post brand brown parcel tape	50	250
Australia Post brand clear packing tape	5	25
Black Low Density Polyethylene Satchel	5	25
Brown Cardboard *	1	5
Brown Envelope *	1	5
Bubble wrap (Coated in white LDPE)	50	250
Grey Cardboard	50	250
High Density polyethylene	100	500
Newspaper	50	250
PPS Kraft Paper – Brown *	1	5
PPS Plainface DL White envelope	50	250
Packing Foam	100	500
Padded Bag – White	50	250
Padded Satchel – White	50	250
Quill Coloured Envelope – C6 Orange	100	500
Reflex A4 White Paper	100	500
Transparent polystyrene	50	250
White Cardboard	50	250
White polystyrene	100	500
White polyvinyl chloride tile	50	250
Wood Grain polyvinyl chloride tile	50	250
Wrapping paper	50	250

Samples in which some fluorescence persisted are denoted with an asterisk (*).

Mock parcels were created using approximately 5 g of atropine held within a wallet sized Ziploc bag made of a polyethylene resin, arranged to create a 5 mm thick layer, which was concealed beneath a layer of the chosen packaging material, to simulate the top surface of a real world drug parcel. Spectra were collected using a spot illumination and in a backscattering geometry with the focal point placed upon the surface of the sample. For all spectra, the x5 microscope

objective was used, along with the same settings that were employed to collect the standard spectra.

To collect the ring illuminated, spatially offset spectra from each mock parcel; the same backscattering geometry and focus upon the sample's surface was maintained, with the axicon held within the lens mount then placed atop the mock parcel, and positioned so that the excitation laser would pass directly through the centre of the lens. This was ensured by viewing the assembly under a spotlight built into the Raman microscope, and making adjustments with the motorised microscope stage when needed.

Importantly, the lens was arranged to be suspended approximately 3 mm above the sample, with the focal point of the microscope than repositioned by decreasing the distance between the objective and the sample by 5 mm. This ensured the axicon would not touch or interfere with the surface layer of the mock parcel, and that the microscope objective and axicon would be sufficiently close that the focal point of the system would not be too dramatically disturbed.

The spatially offset spectra were collected with the 785 nm excitation laser over a range of 120 cm^{-1} to 4000 cm^{-1} with 50% laser power, 10 second exposure time, two spectral accumulations, and a ten second exposure time. If no atropine peaks at 750 cm^{-1} and 1000 cm^{-1} were observed in the spatially offset spectrum obtained, the microscope system was defocused by a further 2.5 mm and the analysis was then repeated.

With both the spot and SORS spectra collected, the WiRE software was used to smooth the spectra and adjust the baseline, before each spectrum was truncated to the wavenumber range of

200 cm^{-1} to 1800 cm^{-1}, and then normalised to a maximum intensity of 25,000 counts to ensure the pairs of spectra were set to the same scale.

Once this pre-processing was completed, it was paramount that the SORS spectrum was corrected to remove the interfering peaks caused by the axicon. To do this, the SORS spectrum and a reference spectrum collected from the axicon were scaled to a maximum intensity of 25,000 counts, then loaded onto the OMNIC software and subjected to Automatic Baseline Correction. The reference spectrum collected from the axicon was then subtracted from the SORS measurement to reveal the unadulterated measurement.

With this correction completed, the two spectra from the mock parcel were loaded onto the OMNIC software, selected, and then subtracted, with the conventional spot spectrum subtracted from the SORS spectrum (SORS – Spot) to yield a subtraction spectrum that resembled the concealed atropine. To identify the concealed atropine, the obtained subtraction spectrum from each mock parcel was cross-checked against a user library containing reference spectra of each packaging type, atropine, cocaine HCl, acetaminophen and a vast number of organic compounds.

9.3 Quantification

While the detection and identification of the concealed compounds was made relatively easy through the use of a comparative database, the ability to accurately quantify the purity of the compounds remained a more difficult task. Previous encounters and recent research indicated that the use of Partial Least Squares Regression was the most effective methodology to approach, however a successful method would require some customisation.

The method detailed below was found to produce accurate, quantitative analysis of each concealed sample and importantly did not sacrifice efficiency too greatly. This meant that a suitably tailored process could be created and applied effectively to detect, identify, and quantify a concealed substance through a variety of packaging types.

Samples of pure atropine were diluted with set weights of baking powder, so that concentrations of 10%, 20%, 40%, 60%, and 80% by weight of atropine could be created for calibration. Pure samples of atropine and baking powder served as 100% and 0% concentrations respectively. A further three concentrations at 25%, 50% and 75% by weight of atropine were also created to be used as test ‘unknowns’ for method validation. The various weights of each compound, along with an accurate concentration of each sample is given below in Table 3.

Table 3 – Weights and concentrations of each test sample used during the study.

Atropine (g)	Baking Powder (g)	Total Weight (g)	Accurate Conc. (%)
4.995	-	4.995	100.0
3.936	1.019	4.955	79.43
3.733	1.224	4.957	75.31
3.028	1.938	4.966	60.98
2.500	2.471	4.971	50.29
1.968	3.010	4.978	39.53
1.252	3.734	4.986	25.11
1.003	4.082	5.085	19.73
0.511	4.486	4.997	10.23
-	5.029	5.029	0.000

Using the same parameters and instrumentation as for the identification stage, ten spatially offset spectra were collected from independent points on the surface of each packaging material. This process was repeated for each of the known, calibration concentrations, so that comprehensive profiles of each parcel and the concealed compounds could be determined.

Once collected, each of the ten sets of spectra were imported into the Unscrambler X program for pre-processing. It is important to note that none of the spectra during the quantification stage were normalised nor adjusted to a set 25,000 counts, so that the observed peak intensities were not changed in any way. With each collection of ten spectra grouped by their concentration, the series underwent a set of pre-processing stages, given in chronological order below;

1. Truncation to between 120 and 1800 cm^{-1}
2. Unit Vector Normalisation
3. SNV & Second Polynomial Detrending
4. Linear baseline subtraction

The series of pre-processing stages were found to accurately convert the varied spectral data into a series of accurate peaks. Importantly, the SNV and Detrending allowed for any curvatures in the spectra to be reduced or removed, while the linear baseline subtraction brought the overall baseline to a level of 0 counts, ensuring that each and every peak height was an accurate representation of the signal's intensity, and not subject to inaccuracies from comparing uneven baselines between measurements.

Once all spectra had been properly processed, the seven concentrations were used to create a Principal Component Analysis model, allowing for the separation between concentrations and any underlying patterns to be examined.

Following the PCA model, a set of values were created for use with the PLS Regression model. These values corresponded to the calibration spectra collected, and allowed for the model to be told what each peak represented. For example, spectra collected from the pure atropine samples were given values of 100, while spectra collected from the 80% atropine sample were given values of 80, and so on until the final baking powder samples were given a value of 0.

The PLS Regression model was then created using the calibration spectra and these values, using the maximum possible number of factors, the NIPALS algorithm and with full validation of the model. The weighting of each sample and response was kept constant at 1**.** Once created, each model was assessed by the Unscrambler X software and given approximate qualities based upon R^2 values and RMSE values for both the Calibration and Validation components.

For the ‘Unknown’ concentrations, the ten spectra from each concentration were imported and pre-processed in the same manner as the calibration spectra. This ensured that no large discrepancies between how the model interpreted each set of spectra would be included in the final results. Using the constructed PLS Regression model, each concentration was analysed and a predicted concentration was generated, along with an estimated deviation (an estimated uncertainty calculated by The Unscrambler X software for each measurement).

Similarly, the ‘Unknown’ concentrations were submitted to the PCA models, allowing for their placement on the observed plots to be examined and a rough estimation of their composition and concentration to be calculated.

9.4 Interrogation of Mixed Compounds

To further test the application of the devised method, a series of complex mixed samples involving atropine, baking powder, caffeine, and crushed Aspirin was created. Each of these samples were created to a set concentration (by weight of atropine) and with an equal ratio of adulterants. The full compositions and concentrations of the complex samples can be found below in Table 4.

Table 4 - Weights and concentrations of each complex sample used during the study.

Conc.	Atropine (g)	Baking Powder (g)	Caffeine (g)	Aspirin (g)	Total (g)
100.0 %	2.0013	-	-	-	2.0013
79.97 %	1.6011	0.1332	0.1344	0.1337	2.0024
74.94 %	1.5045	0.1700	0.1666	01665	2.0076
59.50 %	1.2003	0.2666	0.2781	0.2722	2.0172
50.01 %	0.9998	0.3322	0.3332	0.3341	1.9993
40.18 %	0.7988	0.3998	0.3898	0.3996	1.9880
24.98 %	0.4999	0.4999	0.5001	0.5011	2.0011
20.26 %	0.4213	0.5527	0.5524	0.5527	2.0792
10.18 %	0.2102	0.6184	0.6187	0.6181	2.0655
00.00 %	-	0.6774	0.6776	0.6774	2.0324

For the analysis, five principle packaging types were selected for testing to ensure a diverse collection of matrices were examined. These five samples were chosen based upon their physical characteristics, and their amenability to the technique as observed in the initial examinations. They were the white envelope, HDPE, white cardboard, the Australia Post PB3 padded bag, and the LDPE pre-paid satchel.

Collection of spectra from the complex mixtures concealed within each of the five packaging types was completed using the aforementioned method, however additional pre-processing stages were incorporated in an effort to elucidate the identities of all components present, and not just the target analyte, atropine. Initial pre-processing of the spectra remained consistent with the previous methods, with a sequence of normalisation, SNV, Detrending and baseline adjustments, and a PCA model was created utilising the same specifications and validation methods.

The PCA model proved sufficient to determine the number of principal components (that is the number of pure compounds within each mixture) present in each of the composite spectra

collected from the complex samples. Two subsequent processes followed; the first was a simple screening process involving the comparison of the mixed sample spectra with the OMNIC database, allowing for the dominant compound to be elucidated, while the second was a more in-depth chemometric process involving Multivariate Curve Resolution to decompose the mixed spectra into pure components for identification.

Once constructed, the pure component spectra were then identified against the spectral database created using the OMNIC software. Quantification of each pure component was not attempted, as the MCR process varied the overall intensity of each peak, making any partial least squares model inaccurate.

9.5 Interrogation of Mixed Packaging Types

Although the more complex packaging samples provided a more formidable barrier for the method, and similarly resulted in more complex spectra being collected, the method originally developed for the more simplistic, single layer samples was still applicable.

As such, a new series of concentrations were created using baking powder and aspirin. Each of these samples were created to a set concentration (by weight of aspirin), to the weights shown below in Table 5.

Table 5 - Weights and concentrations of each test sample used during the study on mixed packaging types.

Aspirin (g)	Baking Powder (g)	Total Weight (g)	Accurate Conc. (%)
3.9989	-	3.9989	100.0
3.2084	0.8011	4.0095	80.02
2.9974	1.0084	4.0058	74.83
2.3986	1.6008	3.9994	59.97
2.0048	1.9996	4.0044	50.07
1.6008	2.4020	4.0028	39.99
1.0000	3.0002	4.0002	25.00
0.8002	3.2002	4.0004	20.00
0.3998	3.6004	4.0002	9.99
-	4.0001	4.0001	0.00

Again, the samples made to concentrations of approximately 100%, 80%, 60%, 40%, 20%, 10% and 0% were established as calibration points, while the approximate concentrations of 75%, 50%, and 25% served as validation points. Ostensibly, the method employed to investigate the more complex, multi-layer samples remained the same as previously outlined for the single layer parcels. The reason for this, is that by subtracting the collected spectra, the information received from the multiple layers should also be removed just as if they were a single layer, leading to the only significant difference being the depth being probed.

Chapter 10 - Experimental Results

With each of the twenty-five packaging types assembled into a series of mock parcels and examined using both the conventional Raman procedure and the developed SORS method, the subtraction spectra that were obtained were than identified and quantified. The results obtained throughout the experimental work are given below.

10.1 Detection & Identification Results

10.1.1 Detection of Atropine Concealed Within Mock Parcels

Successful detection of the concealed atropine was considered to have occurred if the final subtraction spectrum obtained showed peaks relating to atropine that could be easily distinguished from the baseline. This was said to occur if the two main peaks, at 750 cm^{-1} and 1000 cm^{-1} could be freely and easily identified. As a result of this parameter, it was found that 19 of the 25 mock parcels (76% of all packaging types) were successfully interrogated, with the concealed atropine revealed with, even if only partially.

To aid in determining the quality of the detection, ranks of Weak, Medium, and Strong were applied to each detection, based upon the height of the peaks at 750 cm^{-1} and 1000 cm^{-1} from the baseline. A Strong signal was noted if the least intense peak height was equal to or greater than 5000 counts above the baseline, a Medium signal for between 2500 and 5000 counts above the baseline, and a Weak signal for a peak height of less than 2500 counts above the baseline.

Table 6 – Summary of Detection Results for the Concealed Atropine Samples

Packaging Type	Atropine Detected	Signal Strength
Australia Post Brand Bubble Wrap	Yes	Strong
Australia Post PB3 Padded Bag	No	-
Australia Post Prepaid Parcel Post Satchel	Yes	Strong
Australia Post Brand Brown Parcel Tape	Yes	Strong
Australia Post Brand Clear Parcel Tape	Yes	Strong
Black LDPE Satchel	No	-
Brown Cardboard	No	-
Brown Envelope	Yes	Weak
Bubble Wrap with White LDPE	Yes	Strong
Generic Padded Bag	Yes	Medium
Generic Padded Satchel	Yes	Weak
Generic Wrapping Paper	Yes	Strong
Grey Cardboard	No	-
Newspaper	Yes	Strong
PPS Kraft Paper – Brown	Yes	Weak
PPS Plainface DL White Envelope	Yes	Strong
Packing Foam	Yes	Strong
Quill Coloured Envelope – Orange	Yes	Strong
Reflex A4 White Paper	Yes	Strong
HDPE	Yes	Strong
Transparent PS	Yes	Medium
White Cardboard	Yes	Weak
White PS	Yes	Medium
White PVC Tile	No	-
Wood Grain PVC Tile	No	-

Of the 19 samples that were successfully found to include additional peaks from the concealed atropine, 12 of those packaging types revealed strong atropine signals (approximately 63%), with a further 3 with medium intensity peaks (approximately 16%). Only 4 samples (approximately 21%) reported weak peak signals corresponding to the concealed atropine.

10.1.2 Identification of Atropine Concealed Within Mock Parcels

While the detection of the two most prominent peaks of atropine, or another more illicit substance, would likely be sufficient for a second detection method and further investigation to be justified, it is not enough to conclusively identify the substance.

The use of OMNIC Spectra software allowed for the rapid identification of the subtraction spectra, and allowed for a qualitative measure of the resulting identification to be obtained (Scale of 0-100). Only the nineteen packaging types in which atropine peaks were detected were cross-referenced with the digital spectral library, with the results shown below in Table 7. In each case, atropine was identified to be the most accurate identification.

Table 7 – Summary of Identification Results for the Concealed Atropine Samples

Packaging Type	Atropine Identified	ID Quality
Australia Post Brand Bubble Wrap	Yes	93.44
Australia Post Prepaid Parcel Post Satchel	Yes	94.18
Australia Post Brand Brown Parcel Tape	Yes	66.34
Australia Post Brand Clear Parcel Tape	Yes	83.89
Brown Envelope	Yes	39.27
Bubble Wrap with White LDPE	Yes	98.18
Generic Padded Bag	Yes	83.15
Generic Padded Satchel	Yes	28.45
Generic Wrapping Paper	Yes	87.26
Newspaper	Yes	90.70
PPS Kraft Paper – Brown	Yes	64.51
PPS Plainface DL White Envelope	Yes	78.89
Packing Foam	Yes	80.50
Quill Coloured Envelope – Orange	Yes	77.02
Reflex A4 White Paper	Yes	86.57
HDPE	Yes	98.02
Transparent PS	Yes	85.94
White Cardboard	No	-
White PS	Yes	76.40

Of these nineteen samples, only the White Cardboard was not successfully identified as atropine. In this one sample, the subtracted spectra were identified with the library search to be most similar to a user recorded spectra entitled ‘Calcium Carbonate 99% (DRIFTS)’, however with a quality of only 11.54.

Impressively, the developed SORS method was found to correctly identify eighteen of the initial twenty-five packaging types examined, resulting in approximately 72% of all samples being susceptible to the technique. Furthermore, it was found that of the successfully interrogated samples, an average quality of identification of 78.48 was achieved, strengthening the potential of the technique as an effective method of detection and identification against concealed samples.

10.1.3 Quantification of Atropine Concealed Within Mock Parcels

Quantification of the concealed atropine samples within each mixed was the secondary aim of the experiment, and an important part of the project. While the method of a scaled subtraction of the spatially offset and spot spectra was effective for the detection and identification of the concealed atropine, the process made conventional methods for quantifying the target analytes impossible. Generally, the intensity of a peak in Raman spectroscopy is proportional to the concentration of the analyte responsible (Greve, Puppels et al. 1999), however after the subtraction, the response will no longer be directly proportional, adding drastic errors into any potential calibration curve. In response to this effect, any quantification would have to be considered from the spatially offset spectra, where no adulteration or subtraction had taken place.

Reduction of the twenty-five collected spectra allowed for more precise predictions of the three validation concentrations through a simple PLS-R model. As seen below in Table 9, only those packaging materials amenable to the initial detection and identification stages were examined here.

Table 8 – Summary of Quantification Results for the Concealed Atropine Samples

Packaging Type	Accurate Conc. (%)	Predicted Conc. (%)	Deviation	RMSE	R Squared
Australia Post Brand Bubble Wrap	75.31	74.94	7.649	7.928	0.947
	50.29	68.19	4.966		
	25.11	24.82	29.95		
Australia Post Prepaid Parcel Post Satchel	75.31	74.15	4.215	4.101	0.986
	50.29	56.51	15.54		
	25.11	28.03	6.115		
Australia Post Brand Brown Parcel Tape	75.31	52.37	7.154	4.502	0.983
	50.29	50.35	1.968		
	25.11	26.42	2.261		
Australia Post Brand Clear Parcel Tape	75.31	86.49	13.19	2.328	0.996
	50.29	52.77	33.20		
	25.11	23.39	3.099		
Brown Envelope	75.31	72.58	7.031	9.953	0.917
	50.29	50.62	10.54		
	25.11	39.65	12.64		
Bubble Wrap with White LDPE	75.31	76.52	30.76	4.165	0.985
	50.29	17.10	23.09		
	25.11	3.785	35.36		
Generic Padded Bag	75.31	76.93	19.20	0.196	0.999
	50.29	46.16	2.957		
	25.11	57.05	2.821		
Generic Padded Satchel	75.31	72.46	2.393	4.123	0.986
	50.29	50.20	3.228		
	25.11	41.87	2.213		
Generic Wrapping Paper	75.31	88.43	4.451	4.276	0.984
	50.29	48.22	29.42		
	25.11	36.23	7.368		

Packaging Type	Accurate Conc. (%)	Predicted Conc. (%)	Deviation	RMSE	R Squared
Newspaper	75.31	81.06	20.78	8.287	0.942
	50.29	61.99	8.636		
	25.11	16.26	4.587		
PPS Kraft Paper - Brown	75.31	79.24	11.32	9.765	0.917
	50.29	32.23	14.69		
	25.11	62.51	9.075		
PPS Plainface DL White Envelope	75.31	75.11	3.091	3.082	0.992
	50.29	58.24	17.12		
	25.11	27.37	3.915		
Packing Foam	75.31	73.16	5.751	3.397	0.996
	50.29	56.51	3.840		
	25.11	28.03	7.292		
Quill Coloured Envelope - Orange	75.31	85.58	10.49	7.940	0.948
	50.29	47.68	12.01		
	25.11	-3.375	21.27		
Reflex A4 White Paper	75.31	75.09	1.754	2.617	0.994
	50.29	49.46	1.755		
	25.11	25.28	8.110		
HDPE	75.31	76.89	2.890	1.465	0.998
	50.29	50.01	14.43		
	25.11	21.24	8.039		
Transparent PS	75.31	96.67	7.220	7.621	0.945
	50.29	87.72	7.192		
	25.11	20.79	5.748		
White PS	75.31	71.89	9.556	1.606	0.998
	50.29	51.83	3.089		
	25.11	26.37	9.520		

When considering the PLS-R models generated, the method developed was able to produce largely accurate results, with the RSME of all models ranging between 0.196 for the padded bag to 9.953 for the brown envelope, and with an average error of only 4.852. Similarly, the R^2 values were equally promising, ranging between 0.917 for the brown paper and brown envelope, to 0.999 for the padded bag; as well as an average R^2 value of 0.973, a respectable value for Raman spectroscopy.

The results of the quantification proved that all 18 packaging types were susceptible to quantification, however not all could be interrogated accurately with varying deviation (uncertainty) noted across the results. The thicker sample of the bubble wrap and white LDPE proved to be too difficult to accurately interpret, generating predictions with large deviations across all three concentrations. Several other samples, such as the HDPE, envelopes, newspaper, wrapping paper, brown tape and brown paper generated large deviations among one of the three concentrations, however these could be attributed to difficulties in collecting accurate spatially offset spectra.

10.2 Determination of Mixed Compounds

As previously mentioned, identification of the more complex mixed compounds required a more complicated methodology, and determination of a larger number of components. As such, MCR proved an effective method for realising the individual components of the compound through each packaging type, enabling for the complex mixtures to be resolved into three relatively pure components.

The OMNIC software then allowed for easy identification of each pure component, shown below in Table 9. For each component, only the identification with the highest quality is shown.

Table 9 - Summary of Identification Results for the Mixed Components

Packaging Type	Component	Component ID	ID Quality
LDPE	1	Atropine	79.70
	2	Baking Powder	7.46
	3	Caffeine	88.90
Padded Bag	1	Atropine	66.67
	2	Atropine	21.05
	3	Caffeine	61.35
Polystyrene	1	Atropine	92.23
	2	Polystyrene	27.67
	3	Caffeine	16.24
White Cardboard	1	White Cardboard	7.47
	2	White Cardboard	7.47
	3	White Cardboard	15.78
White Envelope	1	Aspirin	15.84
	2	Atropine	61.34
	3	Caffeine	60.35

With far more complicated samples, and a more expansive chemometric approach, a decrease in the observed accuracy of the method was to be expected, particularly when dealing with calculated and assumed component spectra. Despite this, the deconvolution of the mixed samples into their relatively pure components, without the adulteration or removal of the packaging, was found to be fairly successful, with three of the four components realised and identified in nearly every sample.

Due to the nature of the samples, where many different powders were combined, quantification was only briefly tried with these samples. The results were found to be largely haphazard, with

the models unable to successfully achieve any predictions without a large (greater than 33%) deviation being present. Due to this persistent pattern in the results, quantification of the complex samples was abandoned at this stage.

10.3 Interrogation of Complex Multi-Layer Parcels

While the method for the investigation the multi-layer samples might not have varied significantly from the optimised method devised, it was expected that a lower accuracy in both identification and quantification would be observed, simply due to the more complex nature and the increased thickness of the packaging. Surprisingly, this prediction did not come to fruition, with the identification results obtained from the multi-layer samples being of comparable accuracy, as shown below in Table 10. For each packaging type, only the identification with the highest quality of match has been shown.

Regarding the 0% concentrations for the LDPE & Bubblewrap and HDPE & Bubblewrap parcels, false positives of atropine and caffeine were noted, as these concentrations only contained aspirin and baking powder. These misidentifications can be accredited to poor scaling across the entire spectrum, which negatively affected the final subtraction result. While important to note, the low quality of identification in both cases means that the false positives are of little concern.

Table 10 - Identification Results from the Complex Packages

Packaging Type	Conc. (%)	Identification	Quality
HDPE & Bubblewrap	100%	Aspirin	16.77
	75%	Aspirin	68.3
	50%	Aspirin	48.12
	25%	Aspirin	33.25
	0%	Atropine	9.28
LDPE & Bubblewrap	100%	Aspirin	19.88
	75%	Aspirin	94.69
	50%	Aspirin	96.09
	25%	Aspirin	74.98
	0%	Caffeine	7.31
Newspaper & Brown Tape	100%	Aspirin	95.02
	75%	Aspirin	63.80
	50%	Aspirin	66.82
	25%	Aspirin	95.52
	0%	Baking Powder	18.48
Padded Bag & Brown Tape	100%	Aspirin	14.59
	75%	Aspirin	16.76
	50%	Aspirin	18.46
	25%	White Cardboard	29.90
	0%	White Cardboard	21.82
Polystyrene + Brown Tape	100%	White Polystyrene	95.77
	75%	White Polystyrene	69.89
	50%	White Polystyrene	97.76
	25%	Aspirin	74.98
	0%	White Polystyrene	95.85
W. Envelope + Brown Tape	100%	Aspirin	74.32
	75%	Aspirin	79.45
	50%	Aspirin	13.41
	25%	Aspirin	24.50
	0%	White Cardboard	20.33

The obtained results showed that all six combinations of packaging types could successfully be examined, however with varying degrees of success. Out of the 20 measurements collected,

66.67% were positive readings for aspirin, while a further single measurement was found to belong to baking powder, the adulterant used in this experiment. A further 7 spectra were found to belong to the packaging itself, with the padded bag exhibiting similar spectra to that of white cardboard. The only results of concern came from the blank measurements of both the LDPE and HDPE samples combined with bubblewrap, in which two false positives were present, with atropine and caffeine identified respectively, albeit with low qualities (less than 10).

For the quantification results, it was found that the more complex packaging types created a more formidable barrier, resulting in irreparable skewing of the peak intensities, and ultimately delivering poor predictions. While the majority of the chemometric models generated were of high quality, exhibiting low RMSE and reputable R^2 values (as seen in Table 11), the results were highly inconclusive, as shown in Table 12 below.

Table 11 - RMSE and R^2 vales for the Calibration and Validation Models

	Calibration		Validation	
Packaging	**RMSE**	**R^2**	**RMSE**	**R^2**
HDPE + Bubblewrap	6.518	0.964	6.997	0.960
LDPE + Bubblewrap	2.253	0.995	4.761	0.983
Newspaper + Brown Tape	8.145	0.942	12.249	0.824
Padded Bag + Brown Tape	11.365	0.889	16.425	0.774
Polystyrene + Brown Tape	3.305	0.991	7.632	0.954
W. Envelope + Brown Tape	2.988	0.992	6.321	0.963

Table 12 - Quantification Results for Complex Packaging Samples

Packaging	Accurate Conc. (%)	Predicted Conc. (%)	Deviation
HDPE + Bubblewrap	74.86	74.38	4.62
	50.06	70.48	7.09
	25.00	45.68	9.34
LDPE + Bubblewrap	74.86	192.67	8.03
	50.06	31.97	3.86
	25.00	16.14	3.96
Newspaper + Brown Tape	74.86	46.44	22.85
	50.06	35.40	14.03
	25.00	110.25	12.90
Padded Bag + Brown Tape	74.86	6.40	16.59
	50.06	6.66	24.70
	25.00	83.36	10.28
Polystyrene + Brown Tape	74.86	52.91	9.60
	50.06	29.16	30.49
	25.00	-208.30	17.32
W. Envelope + Brown Tape	74.86	64.95	3.30
	50.06	95.41	14.21
	25.00	29.04	4.77

Sadly, the level of accuracy in the predictions that was seen in the initial experiments could not be repeated for the more complex packaging samples, with obvious incorrect predictions such as -208.30% noted for samples including polystyrene covered in brown tape. There were noted issues in the models, as well as the predictions, with more complex packaging types producing chemometric models with RMSE and R^2 values well below what is considered accurate. As a result of this, the quantification predictions can be considered poor at best.

10.4 Determination of the Limits of Detection & Quantification

The limit of detection (LOD) and the limit of quantification (LOQ) of an experiment are terms used to describe the smallest possible concentration that could be accurately detected and quantified by an analytical procedure (Armbruster and Pry 2008). To determine these limits for each of the constructed PLS-R regression models, the following equations were used;

$$LOD = 3.3\times (\frac{SD}{S})$$

$$LOQ = 10\times (\frac{SD}{S})$$

In which SD is the standard deviation of the linear regression, and S is the slope of the calibration curve (Shrivastava and Gupta 2011).Using the overview of each model calculated by The Unscrambler X software, the following limits for the calibration of each model were calculated for each of the experiments conducted – these limits of course exclude the complex mixed samples, where the quantification was abandoned and full models were not created.

Table 13 - LOD and LOQ for the Calculated PLS-R Models for Simple Parcels

Packaging Type	Slope	SD	LOD	LOQ
Bubble Wrap	0.9469	2.4127	8.408	25.480
Prepaid Parcel Post Satchel	0.9846	1.2263	4.110	12.455
Brown Parcel Tape	0.9833	0.7409	2.487	7.535
Clear Parcel Tape	0.9955	0.2001	0.6633	2.010
Brown Envelope	0.9172	3.6684	13.199	39.996
Bubble Wrap with White LDPE	0.9855	0.6423	2.151	6.518
Generic Padded Bag	0.9999	0.0015	0.005	0.015
Generic Padded Satchel	0.9854	0.6330	2.120	6.424
Generic Wrapping Paper	0.9844	0.6961	2.334	7.071
Newspaper	0.9417	2.4890	8.722	26.431
PPS Kraft Paper – Brown	0.9174	3.5644	12.822	38.853
PPS Plainface DL White Envelope	0.9920	0.3582	1.192	3.611
Packing Foam	0.9904	0.4274	1.424	4.315
Quill Coloured Envelope – Orange	0.9479	2.2964	7.995	24.262
Reflex A4 White Paper	0.9943	0.2537	2.552	2.552
HDPE	0.9982	0.0761	0.252	0.762
Transparent PS	0.9486	2.3102	8.037	24.354
White Cardboard	0.9986	0.0572	0.189	0.573
White PS	0.9978	0.0956	0.316	0.958

For the simple packaging types, the LOD and LOQ were found to vary drastically depending on the physical characteristics of the packaging. On average, the LOD could be seen to be a concentration of 4.157% (by weight of the target analyte), with the padded bag providing the lowest LOD, and the brown envelope providing the highest. Similarly, the same two samples provided the best and worst LOQ respectively, while the method was noted to achieve an average LOQ of 12.325% (by weight of the target analyte).

Table 14 - LOD and LOQ for the Calculated PLS-R Models for Complex Parcels

Packaging Types	Slope	SD	LOD	LOQ
HDPE + Bubblewrap	0.9641	1.5611	5.343	16.192
LDPE + Bubblewrap	0.9930	0.4113	1.367	4.142
Newspaper + Brown Tape	0.9417	2.5434	8.913	27.009
Padded Bag + Brown Tape	0.8902	5.2101	19.314	58.528
Polystyrene + Brown Tape	0.9938	0.4446	1.477	4.474
W. Envelope + Brown Tape	0.9915	0.3880	1.291	3.913

When concerned with the more complex, multi-layer packages, both the LOD and LOQ of each sample were relatively higher than those previously found in the single layer packages, a result that was to be expected due to the more complex nature. The LOD was found to range between 1.291% for the taped white envelope, and 19.314% for the combination of a padded bag and brown tape, while on average the LOD was seen to be 6.284% (by weight of the target analyte). For the LOQ, the same pattern was observed, while the average LOQ of the method was determined to be 19.043%.

Chapter 11 - Discussion

While the experimental results shown in this research provide a thorough picture of the developed methods' potential and applicability, a more in-depth and critical analysis of the method proved essential to better understand the full scale of its effectiveness and limitations. In this chapter, a full review of the developed method, results, limits, and particulars of the research accomplished is presented.

11.1 Analysis of the Experimental Method

11.1.1 Sample Preparation

One of the greatest advantages in any Raman spectroscopic method is the minimal sample preparation required; an advantage enabling more reliable and simpler methods to be instigated. While simplistic in design, the sample preparation method of weighing the active compound and the base adulterants to set concentrations had proved highly successful when used previously, and when used by more experienced academics such as Ryder et al. (Ryder, O'Connor et al. 2000).

The only prominent problem regarding this method of sample preparation was an inherent lack of sample homogeneity that intermittently persisted within the measurements. In previous research, the use of an agate mortar and pestle had proved sufficient to reduce the most prominent effects of this error, however the continuing sample inhomogeneity was noted by Penido et al. to be the main contributor of error when constructing PLS-R models (Penido, Landulfo Silveira et al. 2012).

It was noted that the degree of uniformity in the mixed samples were most prominently effected by the particle size and physical characteristics such as solidness and crystallinity, with an ideal homogenous mixture being composed of a substance with the same particle distributions and tenuity (Penido, Landulfo Silveira et al. 2012). Ideal conditions in which there is an even and uniform particle size is difficult to create in laboratory conditions, particularly when one component is present in a greater portion than the other, and when the samples are of vastly different morphology.

The simplest method of reducing this specific sample inconsistency was implemented in this research, with the duration and severity of the sample grinding increased, allowing for a more thorough mixing of samples and a marked reduction in particle size differences. A sequential step that was also considered was the addition of a sieve to separate the larger particles from the mix, however the removal of larger particles would alter the measured concentrations within each mixed sample, and so was deemed to be an inappropriate step. A second, more complex method for increasing the homogenisation was found within the research of West and Went, who dissolved their samples in ethanol, so that any problems regarding the differences in particle size could be overcome (West and Went 2011). While successful in their study, such adulteration of the samples would not be possible without first opening the parcel, and so this idea was abandoned for this research.

Ultimately, a partial solution to the inhomogeneity issue was found in the increased spot size utilised in the spatially offset measurements. By increasing the spot size and collecting spectral information from a greater surface area, far more information can be observed, ensuring that the

inaccuracies caused by sample variations, that have large affects in traditional Raman measurements, are relatively small in comparison.

11.1.2 Optimising Raman Parameters

Although proving the success of the method with the replication of previous research was paramount, optimisation of the working experimental parameters was also of critical importance. Initial testing proved that the method was capable of revealing far greater spectral information than a traditional Raman method, however the initial, stoic approach was soon found to degrade and damage some packaging samples due to the high laser power used, as well as not providing the most efficient possible results.

The use of the best possible parameters ensured the most accurate and efficient method, allowing for both rapid and sensitive detection of each mixed samples, while also allowing for the method to be carefully tailored to each packaging type. Part of this development and optimisation involved the examination of the distinct Raman parameters such as the way in which spectra were collected, the spectral range, the choice of excitation wavelength and power level used to analyse the samples, the exposure time and number of accumulations, and finally the objective used when viewing the samples.

11.1.2.1 Selection of Optimum Objective

The Leica DM2500 M microscope used during the research had the capability to provide magnification at 5x, 20x, and 50x objectives. While each of the objectives had their own

advantages and disadvantages, it was found early in the method development that only the 5x objective allowed for sufficient focal depth to be maintained, while also effectively accommodating the axicon and its mount, ensuring that the SORS process could be achieved.

It was found that in order to maintain sufficient focal depth while accommodating the axicon and its mount system, only the 5x objective could be used. In this instance, the additional accuracy and specificity that would be gained from the higher objective had to be sacrificed in order for the SORS technique to be viable.

This unavoidable pre-requisite was not without disadvantages, as the lower objective did not capture the best possible spectral quality, exhibiting a lower accuracy and specificity, than the 20x and 50x objective championed by the likes of Ryder et al. (Ryder, O'Connor et al. 1999). There were some inherent advantages to using the lower objective however, with the lower 5x objective allowing for quick and simple focusing, as well as the easy addition and removal of the axicon lens and mount system.

11.1.2.2 Choice of Excitation Wavelength & Laser Power

The choice of excitation wavelength used through the experimental research was of critical importance to ensure that the most accurate and intense spectra were collected. It is known that the intensity of any band within a Raman spectrum is dependent upon the laser power used and, for the Stokes scattering, it is also known to be proportional to the wavelength of the excitation laser. In essence, and in the absence of fluorescence effects, the lower the wavelength of the excitation laser, the better developed a sample's Raman spectrum will appear (Smith and Dent

2005), an effect that was put to practical application by Sands et al. who used a 244 nm excitation laser in the successful detection of narcotics and explosives (Sands, Hayward et al. 1998).

Another exploitable phenomenon noted in Raman spectroscopy is that far fewer compounds tend to absorb strongly at the longer wavelengths of 750 nm and above, which serves to reduce and potentially suppress fluorescence at the source (Hargreaves 2011). Ideally, a laser with excitation wavelength between these two advantageous extremes would be favourable, and initially three potential wavelengths, of 633 nm, 785 nm, and 1064 nm were examined. The 633 nm laser was quickly excluded from the experiment as it caused intense fluorescence that eclipsed all useful spectral data in the measurements. The 1064 nm laser was similarly excluded in favour of the 785 nm wavelength, as far better peak shape and a less noisy baseline was observed in all test measurements.

A second consideration regarding which laser was selected was the laser power. It has been well documented that the laser power greatly effects the quality of the spectra obtained, and that higher laser powers would lead to far better signal-to-noise ratios and cleaner spectra (Hargreaves 2011). However in this research, the possibility of sample degradation also had to be carefully considered. A higher laser power would damage and even destroy some of the thinner and less resilient packaging types, which would defeat one of the primary aims of this research, and as such, the laser power had to be carefully tuned for each package being interrogated. The result of this trade-off is the table of tailored laser powers previously presented in this work, designed so that each package could be interrogated with the highest possible laser power to

improve the quality of the spectra obtained, while also ensuring that noticeable or obvious physical damage did not occur to any layer within of the parcels.

11.1.2.3 Selection of Spectral Range Collected

The spectral range has a dramatic impact upon the information gained from spectra. Careful observation of the 'fingerprint region', that is the range of 400 to 1800 cm^{-1}, is where the majority of useful spectral information is collected, however it does not include all of the unique bands that needed to identified**.**

In this research, initial spectral measurements were collected over a spectral range of 120 cm^{-1} to 4000 cm^{-1}, obtaining a total of over 5400 data points per spectrum collected. Although this wider range increased the length of time required to collect the full number of spectra, thereby decreasing the efficiency of the method, it enabled the complete spectrum of each sample to be visualised and interrogated, ensuring that even the most minute changes in the data could be observed.

11.1.2.4 Exposure Time and Number of Accumulations

The number of spectral accumulations and the length of time a sample remains exposed to the laser light is known to help increase the quality of the spectra obtained, bettering the signal-to-noise ratio and increasing the prominence of peaks. However, increasing either of these parameters also increases the length of time required to complete a measurement, sacrificing efficiency for improved quality.

However, it was noted in previous experiments on the detection and quantification of cocaine analogues in textiles, that increasing the number of accumulations from 5 to as many as 10 or 15 was not efficient, increasing the collection acquisition time by approximately five minutes with each addition of five accumulations, while providing no real improvement upon the quality of the spectra (Cavasinni 2012). In light of this research, and in keeping with findings repeated in this particular work, it was decided to maintain a single accumulation for each spectral measurement.

Similarly, the exposure time used during the method was kept to the minimum required to obtain adequate and successful results. This practice was selected for two reasons, firstly, so that efficiency of the method could be maintained, but also so that the increased time spent under exposure to the laser did not degrade or irreversibly damage the samples. This resulted in the optimum conditions for collecting spectra over the range of 120 cm^{-1} to 4000 cm^{-1} with 1 spectral accumulation and a 10 second exposure time.

11.1.3 Optimising the Axicon

11.1.3.1 The Axicon Characteristics

Made from borosilicate glass, the axicon lens utilised in this research was selected for its optical and mechanical characteristics, and its high resistance to chemical and environmental damage. This resiliency was important, however the clarity of the lens and its level of absorbance within the visible to 350 nm wavelength range was also of great significance. With minimal absorbance and high clarity, the production of a clean laser ring would be easily possible, while spatially offset spectra would also be relatively free of any interfering signals from the lens itself.

The interfering signals from the axicon lens were unfortunately unavoidable, however a simple subtraction method using a standard spectrum collected from the axicon lens ensured that the SORS measurements collected could be used in a relatively pure form.

11.1.3.2 Axicon Positioning and Focus

While a more acute apex angle would cause greater refraction to occur, a more obtuse apex angle was eventually selected as it was the most easily obtained and cost effective. With a base angle of 2.5°, the axicon lens utilised was not of optimal characteristics, however it provided a powerful glimpse into the full capabilities of the developed method. While a more acute apex angle would have provided a greater level of refraction, thereby generating a wider, more prominent laser ring, axicon lenses of that quality and dimension were beyond the budget of this research.

To help correct for the somewhat diminished quality of the lens, a defocused system was investigated. Obtaining the optimum focus on a sample has been shown to produce a more accurate spectrum with Raman microscopy, particularly when attempting to quantitatively examine a sample (West and Went 2011). This effect is specific to the area and depth being focussed upon, particularly when dealing with multi-layer samples. It was shown by Eliasson et al. that a defocused system was capable of producing a substantial variation in the relative ratio between the signals obtained from the surface and sub-surface layers, and could on many occasions help to enhance the spectra from concealed samples (Eliasson, Claybourn et al. 2007).

Although this practise was known and observed to produce a lessened clarity in the spectra, the additional spectral information gathered in this, and other experiments, proved to be an appropriate trade off. After careful experimentation, it was found that by defocusing the system by an additional 10 mm into the sample, the prominence of characteristic atropine peaks (such as those at 750 cm^{-1} and 1000 cm^{-1}) were increased, while the peaks pertaining to the packaging were greatly diminished. This practise remained equally as effective across multiple packaging types, cementing its inclusion in the final optimised method.

The optimal position of the axicon lens was found to be largely dependent on the focus of the microscope objective. As described by Dépret, Verkerk, and Hennequin, (Depret, Verkerk et al. 2002), maintaining a close distance between the microscope objective and the axicon ensured that the focal points of both lenses are approximately equal. This meant that once focused upon the sample of the packaging, and then defocused inwards by 10 mm, aligning the axicon and objective closely would help to ensure optimal focusing was completed and enhanced results collected.

This theory was examined, and was found to hold firm; as with increasing distance between the microscope objective and the axicon, there was an increasing fluorescence from backscattering light, and a reduction in the visibility of peaks associated with the concealed atropine sample.

11.1.4 Collecting Spectra

While the issue of sample inhomogeneity was seen to persist throughout the experiment, the effect of it was able to be largely circumvented by the collection of multiple spectra from

independent points within each samples, and through the use of a greater laser spot size produced by the axicon lens.

Taking multiple spectra from various independent locations to ensure a more complete and fully representative profile of the sample had been suggested by West and Went, and further supported by the work of Ryder et al., whose work independently showed that taking multiple points greatly increased the accuracy of developed chemometric models. (West and Went 2011) (Ryder, O'Connor et al. 1999).

Ultimately, it was found that while more time consuming, the increased effect of more fully mapping the sample was irreplaceable in this research. The question of efficiency could be drawn at this point, and admittedly it would not suit every situation, particularly those that are time limited, involve very small samples, or where a pure substance is known to be involved. However, when considering the numerous, potential formulations for unknown and illegal narcotics, it is highly likely that the collection of multiple spectra would be an essential step.

11.1.5 Comparison of Traditional Raman and the Developed Method

Improvements in the information obtained from the spatially offset spectra over the traditional Raman measurements were visible almost instantaneously and across all tested packaging (except for those that were found to be unexaminable using this method). There were no packaging types that could be exploited by the traditional Raman that could not be examined equally, or more accurately using the developed SORS method.

While some issues regarding sample fluorescence persisted, the SORS method was able to successfully penetrate thicker samples, ensuring that it's accuracy over the traditional Raman spectroscopic technique was without doubt.

11.1.6 Construction of the Chemometric Models

11.1.6.1 Principal Component Analysis (PCA)

An important precursor to the PLS-R models, and to the identification of the complex mixed samples, was the construction of highly informative PCA models. These models not only allowed for the collected spectra to be examined in terms of their separation and specificity, but also enabled a better understand of the quality of the collected spectra and the number of unique factors that could be used in the later quantitative models.

For all packaging types, and in particular when investigating the complex mixed powders, the PCA models generated were able to produce easily identifiable patterns within each model, helping to reveal the underlying patterns in concentration and sample type, particularly when viewed in a 3D matrix.

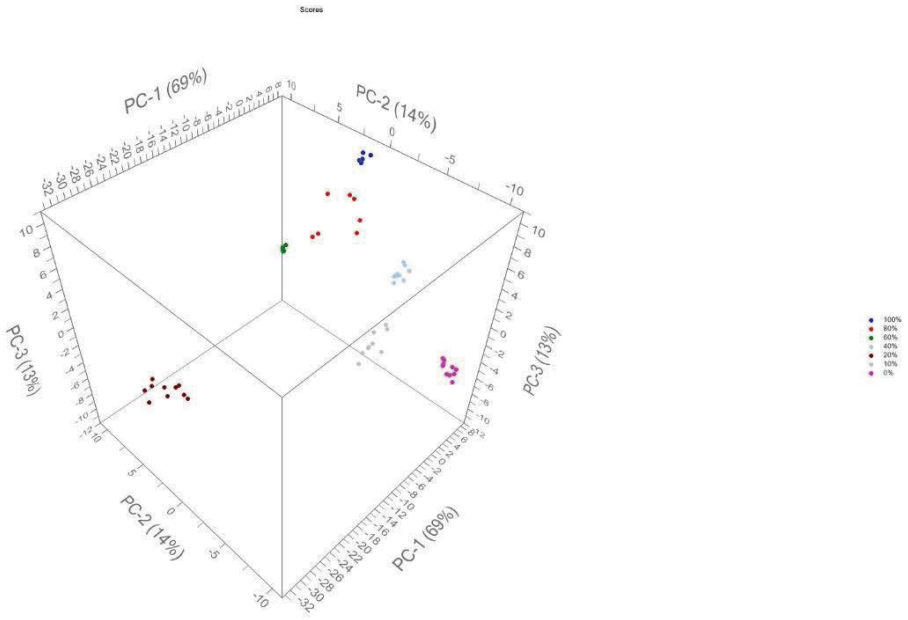

Figure 29 – PCA model generated from the calibration samples concealed with HDPE.

In all cases, the PCA models were found to be an excellent method for reviewing the quality of the models and of the results, allowing for the separation of each sample into their principle, representative points to be closely monitored.

11.1.6.2 Partial Least Squares Regression

The decision to use partial least squares regression as the primary quantification method was due to the method's ability to manage and compute unknown values, while still maintaining a high level of accuracy within the computations. A further noted advantage is that the PLS-R models are built on known concentrations, meaning that a model can be built based on variances that are directly proportional to the concentrations being used (Fenton, Tonge et al. 2011). Importantly, there is also a prominent history of using PLS-R in quantitative studies, with the likes of Ryder et al. and Fenton et al. having used the technique to great success in their own work.

It was also from these works, and from additional research by Noonan et al. (Noonan, Tongue et al. 2009), that helped form the sequence of pre-processing stages used within this study. The inclusion of steps such as Savitsky-Golay smoothing, taking derivatives, and mean centering the data did not provide any noticeable or effective increase in the quality of the data or the models constructed, and so were largely removed from the research at hand.

Despite this, it was found that the PLS-R models benefitted greatly from truncating the data (reducing the number of data points), cosmic ray removal at the initial stages of collection, normalisation, SNV and detrending, and baselines correction. By applying these stages, it was found that the root mean square error of prediction and R^2 values of both the calibration and validation stages of the developed models could be refined and improved, thereby enabling more accurate predictions of the samples concentrations to be made.

While the quality of the calibration and validation segments varied between packaging types and tests completed, they were all generally of a high standard, with average R^2 and RMSEP values achieved that often rivalled work previously published in the field of Raman Spectroscopy (Yang and Ying 2011, Olds, Sundarajoo et al. 2012). The quality of these results is largely due to the stages of collecting addition spectra from each sample, and through the careful application of each pre-processing stage.

11.1.6.3 Pre-processing Stages

The original, un-processed data was found to be afflicted by the various mechanical variations of the axicon lens, laser, and the Raman microscope being used, as well as affected by natural phenomenon such as cosmic rays, sample orientation, and sample inhomogeneity. By applying the selected sequence, it was found that the majority of these variations could be either reduced or removed, allowing for more accurate models to be generated.

Truncation of the full collected spectra was found to be an important stage as it enabled the models to be refined and focused upon only the most prominent segments of the spectra. In this way, many of the variations and disruptions within the collected spectra could be minimised, maintaining the efficiency and accuracy of each developed model. Ideally, this stage allowed for peaks which held little value for quantification to be removed, thereby reducing the number of overall data points, and decreasing the potential for introducing inaccuracies and deviations.

Normalisation was a further pre-processing stage designed to reduce and remove the effects of the many small variations and perturbations that naturally occurred during the course of this experimental work (Renishaw 2006). By smoothing and adjusting the series of collected spectra, the potentially harmful daily and mechanical variations that are inherent in Raman spectroscopic measurements could be accounted for, ensuring that any changes in peak intensities or spectral shapes were solely caused by the change in concentration and composition, and not by any possible secondary or tertiary factors. In this way, the models could once again be refined.

The combined application of SNV and detrending was another important step in the pre-processing, allowing for curvatures and variations within the spectra to be removed, ensuring a linear baseline and more accurate representations of each concentration within each PLS-R model.

Baseline adjustment was relied upon to help ensure that the intensity of the signals received from each peak were accurate reflections of the same concentration, were not enhanced or reduced by baselines which were positioned above or below the zero counts mark, and to maintain a level and consistent baseline intensity for a more accurate comparison of the various samples and concentrations. The addition of a linear baseline adjustment also helped ensure that any remaining variations or perturbations that remained within the data sets could once again be reduced or removed. It was found that using the baseline offset function on The Unscrambler X software provided adequate transformation of the spectra, and allowed for peak intensities to be analysed on the basis of their concentration and composition alone, without other interfering factors skewing the data.

11.1.6.4 Building the PLS Regression Model

The final pre-processing step before a final partial least squares regression model was constructed, was to create a number of transitory PLS regression models, and then use the results generated to better refine the calibration spectra. In this way, each successive PLS regression model generated would have a lower root mean square error and greater linearity. To do this, the optimum factor of each model was identified, and then spectra that differed greatly (a variation

greater than ± 25% from the actual value) between the calibrated and predicted values were removed.

Although this method of refinement called for the removal of data points from each sequence, the increased accuracy and reduced error ultimately justified the decision to include it in the final, optimised procedure. It also followed that the removal of outliers has been a common trend in many scientific experiments, including the identifications and quantitative measurements of narcotics reported by Ryder et al (Ryder, O'Connor et al. 1999).

Three other considerations were involved in constructing partial least squares regression models accurate enough for successful quantification of the concealed samples; these were the algorithm used, form of validation included in the method, and the reduction of multiple spectra into one comprehensive spectrum. Each PLS regression model was constructed using the NIPALS algorithm and full method validation. These two particulars were important in the method development stage, as the different algorithms available from The Unscrambler X software were all suited to different spectral forms. The non-iterative PLS, also known as NIPALS, algorithm, was chosen as it was simple to implement correctly, and was generally recommended for large ill-conditioned data sets. A further advantage of the algorithm was that it is able to easily handle missing data, which gave it some superiority over other possible algorithms (Tauler, Walczak et al. 2009). The use of a full validation method during the development of each model was found to give the best possible results, with each calculated component validated against each other component. While this took longer for each model to be computed, the increased accuracy brought was found to be invaluable, despite the loss of efficiency.

The final consideration when developing the quantification predictions was the reduction of unknown spectra into a single comprehensive spectrum. This approach was noted in the research of Ryder et al. in which spectra were averaged as part of the pre-processing stage (Ryder, O'Connor et al. 2000). The technique was included within this experiment so that a single, comprehensive spectrum could be used with the prediction models. Not only did this enable a more accurate prediction of the concentrations found in each unknown sample, but it also meant that a single prediction was generated and not twenty-five different predicted concentrations, as would be the case for the un-reduced spectra.

Although there were undoubtedly some inefficiencies left within the developed chemometric method, it proved to be an accurate and robust process that was capable of elucidating important information from a large volume of data points. Issues found in the method development stages were countered and overcome as best as possible, including problems regarding sample inhomogeneity, and as such the process was deemed to be a success as it was able to quantify each sample of decent spectra with a relatively high accuracy.

11.2 Analysis of the Results

11.2.1 Identification of Atropine Through Simple Packages

Overall, the identification results of the concealed powders from behind the twenty-five packaging types was highly successful, with 19 of the 25 packaging types successfully interrogated so that the contents could be spectroscopically revealed. Of these 19 mock parcels, it was found that most packaging types (18 of the 19 samples) presented atropine peaks of such quality that identification could be easily achieved.

With an average quality of identification for the concealed atropine of 78.48% across the 18 successful samples, the developed method also boasted no false positives, and only one false negative, seen when examining the sample of white cardboard. In this case, the initial spatially offset results collected from the cardboard were marred by both the density of the cardboard and the light colour of the sample. The combination of these physical characteristics worked together to create a formidable barrier that was difficult to penetrate, with the high density of the cardboard and the light colour preventing any potential spectral information from being obtained. Because of this, the white cardboard produced initial spectra of questionable quality, which in turn reduced the effectiveness of the spectral subtraction and reduced the possibility of collecting an accurate identification of the atropine concealed within.

What can be seen from the spectra collected from the white cardboard however (shown in Figure 30 below), are two characteristic peaks between 710-750 cm^{-1} and at 1000 cm^{-1}, the prominent markers for atropine, which importantly are not present in the conventional spot measurement.

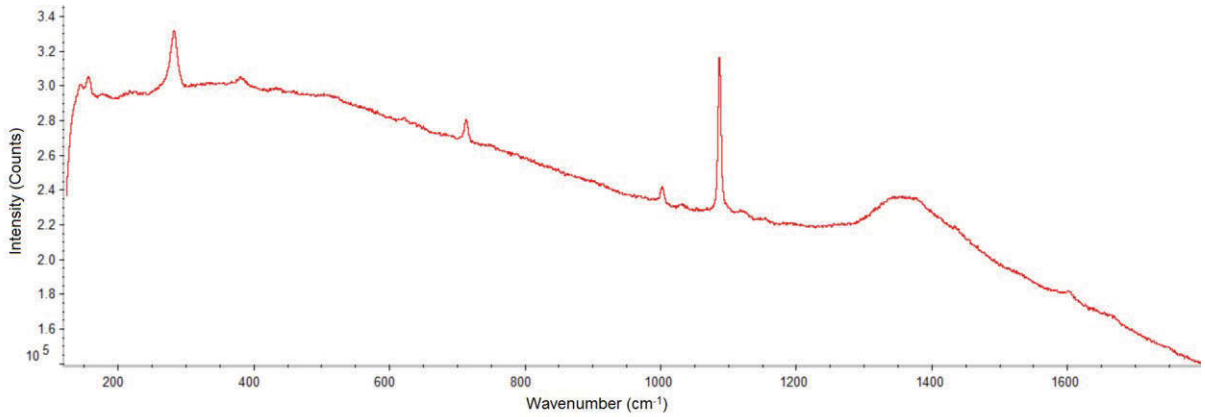

Figure 30 – Spatially offset Raman spectrum collected from white cardboard concealing a sample of pure atropine.

What can be seen from these results, is that a manual inspection of the collected data is essential, as it enables the elucidation of information through a more targeted and nuanced approach, ensuring the all of the small elements of the spectra are examined. This combination of automatic, full-spectrum matching and manual examination of the revealed peaks against known peak markers was found to enable the screening process developed to be used to maximum effectiveness, and importantly, aided in the first potential detection of a substance through cardboard using Raman spectroscopy.

11.2.2 Quantification of Atropine Through Simple Packages

Although the method for collecting enhanced spectral data and identifying the concealed compounds could be refined into a relatively simple process, quantification of the concealed substances was a far more difficult task. While simple comparisons with standard spectra and a known database was sufficient to provide accurate identifications, the ability to accurately quantify collected spectra required the collection of multiple reference spectra and the construction of complex chemometric models. In an effort to save time and reduce the number of ineffectual spectra collected, only the 19 packaging types that could be successfully interrogated were examined quantitatively.

Of these 19 samples, it was found that the majority could be interrogated, with the accurate quantification of the concealed atropine possible without ever opening or removing the packaging. For all models, the RMSE was found to fall within the range of 0.196 and 9.953, depending upon the packaging type, while the R^2 values were found to be within the range of

0.917 and 0.999, also depending upon the sample packaging. On average, a RMSE of 4.852 and an R^2 value of 0.973 was calculated for the complete quantification method.

Although not all packaging types were able to be successfully or partially interrogated it was determined that the effectiveness and accuracy of both the identification and quantification methods ultimately relied upon the characteristics of the packaging itself. The average RMSE and R^2 values calculated are strong indications of this fact (which will be discussed later in this chapter), as well as confirmation that the constructed models and developed method worked effectively within itself.

11.2.3 Interrogation of Complex Mixed Samples

The ability to resolve the complex mixed samples into a series of relatively pure components was an important step forward for the developed method and its application. Using PCA, the number of relative components could be accurately estimated, while also allowing for separation and comparison of spectra with known standards. In this way, the identification of the unknown samples could be initially estimated before the MCR process was applied.

An initial failing in the method was that only three principal components were identified through each packaging type, when there were four components in total, however the reason for this can be seen in the spectra of the components. Caffeine and aspirin both exhibit highly similar spectra, with shared peaks at 550 cm^{-1}, 640 cm^{-1}, ~750 cm^{-1}, 1280 cm^{-1}, and 1600 cm^{-1}. It is because of these similarities, and the almost identical quantities of the components used in each sample, that the two compound's spectra were likely viewed as being one in the same, owing

to them being perceived as a single component in the analysis. Because of this, only three components were found to be significant in each sample.

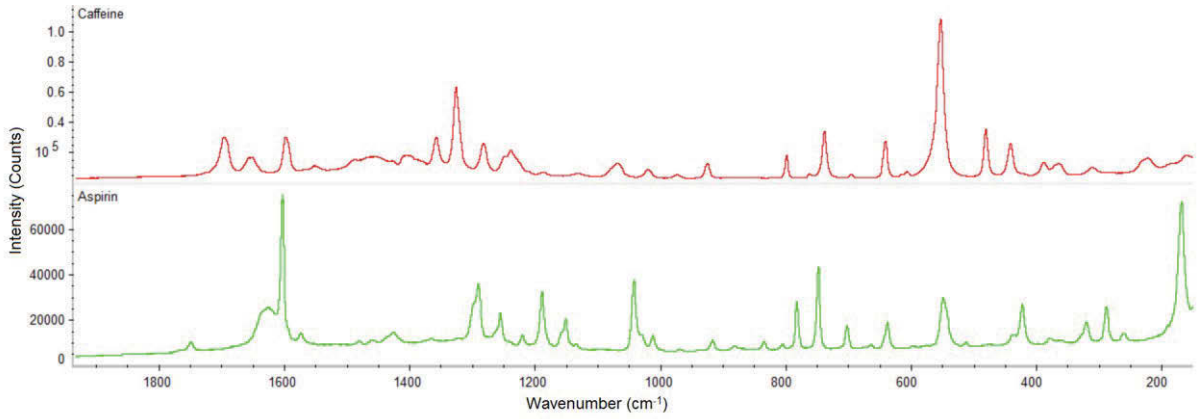

Figure 31 – Comparison of the Raman spectra of Caffeine and Aspirin.

Identification of the resolved component spectra was found to be successful for all samples except for the white cardboard, a pattern that followed on from the results of previous testing. For each of the remaining five samples, the three component spectra were all identified to be either representations of the packaging itself, or representative of the known compounds that were used in creating the samples. Most successful in this examination were the samples including LDPE and the white envelope, where three of the four components were identified successfully with varying degrees of quality.

It was known that far more complicated samples, and a more expansive chemometric approach would likely result in decrease in the observed accuracy of the method, and this expected pattern was easily observed. The MCR analysis proved successful, creating relatively pure spectra from the convoluted mixed samples, while the SORS method developed managed to ensure that the

majority of interfering peaks from the packaging were adequately removed. A major factor that was attributed to the failing of the chemometric models was the large degree of inhomogeneity present within the mixed powder, as well as the overlapping of several peaks, namely within the spectra of caffeine, atropine, and the aspirin, overlapping with peaks across the 550 cm^{-1} to 1600 cm^{-1} region. The other prominent factor was that the MCR created estimated pure spectra, and as such the intensities of the peaks generated could not be trusted as being accurate representations of the true concentrations, making quantification an impossible task.

Despite this and a few noted false positives, it was found that the devised method was more than capable as a first pass screening method, allowing for parcels concealing complex powders to be analysed and identified rapidly without the need for handling or subsampling, while a secondary technique such as gas chromatography-mass spectrometry could then be used to corroborate results and eliminate any false positives that may arise.

11.2.4 Interrogation of Complex Multi-Layer Parcels

While the method for investigation of the multi-layer samples might not have varied significantly from the optimised method devised, it was nevertheless expected that a lower accuracy in both identification and quantification would be observed, simply due to the more complex nature and increased thickness of the packaging. While this was the case, it was encouraging to discover that the optimised method was able to penetrate a sufficient depth that made successful interrogation of the parcels possible.

Highly successful results were observed during the identification stage, with the scaled subtraction method proving capable of removing outside interference from the packaging

material. Interestingly, a low level of quality for the identifications were observed for the 100% aspirin samples concealed within the combinations involving HDPE and LDPE, despite both these spectra and the reference standard sharing sixteen common peaks, predominantly around 1600 cm^{-1}, 1300 cm^{-1}, 1185 cm^{-1}, 1100 cm^{-1}, 750 cm^{-1}, and 525 cm^{-1}.

Understandably, the general trend in the results was that as the concentration of the target analyte decreased, so too did the quality of the identification. This behaviour is not unsurprising as when the concentration of the aspirin was lowered, the prominence of the peaks would decrease, making the identity more difficult to ascertain. Some small exceptions to the trend were noticeable, however they were largely irrelevant.

The main concern within the method were the two false positives noted, where the blank samples of baking powder alone were misidentified as atropine in the HDPE packaging, and caffeine in the LDPE packaging. While troubling, the low quality of these identifications makes their inclusion within the results insignificant.

Of other importance in the results were those spectra identified as being different packaging types than those being investigated. This was most prominent in the spectra from the padded bag, and white envelope, both of which had been covered in brown tape, and of which both were identified to contain white cardboard. This misidentification was similarly of little concern, as the similar nature of the packaging types, and the limited importance of knowing the packaging type, meant they were largely inconsequential errors.

The accuracy observed within quantification results was largely dependent upon the characteristics of the packaging being interrogated, with the more formidable barriers reducing the apparent accuracy of the models and predictions. The padded bag fastened with brown tape proved to be the most difficult parcel to exploit, with the additional thickness and fluorescence from the brown tape skewing the peak intensities and reducing the linearity of the overall model. Similarly, the newspaper was found to be a difficult packaging type to analyse, largely because it was necessary to use a lower laser power so that no thermal degradation occurred.

As a result, quantification of the powders concealed within these packages gave largely inaccurate results for the majority of concentrations. For the remaining four packaging types, it was found that the results remained haphazard, occasionally producing accurate results, but often producing results far from the known concentrations. This was particularly evident in the white polystyrene samples where a value of -208.30% was obtained, an issue largely attributed to the complex and overlapping nature of the spectra.

11.3 Examination of Packaging Characteristics

While sample inhomogeneity proved to be one of the more dominant reason for reduced accuracy, the sample characteristics also played an important role, adding to the complications in the method.

11.3.1 Density

The light propagation inside a sample depends upon the optical density of a material, which influences the probability of a photon being absorbed or being converted to a Raman photon at

each step of the process. Consequently, when a laser beam hits a highly turbid sample, the photons will propagate in a random fashion, and due to the random scattering of the photons in the sample material, the surface interrogated will increase with increasing depth (Cletus, Olds et al. 2012). This effect helps to make the SORS method successful, but will also vary dramatically with the type of sample being interrogated.

When considering the plastic and polymer based samples, the density and crystallinity of the samples has a measured effect, with the difference notable between LDPE and HDPE samples. The greater crystallinity present in the HDPE sample will cause a sharper and clearer spectrum to arise, while the more diffuse spectrum will be obtained from the LDPE sample (Gall and Hendra 1971).

There is an opposite effect that can be seen in organic samples that are prone to excessively absorbing the laser light, such as paper and cardboard (Bloomfield, Matousek et al. 2013). The higher density of cardboard, coupled with its ability to strongly absorb the excitation laser light ensures that the sample blocks all potential transmission, and ultimately burns, while the less dense paper allows for some transmission of the laser light, leading to the successful interrogation of the sample.

11.3.2 Thickness

It was shown experimentally in this work, and in work by Liao et al., that as the thickness of the top layer of a sample increases, the intensity of concealed layers will decrease (Liao, Sinjab et al. 2016). In their work, it was shown that increasing the thickness of a top-layer caused a noted

attenuation in the Raman signal of the bottom layer, indicating that a thicker sample presented a more formidable barrier and reduced the efficacy of the technique.

In the work demonstrated here, the same effect can be seen. Thicker layers of white paper can be seen to reduce the prominence of the peaks from the atropine concealed within. These results mirror those found in the work by Liao et al., proving how the thickness of the sample can drastically alter the quality and sensitivity of the method. This effect largely explains the lack of success when investigating the PVC tiles.

11.3.3 Opacity

It was noted in work by Shelly Li, that the opacity of a sample could potentially have an effect on the intensity of the Raman signal obtained (Li 2010). In theory, a more transparent sample will allow a freer scattering and easier transmission of light, resulting in spectra of greater intensity. This theory is seen in action when considering the different packaging types present in this research, particularly the two samples of polystyrene.

Both samples of polystyrene exhibited similar thicknesses and densities, and differed predominantly only in their colour and opacity. When considering the results obtained from the samples, it can be seen that more intense peaks and more accurate results were obtained from , the transparent, colourless sample of polystyrene. These results add weight to the theory noted by Shelly Li, and also go to show how the effects of opacity can alter the quality of spectra obtained.

It has previously been reported that sample opacity, along with orientation and laser power can have a noted and direct effect on Raman intensity (Sasic 2008), and that the opacity of a sample will limit the effective path length, resulting in less depth being probed in each measurement (McCreery 2005). If a material is transparent, then the depth of focus and focal volume of the laser beam will be dictated by the numerical aperture of the lens, the wavelength of the laser light, and the real component of the sample's refractive index at that wavelength. However, if the sample is closer to opaque, then the depth of light penetration will be dictated not by the physical optics but by the absorptivity of the sample at that wavelength (Tuschel 2016). As such, it can be easily seen how the apparent opacity of a sample can greatly change the intensity of the Raman signal obtained.

11.3.4 Colour

The last of the dominant physical characteristics that were found to affect the quality and intensity of the Raman signals obtained is the colour of the samples being interrogated. It had already been shown that dark coloured samples such as brown and green bottles are notoriously difficult to analyse, either due to fluorescence or adsorption of the laser light (Bumbrah and Sharma 2016).

It has also been shown that the Raman signals observed from dark samples, such as black, grey, and dark blue packages and specimens were very low in intensity, a common occurrence due to the laser light being absorbed by carbon black (NIRSystems 2016). This effect was also seen in the work conducted for this research, with no observable peaks obtained from paper samples that were coloured black or brown. Lighter colours, such as blue, green, pink, purple, white, and red

seemed to have little or no effect on the intensity of the Raman peaks, however it was observed that yellow and orange samples had weaker Raman signals when examined using the 785 nm laser.

Particularly for paper and polymer based samples, it was observed how colour of the sample can have a noticeable effect on the quality of the Raman spectra obtained, and the intensity of the Raman signal achieved.

11.4 Analysis of the Developed Method

Although the developed method worked more than adequately for nineteen of the twenty-five packaging types, and for the more complex packaging types examined, it had some drawbacks and limitations. Notably, the quality of the spectra obtained, and so the quality of the identification and quantification methods, was highly susceptible to the physical characteristics of the packaging types, and largely dependent upon the quality of the subtraction undertaken. In this brief section, an analysis of the drawbacks found within the method will be presented, along with potential solutions to overcome them.

11.4.1 Critical Analysis of the Identification Method

Based solely upon the results, the devised method can be seen as wholly successful, bringing about the rapid and accurate detection and identification of concealed powders through a variety of packaging types without damaging the exterior of the packaging. Although not all packaging types could be successfully permeated with the laser light, those that were susceptible were analysed to a high degree of accuracy and sensitivity.

Two main issues persisted throughout the experimentation, that of sample inhomogeneity, and the resistance of the packaging due to their physical characteristics. Regarding the first issue, sample inhomogeneity proved to be partially overcome by prolonged grinding with the agate mortar and pestle, and the larger spot size of the laser produced by the axicon lens. With the prolonged grinding method not an option for real-world scenarios, other methods were also found to help overcome this issue and to lower the number of negative or incorrect identifications, such as increasing the number of accumulations and acquisitions collected in each run. While both these motions would increase the length of time required to collect the data, thereby decreasing the efficiency of the method, they would also enhance the sensitivity of the results, increasing the prominence of important Raman peaks required for identification. Another potential method would be to use a laser of lower wavelength such as 244 nm which would give better quality spectra, however this may cause additional problems regarding fluorescence of the packaging that would have to be combated.

Regarding the second issue, there is unfortunately no way to reduce the effects of the packaging, as the thickness, opacity and density of the samples are set, however, it might be possible to reduce the effects of colour. It was shown previously that the colour of a sample is capable of both promoting fluorescence and absorbing the laser light. Both effects greatly reduce the effectiveness of the method, with the fluorescence causing important peaks to be eclipsed and making the scaled subtraction impossible, while the absorption of the laser light causes a great reduction in the amount of laser light that is transmitted to the sample, causing a noticeable reduction in the quality of the results obtained. While it was not tested, one potential solution would be to place a small piece of white, or similarly coloured material atop the parcel being

tested. Such a material would reduce the effects of the packaging's colour, while not being thick or dense enough to greatly alter the results obtained.

One further difficulty encountered within the method was ensuring that an accurate subtraction between the spatially offset spectrum and the conventional spot spectrum could be achieved. Two methods were used to ensure that this step was carried out effectively and with minimal adulteration of the target peaks, namely, a normalising, scaling of all spectra to a level of 25,000 counts, and the use of an external standard to correct for daily variations that arose from the Raman microscope. By incorporating both of these stages into the final, optimised method, it could be ensured that any spectral adulteration was done in a controlled and responsible manner.

11.4.2 Critical Analysis of the Quantification Method

Coupling of the novel SORS method developed with powerful chemometric methods was found to produce favourable results when looking to quantify concealed powders hidden inside parcels. The selection of PLS-R over other available chemometric processes such as principal component analysis was found to be successful, allowing for accurate, informative models to be easily generated. Models were found to generally exhibit low RMSE and high R^2 values, which potentially could be accurate enough for routine forensic analysis (Ryder, O'Connor et al. 2000).

Some key issues prevailed throughout the refinement of the method, issues which need to be addressed and overcome. Firstly, the sample inhomogeneity was the largest factor that lowered the accuracy of each chemometric model. While the larger spot size of the laser helped to collect more information from each run, ensuring that a more complete picture of the mixed powder was

collected, there was still the potential for large portions of heterogeneous sample to persist and skew measurements. In an effort to overcome this effect, a larger number of independent points upon the sample would need to be probed, so that a more comprehensive view of the parcel's contents can be viewed. While taking more than twenty-five spectra per concentration would begin to diminish the efficiency of the method, and would not always be practical for every possible narcotic formulation (Ryder, O'Connor et al. 2000), it is currently one of the most effective solutions to the problem, even if issues can persist.

A second prominent issue was regarding the efficiency of the method. While taking a larger number of independent samples proved largely effective in this research, it was found that even after collecting twenty or more spectra from a sample, some errors and inconsistencies persisted. Capturing a larger number of independent points would greatly decrease the efficiency of the method, with the amount of work and time required to build each model greatly increased, but there are some potential solutions to this issue. A list of new techniques and technology such as Raman mapping and imaging has been shown to make the manual process more efficient by automating the process, allowing for a quicker and less hands-on method to be constructed (Bernard, Beyssac et al. 2008, Zoubir 2012).

While these issues were able to be generally overcome in this research, further refinement and optimisation is of constant interest. The ability to increase accuracy and maintain, or better, the overall efficiency of the method is of specific interest. Combining the developed technique with more automated methods should improve upon both qualities, as long as the focus with both the sample and axicon can be maintained.

11.4.3 Determination of Limits of Detection & Quantification

An accurate comparison of the limits of detection and quantification for the developed SORS method was difficult to come by, particularly for a method that serves to look through a variety of packaging types. Some data was found from previous research and development, with Cobalt's TRS-100 spectrometer reaching an LOD of 1-2% of the active pharmacological ingredient (API), while their portable RapID indicated impressive penetration ability of 2 mm thick plastic bags, 4 mm of opaque/coloured HDPE, and 4-5 layers of multi-layered paper/plastic sacks (Cobalt 2016).

For the developed method, the LOD for simple samples can be compared favourably, with an average LOD found to be approximately double that of Cobalt's results at 4%. When considering that the developed method is devised to be a cheap and simple method to convert a traditional Raman microscope into a functional SORS method. The depth and power of penetration is another important comparison, and again it favourably compares to that of Cobalt's RapID. While multi-layer samples only up to three layers were examined, the results show the potential for even more complex parcels to be successfully analysed. Furthermore, samples such as the packing foam were successfully analysed and featured a greater thickness than the 4 mm reported by Cobalt, while the 2 mm reported for plastic bags was easily mirrored in the padded bag examined.

Chapter 12 – Conclusion

Although the manners and methods in which drugs are sold and trafficked has become digitised, modernised, and made far more difficult to combat, the social and economic costs of drug abuse have remained a frightening constant. Through the advent of new and more sophisticated ways of transporting and selling illicit drugs, the prominence of drugs of abuse in society, both domestically and internationally has dramatically increased, and so it is paramount that new methodologies to tackle the increasing threat are developed.

While these new and more intricate smuggling methods are becoming more sophisticated and increasingly varied, the majority of recreationally used drugs, particularly cocaine is known to arrive through parcels and in simple packaging delivered through the mail. Purchased online through the Darknet, where these drugs can be bought and sold with almost absolute anonymity, the trafficking of these illicit substances has become steadily more covert and difficult to trace, and the best hope for combating the current damage of drug abuse now appears to be through improving the ability to detect and intercept the illicit substances in transit.

One of the most discussed and researched techniques for such methods of identification and quantification in current years, is that of Raman spectroscopy. The prominence of Raman spectroscopy in the field of drug detection and quantification is largely attributed to the technique's ability to provide rapid, sensitive, non-destructive, and in-situ analysis of a variety of drug samples (West and Went 2011). Although powerful, traditional Raman spectroscopy is limited in its ability to profile thick samples, causing it to have serious limitations when dealing with parcels in transit.

In an effort to subvert this issue, as well as to further simplify and improve the basic method of Raman spectroscopy, the new technique of Spatially Offset Raman Spectroscopy (SORS) has been created. This technique has been ideally reported to be able to produce accurate identification of both solids and liquids within containers in several previous trials. Importantly, this technique can analyse substances without the need for any sample pre-treatment, meaning that a suspected illicit substance can be identified and potentially quantified without disturbing its packaging. While literature regarding this technique is still limited, there is sufficient indication that SORS is a prominent and highly important modern spectroscopic technique.

In this research, a newly developed SORS method that was amenable to conventional Raman spectrometers was presented. The method developed was able to detect, identify, and quantify various mixed samples involving atropine and a number of adulterants through twenty-five common and frequently used packaging types, as well as several simulated parcels created directly from recent news stories and global events.

In this research, a simple but effective SORS method was developed that could easily be used in conjunction with a traditional Raman spectrometer. The method was able to successfully investigate nineteen of the most common parcels types, including envelopes, tapes, plastics, and wrapping paper, while also being able to successfully detect, identify, and quantify various samples of concealed compounds. Furthermore, the method was able to successfully interrogate complex mixed powders, and complex multi-layer parcels, furthering the applicability of the technique.

Although some flaws persisted, particularly when considering the overall efficiency of the method, it was shown that the use of a simple axicon, coupled with a traditional Raman microscope and chemometric processes, could interrogate the majority of common packaging types available. Limitations persisted for some packaging types, such as metals, cardboard, and thick polymers, however, it was easily shown that a far greater amount of spectral information could be gathered using the SORS method. In addition to these findings, a deeper understanding on the limitations and potentials of the SORS technique was achieved, with the power of the method examined through the use of more complex samples and parcel types.

In conclusion, this research confidently showed the benefits of using a SORS method, while also showing that the technique could be easily achieved through the simple transformation of a traditional Raman microscope, alleviating the need to purchase entirely new instrumentation at a much greater cost. As such, it was proven that the SORS method, with refinement, could potentially be a powerful new technique in the ever-evolving war on drugs.

Appendix

Physical characteristics of the twenty-five packaging samples tested.

Packaging	Weight (g)	Length (cm)	Width (cm)	Thickness (cm)	Area Density (g/m^2)
Australia Post Brand Bubble Wrap	0.1867	4.20	6.0	0.190	74.09
Australia Post PB3 Padded Bag	8.0102	12.7	17.8	0.309	354.34
Australia Post Prepaid Parcel Post Satchel	0.6958	6.0	10.4	0.028	111.51
Australia Post Brand Brown Parcel Tape	0.0632	5.5	2.5	0.010	45.96
Australia Post Brand Clear Parcel Tape	0.0657	5.5	2.5	0.011	47.78
Black LDPE Satchel	0.3728	6.0	4.9	0.040	155.33
Brown Cardboard	2.4047	8.5	6.5	0.170	435.24
Brown Envelope	0.9385	9.0	7.5	0.056	139.04
Generic Bubble Wrap with White LDPE	0.4256	6.0	4.0	0.258	177.33
Generic Padded Bag	0.3499	5.0	4.5	0.208	155.51
Generic Padded Satchel	0.4025	6.3	3.5	0.362	101.76
Generic Wrapping Paper	0.1695	4.2	5.7	0.010	70.80
Grey Cardboard	4.7248	8.7	6.3	0.157	862.03
Newspaper	0.1284	5.0	5.0	0.010	51.36
PPS Kraft Paper – Brown	0.1268	4.0	5.0	0.013	63.40
PPS Plainface DL White Envelope	0.3737	8.5	6.0	0.019	73.27
Packing Foam	0.2137	6.0	3.5	0.556	101.76
Quill Coloured Envelope – C6 Orange	0.3296	7.0	5.0	0.057	94.17
Reflex A4 White Paper	0.4626	5.7	10.0	0.015	81.16
HDPE	1.4672	4.6	4.8	0.080	654.10
Transparent PS	0.3852	4.0	5.2	0.019	185.19
White Cardboard	1.1231	7.5	6.0	0.157	249.58
White PS	0.7321	5.3	5.4	0.060	255.80
White PVC Tile	47.4682	9.8	26.5	0.554	1827.81
Wood Grain PVC Tile	99.1364	10.0	32.0	1.042	3098.01

$$GSM = grams\ per\ square\ meter = \ Weight \ \div (Length \times Width)$$

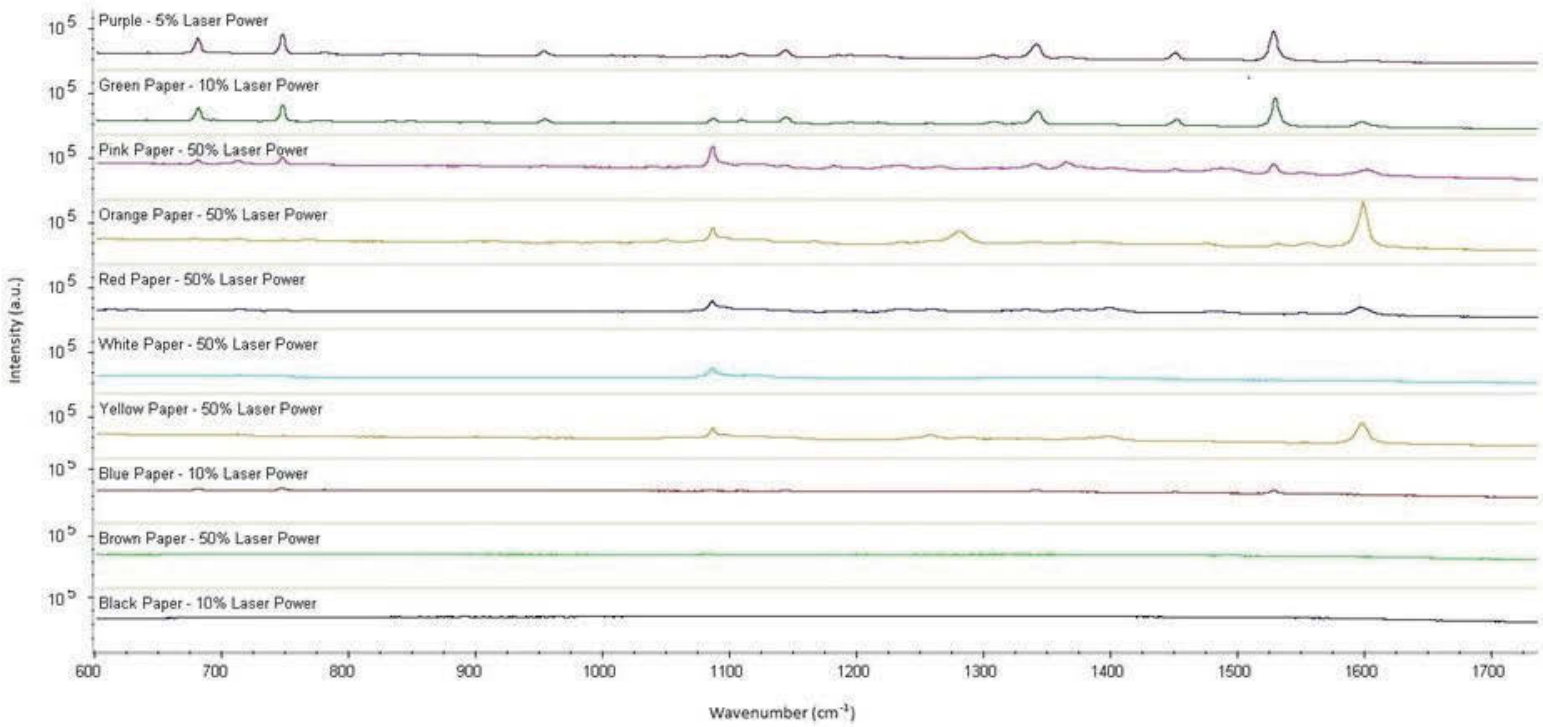

Comparison of conventional Raman spectra collected from various coloured papers with a 785 nm excitation laser. Spectra are shown on a common scale, and the various laser powers used for each spectrum are given.

References

AAP (2005). Cocaine sent through mail. The Age.

Ali, M. A., et al. (2009). "In Situ Detection of Cocaine Hydrochloride in Clothing Impregnated with the Drug Using Benchtop and Portable Raman Spectroscopy." Journal of Raman Spectroscopy.

Anderson, D. (2015). A Question Of Trust, Meshed Insights Ltd.

Armbruster, D. A. and T. Pry (2008). "Limit of Blank, Limit of Detection and Limit of Quantitation." The Clinical Biochemist Reviews **29**(1): 49-52.

Bartick, E. (2002). Forensic Analysis by Raman Spectroscopy: An Emerging Technology. M. Editore. Bologna, Italy, Proceedings of the 16th Meeting of the International Association of Forensic Sciences**:** 45-50.

Bartlett, J. (2014). The Dark Net: Inside the Digital Underworld, Random House.

Beebe, K. R., et al. (1998). "Chemometrics: A Practical Guide." John Wiley & Sons.

Bell, S. E., et al. (2000). "Composition Profiling of Seized Ecstasy Tablets by Raman Spectroscopy." Analyst **125**(10): 1811-1815.

Bell, S. E. J., et al. (2004). "Development of Sampling Methods for Raman Analysis of Solid Dosage Forms of Therapeutic and Illicit Drugs." Journal of Raman Spectroscopy **35**(5): 409-417.

Bernard, S., et al. (2008). "Raman Mapping Using Advanced Line-Scanning Systems: Geological Applications." Applied Spectroscopy **62**(11): 1180-8

Bloomfield, M., et al. (2010). "Detection of concealed substances in sealed opaque plastic and coloured glass containers using SORS." in Optics and Photonics for Counterterrorism and Crime Fighting VI and Optical Materials in Defence Systems Technology VII, Proceedings of SPIE **7838**.

Bloomfield, M., et al. (2013). "Non-invasive identification of incoming raw pharmaceutical materials using Spatially Offset Raman Spectroscopy." Journal of Pharmaceutical and Biomedical Analysis **76**: 65-69.

Brenan, C. J. H. and I. W. Hunter (1996). "Volumetric Raman Microscopy Through a Turbid Medium." Journal of Raman Spectroscopy **27**(8): 561-70

Brookshire, B. (2015). Caffeine Gives Cocaine an Addictive Boost. ScienceNews.

Buckley, K., et al. (2014). "Decomposition of in vivo Spatially Offset Raman Spectroscopy Data Using Multivariate Analysis Techniques." Journal of Raman Spectroscopy **45**(2): 188–192.

Bumbrah, G. S. and R. M. Sharma (2016). "Raman spectroscopy – Basic principle, instrumentation and selected applications for the characterization of drugs of abuse." Egyptian Journal of Forensic Sciences **6**: 209-15

Caliberto, E. and G. Spoto (2000). Modern Analytical Methods in Art and Archaeology. Chemical Analysis Series. Chichester.

Carr, A. (2012). Carlisle man sent to prison after receiving package of cocaine in mail. The Sentinel.

Cavasinni, B. (2012). Detection & Quantification of a Cocaine Analogue & its Adulterants in Textiles. Faculty of Science, University of Technology, Sydney. **Bachelor of Forensic Science (Honours) in Applied Chemistry**.

Chalmers, J. M., et al. (2012). Infrared and Raman Spectroscopy in Forensic Science, John Wiley & Sons.

Chalmers, J. M. and P. R. Griffiths (2001). Handbook of Vibrational Spectroscopy, John Wiley & Sons.

Cletus, B., et al. (2011). "Concealed substance identification using a defocused inverse spatially offset Raman spectrometer." Queensland University of Technology. 1339-41

Cletus, B., et al. (2012). "Combined time- and space-resolved Raman spectrometer for the non-invasive depth profiling of chemical hazards " Analytical and Bioanalytical Chemistry. **403**(1): 255-63

Cobalt (2016). "Cobalt RapID and TRS100." Retrieved November 2nd, 2016, from http://www.ablelab.eu/products/spectroscopy/cobalt-rapid-es-trs100.

Conti, C., et al. (2015). "Subsurface analysis of painted sculptures and plasters using micrometre-scale spatially offset Raman spectroscopy (micro-SORS)." Journal of Raman Spectroscopy **46**: 476-482.

Conti, C., et al. (2015). "Noninvasive analysis of thin turbid layers using microscale spatially offset Raman spectroscopy." Analystical Chemistry. **87**(11): 5810-5

Croke, B. F. W. (1995). "Removal of Cosmic-Ray Events in Spectroscopic CCD Data." Publications of the Astronomical Society of the Pacific.

Das, B. B., et al. (1997). "Time-Resolved Fluorescence and Photon Migration Studies in Biomedical and Model Random Media." Rep. Prog. Phys. **60**(227): 227-92

Das, R. S. and Y. K. Agrawal (2011). "Raman Spectroscopy: Recent Advancements, Techniques and Applications." Vibrational Spectroscopy **57**: 163-176.

DeepDotWeb (2013). "Updated: List of Dark Net Markets (Tor & I2P)." Retrieved November 4th, 2016, from https://www.deepdotweb.com/2013/10/28/updated-llist-of-hidden-marketplaces-tor-i2p/

Demsar, U., et al. (2012). "Principal Component Analysis of Spatial Data: An Overview." Annals of the Association of American Geographers **103**(1): 106-128.

Depret, B., et al. (2002). "Characterization and modelling of the hollow beam produced by a real conical lens." Optics Communications **211**: 31-38.

Di, Z., et al. (2015). "Spatially offset Raman microspectroscopy of highly scattering tissue: theory and experiment." Journal of Modern Optics **62**(2): 97-101.

Dickey, F. M. (2014). Laser Beam Shaping: Theory and Techniques, CRC Press.

Dieing, T., et al., Eds. (2010). Confocal Raman Microscopy, Springer.

Durkin, A. J., et al. (1998). "Quantification of Polydimethylsiloxane Concentration in Turbid Samples Using Raman Spectroscopy and the Method of Partial Least Squares." Lasers in Medical Science **13**: 32-41.

Edwards, H. G. M. and J. M. Chalmers (2005). Practical Raman Spectroscopy and Complementary Techniques. Raman Spectroscopy in Archaeology and Art History. Cambridge, The Royal Society of Chemistry.

Edwards, H. G. M. and J. M. Chalmers (2005). Raman Spectroscopy in Archaeology and Art History. Cambridge, Royal Society of Chemistry Publishing.

Edwards, H. G. M., et al. (2005). "Raman Spectroscopic Characterisations and Analytical Discrimination Between Caffeine and Demethylated Analogue of Pharmaceutical Relevance." Spectrochimica Acta. **61**(7): 1453-9

Eliasson, C., et al. (2007). "Deep Subsurface Raman Spectroscopy of Turbid Media by a Defocused Collection System." Applied Spectroscopy **61**(10): 1123-1127.

Eliasson, C., et al. (2007). "Non-Invasive Detection of Concealed Liquid Explosives Using Raman Spectroscopy." Analytical Chemistry **79**(21): 8185-8189.

Eliasson, C., et al. (2008). "Non-invasive quantitative assessment of the content of pharmaceutical capsules using transmission Raman Spectroscopy." Journal of Pharmaceutical and Biomedical Analysis **47**: 221–229.

Eliasson, C., et al. (2007). "Non-Invasive Detection of Cocaine Dissolved in Beverages Using Displaced Raman Spectroscopy." Analytica Chimica Acta **607**: 50-53.

Eliasson, C. and P. Matousek (2007). "Non-Invasion Detection of Counterfeit Drugs Using Spatially Offset Raman Spectroscopy (SORS)." Central Laser Facility Annual Report.

Eliasson, C. and P. Matousek (2007). "Non-Invasive Authentication of Pharmaceutical Products Through Packaging Using Spatially Offset Raman Spectroscopy." Analytical Chemistry **79**(4): 1696-1701.

Elshout, M., et al. (2011). "Detection of Raman Spectra in Ocular Drugs for Potential In Vivo Application of Raman Spectroscopy." Journal of Ocular Pharmacology and Therapeutics **27**(6): 445-51

Esse, K., et al. (2011). "Epidemic of illicit drug use, mechanisms of action/addiction and stroke as a health hazard." Brain and Behavior.

Everall, N. (1994). "Quantitative Study of Self-Absorption in Near-Infrared Fourier Transform Raman Spectroscopy." Journal of Raman Spectroscopy **25**: 813-819.

Everall, N. J. (2000). "Modelling and Measuring the Effect of Refraction on the Depth Resolution of Confocal Raman Microscopy." Appl. Spectrosc. **54**: 773.

Farquharson, S. and W. Smith (2004). "Differentiating Bacterial Spores from Hoax Materials by Raman Spectroscopy " Proceeding of SPIE.

Fenton, O. S., et al. (2011). "Quantitative Analysis of Simulated Illicit Street-Drug Samples Using Raman Spectroscopy and Partial Least Squares Regressions." Spectroscopy Letters **44**: 229-234.

G., C., et al. (1984). "Raman Spectroscopy of Urea-Formaldehyde Resins and Model Compounds." Journal of Applied Polymer Science **29**: 2749-62

Gall, M. J. and P. J. Hendra (1971). "Laser-Raman Spectroscopy of Polymer Samples." The Spex Speaker **16**(1).

Gaubert, A., et al. (2016). "Characterization of Surfactant Complex Mixtures Using Raman Spectroscopy and Signal Extraction Methods: Application to Laundry Detergent Deformulation." Analytica Chimica Acta **915**: 36-48.

Geladi, P. and B. R. Kowalski (1986). "Partial Least-Squares Regression: A Tutorial." Analytica Chimica Acta **185**: 1-17.

Giles, J. H., et al. (1999). "Quantitative Analysis Using Raman Spectroscopy Without Spectral Standardization." Journal of Raman Spectroscopy **30**: 767-771.

Goodin, D. (2012). Feds shutter online narcotics store that used TOR to hide its tracks, ARS Technica.

Greenberg, A. (2013). New Silk Road Drug Market Backed Up To '500 Locations In 17 Countries' To Resist Another Takedown. Forbes.

Greenberg, A. (2014). "Drug Market 'Agora' Replaces The Silk Road As King of the Dark Net."

Greve, J., et al. (1999). Spectroscopy of Biological Molecules: New Directions. 8th European Conference on the Spectroscopy of Biological Molecules, Enschede, The Netherlands, Springer Science & Business Media.

Guineau, B., et al. (2001). "Manganese Black Pigments in Prehistoric Paintings: the Case of the Black Frieze of Pech Merle"Archaeometry. **43**(2)**:** 211-15.

Haaland, D. M. and E. V. Thomas (1988). "Partial Least-Squares Methods for Spectral Analyses." Anal. Chem. **60**: 1193-1202.

Hargreaves, M. D., et al. (2008). "Application of Portable Raman Spectroscopy and Benchtop Spatially Offset Raman Spectroscopy to Interrogate Concealed Biomaterials." Journal of Raman Spectroscopy **40**: 1875-1880.

Hargreaves, M. D., et al. (2008). "Analysis of Seized Drugs Using Portable Raman Spectroscopy in an Airport Environment: A Proof of Principle Study." Journal of Raman Spectroscopy **39**: 873-880.

Hargreaves, M. D. E., Howell G.M. Chalmers, John M. (2011). Infrared and Raman Spectroscopy in Forensic Science (2nd Edition). Hoboken, NJ, USA, Wiley.

Harroun, S. G., et al. (2011). "Surface-Enhanced Raman Spectroscopy Analysis of House Paint and Wallpaper Samples from an 18th Century Historic Property." Analyst **136**: 3453-3460.

Hendra, P. J. (2002). Sampling Considerations for Raman Spectroscopy. Handbooks of Vibrational Spectroscopy. J. M. Chalmers and P. R. Griffiths, John Wiley & Sons. **Volume 2**.

Hoffmann, A. (2015). Before Darknet Markets Were Mainstream, Deep Dot.

Hopkins, R. J., et al. (2012). "Short-Wave Infrared Excited Spatially Offset Raman Spectroscopy (SORS) for Through-Barrier Detection." Analyst **137**(19): 4408-10

Huang, J., et al. (2010). "Practical Considerations in Data Pre-treatment for NIR and Raman Spectroscopy." Retrieved January 2nd, 2017 from http://www.americanpharmaceuticalreview.com/Featured-Articles/116330-Practical-Considerationsin-Data-Pre-treatment-for-NIR-and-Raman-Spectroscopy/

Hurley, D. (2014). Crime lords send drugs through mail in tiny packages to avoid detection. Herald Sun.

Jaumot, J., et al. (2005). "A Graphical User-Friendly Interface for MCR-ALS: A New Tool for Multivariate Curve Resolution in MATLAB." Chemometrics and Intelligent Laboratory Systems **76**: 101-110.

Jevatovic, P. and ACC (2014). 2012-12 Illicit Drug Data Report. Canberra, Australian Crime Commission.

Karch, S. B. (2005). A Brief History of Cocaine, CRC Press.

Katainen, E., et al. (2007). "Quantification of the Amphetamine Content in Seized Street Samples by Raman Spectroscopy." Journal of Forensic Sciences **52**(1): 88-92.

Kaur, H. S. (2006). Instrumental Methods of Chemical Analysis. Meerut, Pragati Prakashan.

Kwok, K. and L. S. Taylor (2012). "Analysis of Counterfeit Cialis Tablets Using Raman Microscopy and Multivariate Curve Resolution." Journal of Pharmaceutical and Biomedical Analysis **66**: 126-135.

Laikin, M. (2006). Lens Design, CRC Press.

Landsberg, G. and L. Mandelstam (1928). "Eine neue Erscheinung bei der Lichtzerstreuung in Krystallen." Naturwissenschaften **16**(28): 557.

LaPlant, F. (2010). "Lasers, Spectrographs, and Detectors." Springer.

Laufer, G. (1996). Introduction to Optics and Laser in Engineering, Cambridge University Press.

Lei, M., et al. (2012). "Long-Distance Axial Trapping with Focused Annular Laser Beams." PLoS ONE **8**(3): e57984.

Lewis, I. R. and H. Edwards (2001). Handbook of Raman Spectroscopy: From the Research Laboratory to the Process Line, CRC Press.

Li, S. (2010). "Application of Online Reaction Monitoring by Raman and Infrared Spectroscopy in Early Drug Development: Halogen-Lithium Exchange Chemistry." American Pharmaceutical Review.

Liang, N. T., et al. (1993). "Laser Power Dependence of Raman Scattering on YBazCu307-x Thin Films." Journal of Raman Spectroscopy **24**: 179-181.

Liao, Z., et al. (2016). "DMD-based software-configurable spatially offset Raman spectroscopy for spectral depth profiling of optically turbid samples." Optics Express **24**(12): 12701-12

Littleford, R. E., et al. (2004). "Raman Spectroscopy of Street Samples of Cocaine Obtained Using Kerr Gated Fluorescence Rejection." The Analyst **129**(6): 505-6

Loadman, M. J. (1999). Analysis of Rubber and Rubber-like Polymers, Springer.

Loeffen, P. W., et al. (2011). "Spatially Offset Raman Spectroscopy (SORS) For Liquid Screening." SPIE Proceedings **8189**.

Long, D. A. (2002). The Raman Effect: A Unified Treatment of the Theory of Raman Scattering by Molecules, John Wiley & Sons.

Macleod, N. A., et al. (2008). "Prediction of Sublayer Depth in Turbid Media Using Spatially Offset Raman Spectroscopy." Analytical Chemistry **80**(21): 8146-52

Maher, J. R. and A. J. Berger (2010). "Determination of Ideal Offset for Spatially Offset Raman Spectroscopy." Applied Spectroscopy **64**(1): 61-65.

Martens, H. and T. Naes (1992). Multivariate Calibration, John Wiley & Sons.

Matousek, P. (2006). "Inverse Spatially Offset Raman Spectroscopy for Deep Non-Invasive Probing of Turbid Media." Applied Spectroscopy **60**(11): 1341-1347.

Matousek, P., et al. (2005). "Subsurface Probing in Diffusely Scattering Media Using Spatially Offset Raman Spectroscopy." Applied Spectroscopy **59**(4): 8.

Matousek, P. and M. D. Morris (2010). Emerging Raman Applications and Techniques in Biomedical and Pharmaceutical Fields, Springer.

McCreery, R. L. (2000). Raman Spectroscopy for Chemical Analysis. New York, John Wiley & Sons.

Mehta, M., et al. (2004). "Effects of cocaine and caffeine alone and in combination on cardiovascular performance: an experimental hemodynamic and coronary flow reserve study in a canine model." International Journal of Cardiology **97**(2): 225-232.

Morrison, A. (2013). Man busted importing drugs after post boxes raise alarm. Sunshine Coast Daily.

Mosier-Boss, P. A., et al. (1995). "Fluorescence Rejection in Raman Spectroscopy by Shifted-Spectra, Edge Detection, and FFT Filtering Techniques." Applied Spectroscopy **49**(5):630-9

Murphy, D. B. (2001). Fundamentals of Light Microscopy & Electronic Imaging, John Wiley & Sons.

Naes, T., et al. (2002). Multivariate Calibration and Classification, NIR Publications.

NIRSystems, M. (2016). "Identification of polymers using handheld Raman spectroscopy." Raman Spectroscopy Application Note RS–1 **1**.

Noonan, K. Y., et al. (2009). "Rapid Classification of Simulated Street Drug Mixtures Using Raman Spectroscopy and Principal Component Analysis." Applied Spectroscopy **63**(7): 742-7

O'Connell, M.-L., et al. (2010). "Qualitative Analysis Using Raman Spectroscopy and Chemometrics: A Comprehensive Model System for Narcotics Analysis." Applied Spectroscopy **64**(10): 1109-1121.

Olds, W. J., et al. (2011). "Spatially Offset Raman Spectroscopy (SORS) for the Analysis and Detection of Packaged Pharmaceuticals and Concealed Drugs." Forensic Science International **212**(1): 69-77.

Olds, W. J., et al. (2012). "Non-invasive, quantitative analysis of drug mixtures in containers using spatially offset Raman spectroscopy (SORS) and multivariate statistical analysis." Society for Applied Spectroscopy. **66**(5): 530-7

Ormsby, E. (2012) The Drug's in the Mail.

Osuh, C. (2014). Drugs fixer jailed after smuggling cocaine through the post for THREE years. Machester Evening News.

Penido, C. A. F. d. O., et al. (2012). "Quantification of Binary Mixtures of Cocaine and Adulterants Using Dispersive Raman and FT-IR Spectroscopy and Principal Component Analysis." Instrumental Science and Technology **40**: 441-456.

Power, M. (2013). Online highs are old as the net: the first e-commerce was a drugs deal. The Guardian.

Qian, J. and L. Chandler (2013). "Multi-Wavelength Confocal Raman Microscope for Non-Destructive Pharmaceutical Ingredient Analysis." BaySpec.

Raman, C. V. (1928). "A New Radiation." Indian Journal of Physics **2**: 387-398.

Renganayaki V., et al. (2012). "Vibration Spectroscopy Investigation on Aspirin Using Semi-Empirical Calculations." International Journal of ChemTech Research **4**(3): 983-990

Renishaw (2006). "Chemometric Analysis and Pre-processing Techniques Applied to Raman Mapping Experiements in Forensic Science." SPD/AN **105**(1).

Ryder, A. G. (2002). "Classification of narcotics in solid mixtures using principal component analysis and Raman spectroscopy." Journal of Forensic Sciences **47**: 275-284.

Ryder, A. G., et al. (1999). "Identifications and Quantitative Measurement of Narcotics in Solid Mixtures Using Near-IR Raman Spectroscopy and Multivariate Analysis." Journal of Forensic Sciences **44**(5): 1013-1019.

Ryder, A. G., et al. (2000). "Quantitative Analysis of Cocaine in Solid Mixtures Using Raman Spectroscopy and Chemometric Methods." Journal of Raman Spectroscopy **31**(3): 221-227.

Salzer, R. (2012). Biomedical Imaging: Principles and Applications, John Wiley & Sons.

Sands, H., et al. (1998). "UV-Excited Resonance Raman Spectroscopy of Narcotics and Explosives." Journal of Forensic Sciences **43**(3): 509-513.

Sasic, S., Ed. (2008). Pharmaceutical Applications of Raman Spectroscopy, John Wiley & Sons. 1-28

Sasic, S. and S. Ekins (2007). Pharmaceutical Applications of Raman Spectroscopy, John Wiley & Sons.

Sato, H., et al. (2002). "Raman Spectra of High-Density, Low-Density, and Linear Low-Density Polyethylene Pellets and Prediction of Their Phsyical Properties by Multiavariate Data Analysis." Journal of Applied Polymer Science **86**: 443-448.

Schrader, B. (1995). Infrared and Raman Spectroscopy. Methods and Applications, . Weinheim, VCH.

Schulmerich, M., et al. (2007). "Subsurface and transcutaneous Raman spectroscopy and mapping using concentric illumination rings and collection with a circular fiber-optic array." Applied Spectroscopy **61**(7): 671-678.

Schulmerich, M. V., et al. (2006). "Transutaneous Fiber Optic Raman Spectroscopy of Bone Using Annular Illumination and a Circular Array of Collection Fibers." J. Biomed. Opt. **11**(6).

Schwartz, M. J. (2012). "Feds Bust 'Farmer's Market' For Online Drugs."

Sharma, B., et al. (2013). "Seeing Through Bone with Surface-Enhanced Spatially Offset Raman Spectroscopy." Journal of the American Chemical Society **135**(20): 17290-3

Shrivastava, A. and V. B. Gupta (2011). "Methods for the Determination of Limit of Detection and Limit of Quantitation of the Analytical Methods." Chronicles of Young Scientists **2**: 21-25.

Siesler, H. W., Ed. (2014). Infrared and Raman Spectroscopic Imaging, Wiley.

Smekal, A. (1923). "Zur Quantentheorie der Dispersion." Zuschriften Und Vorläufige Mitteilungen **11**(43): 873-875.

Smith, E. and G. Dent (2005). Modern Raman Spectroscopy - A Practical Approach. Chichester, John Wiley & Sons, Ltd.

Smith, E. and G. Dent (2013). Modern Raman Spectroscopy: A Practical Approach, John Wiley & Sons.

Smith, F. (2004). Handbook of Forensic Drug Analysis, Academic Press.

Smith, W. J. (2000). Modern Optical Engineering, McGraw-Hill.

Socrates, G. (2004). Infrared and Raman Characteristic Group Frequencies: Tables and Charts, John Wiley & Sons.

Stewart, S. P., et al. (2012). "Raman Spectroscopic for Forensic Examination of Beta-Ketophenethylamine "Legal Highs": Reference and Seized Samples of Cathinone Derivatives." Analytica Chimica Acta **711**: 1-6.

Tauler, R., et al. (2009). Comprehensive Chemometrics: Chemical and Biochemical Data Analysis, Elsevier.

Tedesco, J. and J. Slater (2000). "785-nm Laser Benefits Raman Spectroscopy." Retrieved 26th of May, 2014.

Tracy, T. and B. Paddock (2015). NYC drug ring busted after cocaine shipped in packages disguised as kids' birthday gifts: officials. Daily News.

Traynor, L. (2015). Drug peddlers POSTING heroin and cocaine into Britain's jails - with 2 packages intercepted every day. Mirror.

Tuschel, D. (2016). "Selecting an Excitation Wavelength for Raman Spectroscopy." Spectroscopy **31**(3).

UNODC (2015). World Drug Report 2015.

Vandenabeele, P., et al. (2007). Chemical Reviews. **107**.

Veij, M. d., et al. (2008). "Detection of Counterfeit Viagra with Raman Spectroscopy." J. Pharm. Biomed. Anal. **46**(2): 303-9.

Veij, M. d., et al. (2007). "Fast detection and identification of counterfeit antimalarial tablets by Raman spectroscopy." Journal of Raman Spectroscopy **38**(2): 181-7

Veloso, F., et al. (2005). "Comparison Between Laser Initiated Hollow Gas Embedded Z-pinches with Different Initial Radius." Plasma and Fusion Science: 16th IAEA Technical Meeting on Research using Small Fusion Devices.

Verster, J. C., et al. (2012). Drug Abuse and Addiction in Medical Illness: Causes, Consequences and Treatment, Springer Science & Business Media.

WCO (2012). "Customs operation nets exceptional quantities of drugs in postal parcels."

WCO (2013). Illicit Trade Report 2013, World Customs Organisation.

West, M. J. and M. J. Went (2011). "Detection of Drugs of Abuse by Raman Spectroscopy." Drug Testing and Analysis **3**(9): 532-538.

Wieboldt, D. (2010). "Understanding Raman Spectrometer Parameters."

Wikstorn, H., et al. (2005). "Comparison of Sampling Techniques for In-Line Monitoring Using Raman Spectroscopy." Applied Spectroscopy **59**(7): 934-941.

Winburn, D. C. (1989). Practical Laser Safety, CRC Press.

Wold S., Martens H., and Wold. H (1982) The Multivariate Calibration Problem in Chemistry Solved by PLS Method. Springer-Verlag, Heidelberg.

Wu, J., et al. (1995). "Three-Dimensional Imaging of Objects Embedded in Turbid Media with Fluorescence and Raman Spectroscopy." Applied Optics **34**(18): 3425-30

Yang, D. and Y. Ying (2011). "Applications of Raman Spectroscopy in Agricultural Products and Food Analysis: A Review." Applied Spectroscopy Reviews **46**(7): 539-560.

Yu, X., et al. (2014). "Optimization design of a diffractive axicon for improving the performance of long focal depth." Optics Communications.

Zhang, X., et al. (2013). "Study of Raman Spectroscopy to detect the Underlying Substance Concealed below Diffusely Scattering Medium." Optics and Photonics Journal **3**: 272-276.

Zhang, Y. (2008). "Analytical expression for the diffraction field of an axicon using the ray-tracing and interference method." Applied Physics B **90**: 93-96.

Zoubir, A. (2012). Raman Imaging: Techniques and Applications, Springer.